


Review

# Chiral Heterocycle-Based Receptors for Enantioselective Recognition

Vaibhav N. Khose <sup>1</sup>, Marina E. John <sup>1</sup>, Anita D. Pandey <sup>1</sup>, Victor Borovkov <sup>2,\*</sup>   
and Anil V. Karnik <sup>1,\*</sup>

<sup>1</sup> Department of Chemistry, University of Mumbai, Vidyanagari, Mumbai 400 098, India; vnkbose@gmail.com (V.N.K.); marinajohn126@gmail.com (M.E.J.); anitadpandey@gmail.com (A.D.P.)

<sup>2</sup> Department of Chemistry and Biochemistry, Tallinn University of Technology, Akadeemia tee 15, 12618 Tallinn, Estonia

\* Correspondence: victor.borovkov@ttu.ee (V.B.); avkarnik@chem.mu.ac.in (A.V.K.); Tel.: +91-022-26526091 (A.V.K.)

Received: 27 December 2017; Accepted: 12 January 2018; Published: 24 January 2018

**Abstract:** The majority of biomolecules found in living beings are chiral, therefore chiral molecular recognition in living systems is crucial to life. Following Cram's seminal work on the crown-based chiral recognition, prominent research groups have reported innumerable chiral receptors with distinctly different geometrical features and asymmetry elements. Main applications of such chiral receptors are found in chiral chromatography, as for analytical purposes and for bulk separation of racemates. Incorporation of heterocyclic rings in these recognition systems added a new dimension to the existing group of receptors. Heterocycles have additional features such as availability of unshared electron pairs, pronounced conformational features, introduction of hydrogen bonding and presence of permanent dipoles as well as specific spectral properties in certain cases. These features are found to enhance binding properties of the receptors and the selectivity factors between opposite enantiomers, allowing them to be effectively separated. The review presents the synthetic approaches towards these heterocyclic receptors and their distinctly different behavior vis-à-vis carbocyclic receptors.

**Keywords:** heterocycle; receptors; enantioselective recognition; hydrogen bonding; conformational rigidity; configuration; diastereomeric interactions; macrocycle size; pyridine; dipolar interactions

## 1. Introduction

Chiral Analytical techniques have become indispensable tools in pharmaceutical and fragrance industries. Qualitative and quantitative analyses of the enantiomerically pure or enriched compounds used in these industries are essential in the view of criteria set by regulating authorities [1,2]. Most of these techniques are based on the non-bonded diastereomeric interactions between a host and enantiomeric guests. Such diastereomeric interactions are the genesis of the chiral manifestations in natural and man-made systems.

Indeed, chiral molecular recognition remains one of the most expanding research fields in organic chemistry [3]. Various biological phenomena such as enzyme-substrate, antibody-antigen and drug-biomolecule interactions are a manifestation of the importance of enantiospecific supramolecular processes in living organisms [4]. The importance of chirality in the fields of medicine [5,6], asymmetric synthesis, [7,8] catalysis [9], flavor [10], fragrances [11], biochemistry [12] and material science chemistry [13] has already been well established. While the area of asymmetric synthesis has witnessed a tremendous growth, the practicality of preparing homochiral compounds still remains a challenge. Thus, the stimulus for interest in the separation of racemic mixtures exploiting host-guest chemistry has gained popularity over the years.

The earliest studies on enantiomeric recognition of chiral organic ammonium salts by chiral crown ethers were carried out by Cram and coworkers [14]. Since then, the importance of furnishing chiral macrocyclic ligands has been realized. Some of these ligands include amino acid units [15], sugar molecules [16], diaza-crown moieties [17], and crown ethers containing a pyridine sub-cyclic fragment [18]. In the last few decades, strategies and methods for synthesizing simpler organic compounds that mimic the biological receptors have been the prime focus in this research area [19–21]. Thus, the artificial receptors having diverse chiral backbones with different elements of chirality [22–25], incorporating aromatic/heteroaromatic alicyclic rings [26–28] in the core structural motif with multiple functionalities [29] have been reported. The receptors containing heteroaromatic ring/heteroalicyclic rings have attracted widespread interest due to their excellent chiral discriminating ability [30]. The receptors with five/six membered heterocycles offer additional advantages while binding the chiral guests through several non-covalent interactions such as hydrogen bonding, electrostatic interactions, hydrophobic binding, cation- $\pi$  interactions,  $\pi$ - $\pi$  stacking, steric complementarity, etc. in the enantioselective recognition processes [31]. Analytical techniques such as NMR, UV-Vis, circular dichroism, and fluorescence spectroscopy are commonly used to study chiral recognition, among which the fluorescence approach provides the highest sensitivity and real-time measurement.

Till date, there is no comprehensive review emphasizing heterocycle-based chiral receptors in enantioselective processes. The present review article presents a detailed account of the recent developments in the design and synthesis of various chiral receptors with heterocyclic motif such as pyridine [18], chromene [32,33], imidazole [34], benzimidazole [35,36], furan [37], thiophene [38], oxazole [22–25] etc. and its application in the enantioselective recognition of different classes of chiral analytes [39,40].

## 2. Components of Chiral Molecular Recognition

### 2.1. Different Types of Forces

Various non-covalent and covalent interactions are the key elementary factors involved in the host-guest molecular recognition phenomena. Much effort in recent years have moved to more keen understanding for the basis of molecular recognition and the physical principles governing this phenomenon have been the focus of many researchers for centuries. Besides, a wide range of the controlled separation and chemical transformation processes in the drug design, scientific and engineering fields relies on the host-guest chemistry. This section comprehensively addresses the different types of interaction forces in detail.

### 2.2. Non-Covalent Interactions

Non-bonded interactions are susceptible to thermal fluctuations and other external factors unlike covalent linkages. Weak forces by themselves are able to form strong intra and intermolecular significant interactions only upon working together or in combination with a covalent binding. They are most ubiquitous in nature and are crucial in determining the three-dimensional structures adopted by proteins and nucleic bases.

Depending upon the origin, non-covalent interactions are divided into the following sub classes; Electrostatic Interactions, Hydrogen Bonding,  $\pi$ -electronic effects, Van der Waals forces and Hydrophobic binding, which are summarized briefly below.

#### 2.2.1. Electrostatic Interactions

Electrostatic or Ionic interactions [41] are strong coulombic attractive forces between opposite charges, observed in the case of several receptors, such as cations and anions, binding effectively to the corresponding guest in place. This type of interaction is non-directional, whilst for the ion-dipole interactions the dipole must be suitably aligned for optimal binding efficiency. The high strength of electrostatic interactions has made them an invaluable tool amongst supramolecular chemists for



achieving strong binding. Ionic interactions are basically of two types; the classic ionic bond which is a non-directional attractive force, for example between a positively charged metal ion and negatively charged non-metal, and the salt bridge wherein there is a balance of the electrostatic forces between three or more atoms with partial charges. Such strong attractive interactions stabilize the host guest complex extensively.

### Hydrogen Bonding Interaction

Hydrogen bonding [41,42] is attractive electrostatic interaction between the hydrogen atom, bearing a partial positive charge, covalently attached to an electronegative atom and another electronegative atom which has a partial negative charge developed on it. Hydrogen bonding is the most widely employed dipole-dipole interaction in the field of supramolecular chiral discrimination. Most receptors have electronegative heteroatoms such as Nitrogen, Oxygen as binding sites involved in hydrogen bonding.

#### 2.2.2. $\pi$ -Electronic Interactions

##### $\pi$ - $\pi$ Interaction

$\pi$ - $\pi$  Interactions [43] are rather weak bindings occurring in the face-to-face or edge-to-face or edge-to-edge manners, which play a major role in many aspects of biological, solid-state and host-guest supramolecular chemistry. The quadrupole-quadrupole forces are responsible for the  $\pi$ - $\pi$  stacking of aromatic rings. Aromatic rings such as benzene, naphthalene, pyridine, imidazole, triazole, indole etc. are often incorporated into the chiral macrocycle for increasing the capacity for chiral recognition to a greater extent owing to the  $\pi$ - $\pi$  stacking interaction of the host and guest systems.

##### Cation- $\pi$ Interaction

The interaction between a cation and delocalized  $\pi$ -electron cloud of the aromatic system exemplifies the cation- $\pi$  interaction [44]. The simplest view of this non-bonding interaction is in the gas phase. In this case, there is no solvent and stabilization of the system is entirely dependent on the cation and  $\pi$  system of interest. The cation- $\pi$  interactions between the hydrogen-bonded ammonium ion and the aromatic ring of host, exemplifies the chiral recognition of organic ammonium ions by various chiral receptors.

#### 2.2.3. Van der Waals Forces

Van der Waals forces [45] are an attractive noncovalent type of interactions between the fixed dipole in one molecule and induced instantaneous oscillating dipole in another molecule via the corresponding distortion of electron clouds. These forces though underappreciated, are of immense importance to the supramolecular properties of all molecules. However, it is difficult to rationally design the receptors specifically, as this type of interactions is very common to most molecules. The binding of guest into the hydrophobic cavity of host is driven by an enthalpy stabilization. Therefore, even small molecules can make a large number of the Van der Waals contacts and each of them add in a synergistic manner.

Additionally, there is one specific subclass in this category called the “London dispersion forces” and attributed to two induced dipoles.

#### 2.2.4. Hydrophobic Interactions

Hydrophobic interactions [46] are a result of the nonpolar side chains (aromatic rings and hydrocarbon groups) holding tightly in polar solvents, especially water. In this case, there is no sharing of electrons between any groups, therefore it does not produce a true bond. The hydrophobicity of receptors can be manipulated by introducing long side chains. On binding of a guest, the water molecules around a polar surface of the hydrophobic cavity of the host are released into the bulk solvent,

which in turn leads to enhancement of its hydrogen bonding capabilities simultaneously increasing the entropy of the system. The hydrophobic interactions are comparatively stronger than Van der Waals forces or Hydrogen bonding. For example, cyclophanes and cyclodextrins being macrocyclic itself possess inbuilt hydrophobicity contributing to the host-guest affinity and are well-designed to encapsulate guest molecules from an aqueous solution.

### 3. Analytical Tool for Chiral Recognition

For efficient enantioselective discrimination, the chiral host-guest interactions should result in certain chemical-physical changes that can be read out by various analytical techniques. Depending on spectral properties of the host-guest complexes, analytical techniques such as fluorescence, UV-visible absorption, circular dichroism, NMR, HPLC, electrochemistry, IR, and mass spectrometry could be used as effective tools to measure the chiral recognition phenomenon. The detailed description of each technique is presented below.

#### 3.1. Fluorescence

Fluorescence spectroscopic technique received considerable attention because it is able to provide special advantages which include simplicity, low cost, high sensitivity, adaptation to automation and real-time analysis, diverse signal output modes and small quantity of host and guest. This technique allows multiple detection modes such as emission, excitation and lifetime measurements.

For chiral analysis/recognition fluorophores (fluorescent chromophoric systems) should be either intrinsically chiral or made chiral by attaching an enantiopure moiety. The corresponding diastereomeric interactions with the concerned chiral analyte give different fluorescence responses; i.e., the recognition. Such sensors generally respond via the fluorescence enhancement or quenching. The fluorescence quenching is observed due to loss of the energy of the excited state by a non-radiative decay. Such systems are commonly studied by the Stern-Volmer equation [47] (see below).

$$F_0/F = 1 + K_{sv} [Q]$$

where

$F_0$  = Initial emission intensity of the host

$F$  = Intensity of the host after addition of analyte (Guest)

$K_{sv}$  = Stern-Volmer constant/Stability constant for the complex

$[Q]$  = Concentration of the analyte (Guest)

The Stern-Volmer plot of fluorescence intensity ratio,  $F_0/F$  vs.  $[Q]$ , concentration of guest enantiomers would exhibit the linear relationship with host and from the graph, Stern-Volmer constant can be calculated.

However, when complexation results in the enhancement of fluorescence, the system is studied by using the Benesi-Hildebrand equation [48] (see below).

$$I_0/(I - I_0) = [b/(a - b)] [1/(K[M]) + 1]$$

where

$I_0$  = Initial emission intensity of the host

$I$  = Intensity of the host after addition of analyte (Guest)

$K$  = Stability constant for the complex

$a, b$  = Constants terms

$[M]$  = Concentration of the analyte (Guest)

The  $[b/(a - b)]$  can be found out by plotting the  $I_0/(I - I_0)$  against the inverse of the concentration of analyte,  $M^{-1}$ .

The Benesi-Hildebrand equation is similar to equation for straight line,  $y = mx + C$ . The intercept of the graph gives the  $[b/(a - b)]$ ; the  $I_0$  and  $I$  are found out experimentally and hence  $K$  can then be calculated.

### 3.2. UV-Vis Absorption

UV-vis spectroscopy is one of the widely used methods for chiral recognition as it provides high sensitivity and simplicity to the host-guest binding study. In this case, the host molecule should contain a chromophoric system with the absorption band in the UV-Vis range, while the host-guest complex generally has a different absorption band. The difference in the absorbance of host and corresponding host-guest complex is used for determination of the extent and strength of binding in a quantitative manner.

The association constants related to binding process of the opposite guest enantiomers with the chiral host can be calculated by using the modified Benesi-Hildebrand equation [35] as follows.

$$[H]_0[G]_0 = \frac{1}{K_a \Delta \epsilon} + \frac{[G]_0}{\Delta \epsilon}$$

Further modified equation, where a double reciprocal plot can be made with  $1/\Delta A$  as a function of  $1/[G]_0$ . {where  $[G]_0 \gg [H]_0$ }.

$$\frac{1}{\Delta A} = \frac{1}{K_a \Delta \epsilon [H]_0 [G]_0} + \frac{1}{\Delta \epsilon [G]_0}$$

where,

$[H]_0$  and  $[G]_0$  are total concentrations of host and guest, respectively,

$\Delta \epsilon$  is the change of molar extinction coefficient between the free and complexed host,

$\Delta A$  represents the absorption change of host upon the addition of opposite guest enantiomers.

The plots of  $1/\Delta A$  against  $1/[G]_0$  values, usually give an excellent linear relationship, indicating the corresponding binding process between the host and guest enantiomers. The  $\Delta \epsilon$  value can be derived from the intercept, while  $K_a$  (association constant) can be calculated from the slope. The binding constants,  $K(R)$  or  $K(S)$  and associated free energy change ( $\Delta G_0$ ) for the host molecule upon the complexation are obtained by the curve fitting analysis of observed absorbance changes.

### 3.3. Circular Dichroism (CD)

Circular dichroism (CD) spectroscopic technique responds to the spatial asymmetry change in conformation and/or configuration, and hence is effectively used for investigating the chiroptical properties of chiral hosts and their complexes with enantiomeric guests. It enables probing the discrimination efficiency of supramolecular hosts and determination of complex stoichiometry and stability.

In general, two or more electronic transitions of the chromophoric units around a chiral center excitonically couple with each other generating bisignate CD signals. It allows the reliable determination of enantiomeric preference by comparing the corresponding amplitudes of exciton couplets from exciton-coupled circular dichroism (ECCD) spectra of the resulting complexes. The sign of the Cotton effect can be used to assign the absolute configuration or relative conformation [3].

### 3.4. Nuclear Magnetic Resonance (NMR) Analysis

Enantioselective recognition can be readily studied by using NMR spectroscopy as the diastereomeric interaction between a chiral host and enantiopure guest that is usually accompanied by significant chemical shift changes. This technique is useful for both liquid and solid compounds, while only milligram quantities of samples are required. The recognition process via NMR can be carried out by two main approaches: the use of chiral solvating agents (CSA) and enantiopure

chiral derivatizing agents (CDA). In the case of CSA [49] based on non-covalent interactions, the corresponding diastereomeric complexes are formed between a solute and chiral solvent and the resultant NMR signals deduce the chirality of molecule of interest. A sub-class of CSA is chiral shift reagents (CSR), where a paramagnetic metal ligated to chiral ligands. In the case of CDA [50], the covalent bonded diastereomeric derivatives are formed and their NMR pattern helps in assignment of the configuration of the target compound. Determination of the enantiomeric purity of the samples with certain enantiomeric excess is also possible by using NMR [51]. Furthermore, the variable-temperature  $^1\text{H}$  NMR measurements are useful in estimating a kinetically more stable complex and exhibit the enantiomeric recognition effect.

Presence of aromatic moieties in the host as well as in the guest generally gives better results due to the magnetic anisotropic effect. It is expected that the protons present in the vicinity of chiral center are affected by the shielding or deshielding effect during the formation of diastereomeric complexes. It results in better separation of the peaks for these protons in both the diastereomers; hence enhancing the chiral recognition.

### 3.5. High Performance Liquid Chromatography (HPLC)

Chiral HPLC [52] serves as the most extensively used analytical method for resolving enantiomers of the chiral samples. A stationary phase of the chiral HPLC columns contains an enantiomeric form of the chiral materials such as cellulose or cyclodextrin. Two opposite enantiomers of the analyte are distinct in affinity to the chiral stationary phase (CSP), and therefore show different retention times.

The chiral compounds synthesized in laboratory in a racemic form or enantio-enriched form via asymmetric synthesis are commonly analyzed by chiral HPLC. The separation of enantiomers on chiral HPLC column is based on the diastereomeric binding via three point interactions with a chiral coating present in the column. The difference in the retention time of enantiomers is an example of chiral molecular recognition between the chiral column packing materials and the enantiomers. The most popular chiral columns are Chiralcel OD and Chiralpak AD. Chiralcel OD has the tris(3,5-dimethylphenyl carbamate)s derivative of cellulose as CSP, whereas Chiralpak AD has the same derivative but of amylose (Figure 1). These polysaccharide-based chiral columns are nearly universal with the capability to resolve chiral compounds being almost 80–90% as reported so far using hexane-alcohol as eluents. Most commercially available chiral HPLC columns are carbohydrate-based such as Chiralcel OD and Chiralpak AD, crown ether-based column includes crown pack CR, crown pack CR (+), crown pack CR (−) etc. Thus, re-emphasizing the role of heterocycles in chiral supramolecular chemistry.

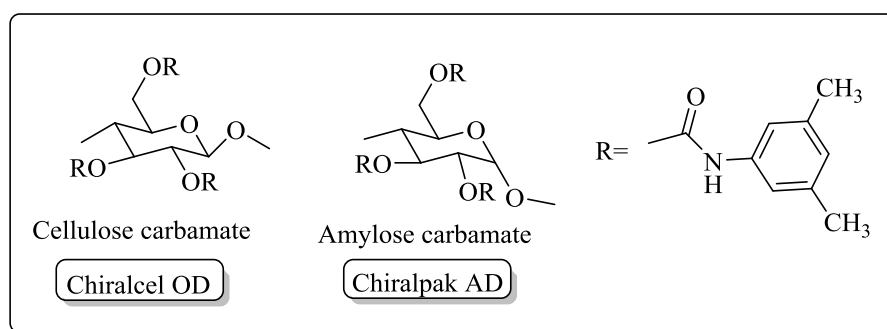


**Figure 1.** Chiral column packing materials, of cellulose carbamate and amylose carbamate.

### 3.6. Mass Spectrometry

Mass spectrometry [23,53] is the ubiquitous powerful analytical tool for the chiral molecular recognition. The chiral recognition using fast atom bombardment mass spectrometry (FAB-MS) and electrospray ionization mass spectrometry (ESI-MS) are the most significant ways to quantify the

recognition phenomena. The methodology working on the basis of isotopic labeling of one of the guest ( $G^+$ ) enantiomers is carried out followed by comparing the peak intensities of 1:1 mixture of the unlabeled ( $G_R^+$ ) and labeled enantiomer guests ( $G_{S-dn}^+$ ). Chiral recognition of the given host is simply measured by using the following equation.

'IRIS' value was defined to be peak intensity ratio,  $I[(H + G_R^+)]/I[(H + G_{S-dn}^+)] = I_R/I_{S-dn}IRIS$ , of two diastereomeric host-guest complex, exhibited in the  $n$  mass unit difference in the mass spectrum.

There are three possible cases of *IRIS*.

- (1)  $IRIS > 1.0$  means that the given chiral host binds more strongly (*R*)-enantiomer of the guest, hence indicating the (*R*)-enantiomer preference; the larger  $I_R/I_{S-dn}$  value corresponds to the higher degree of chiral recognition of the host.
- (2) In contrast,  $IRIS < 1.0$  means that the given chiral host binds more strongly (*S*)-enantiomer of the guest, indicating the (*S*)-enantiomer preference with the opposite tendency for the  $I_R/I_{S-dn}$  value.
- (3)  $IRIS = 1.0 \pm 0.05$  means that the given chiral host cannot differentiate the chirality of the guest.

### 3.7. Electrochemical Methods

Electrochemical methods have attracted much attention due to their high sensitivity, operational simplicity, and cost efficiency.

Electrochemical methods such as ion-selective electrodes (ISEs) for pH and cyclic voltammetry (CV) enable the qualitative as well as quantitative determination of the target analyte along with the elucidation of thermodynamics and kinetics of the electron transfer reactions. These techniques convert the chemical and/or physical information of analyte into the electrical signal of either potential or current or both, which is then processed to reveal the accurate chemical information.

The chemical or physical change may be induced directly by the target analyte interacting with the electrode, thereby generating the electric signals monitored as a potential, or current change, or both. Detection based on each of these signals is termed *potentiometry*, *amperometry* (including *coulometry*), and *voltammetry*, respectively.

Electrochemical detection has been applied mainly to the redox-active targets that are charged, that are, ions, and/or capable of undergoing the redox reactions on an electrode leading to either oxidation or reduction of the target.

#### Cyclic Voltammetry

Simultaneous recording and analyzing the potential and current variations with time are the merits of voltammetry [54]. In particular, to make the control and analysis easier, the change of potential can be made linear against time. The corresponding voltammetry is called *linear sweep voltammetry*. Further, the potential can be linearly increased and then decreased in a cyclic manner, and such a method is called *cyclic voltammetry*. Upon combining with the three-electrode cell it becomes the widely used electrochemical technique for either fundamental studies or detection applications. The most important result from such a measurement is the cyclic *voltammogram*, or simply CV, which plots the variation of current against the linearly changing electrode potential  $E$ .

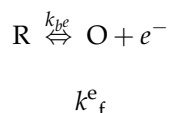
CV is nowadays conventionally performed on a computer-controlled potentiostat as commercially supplied. The user needs to input at least three parameters into the potentiostat: the initial and final potentials  $E_i$  and  $E_f$  of the potential scan, and the potential scan rate  $dE/dt$ . The equations below describe the relationships between these parameters:

$$dE/dt = (E_f - E_i)/(t_f - t_i)$$

$$E = E_i + t \times dE/dt$$

where  $t$  is the variable time. In this equation, the start ( $t_i$ ) and final ( $t_f$ ) times of potential scan are used here to explain the relationship, but are not independent because they are determined by  $E_i$ ,  $E_f$ , and  $dE/dt$ . Also, it is of note that the scan rate  $dE/dt$  is positive when  $E_f > E_i$  and negative when  $E_f < E_i$ .

The electrode reaction potential and kinetics of redox active molecule are well reflected by the peak potentials and the shape of CV. In general, for a one-electron reaction that converts a molecule in the reduced state R to the oxidized state O, the reaction proceeds as follows:



where  $k_f^e$  and  $k_b^e$  are the rate constants for the forward and backward electron transfer reactions, respectively. If  $k_f^e \approx k_b^e$  and both are sufficiently large, the reaction represents a reversible electrode process. If  $k_f^e \gg k_b^e$ , the reaction is electrochemically irreversible, even though it may be chemically reversed given a sufficiently long time. Between these two-edged points, the reaction is regarded as quasi-reversible. These situations can be mathematically processed, giving rise to useful conclusions in relation to CVs, particularly for electrochemical detection.

#### 4. Special Features of Heterocyclic Receptors for Enantioselective Recognition

Chiral molecular recognition is dependent on several parameters. To facilitate and exploit these parameters, the design of chiral receptors is the most crucial factor. The research community continuously broadens the scope of chiral receptors containing the aromatic/heteroaromatic/aliphatic rings. The present review covers a variety of hosts containing one or more heterocyclic rings as a vital part for enantiodiscrimination. Thus, these heterocyclic rings can be of different sizes and structure, for example aromatic rings such as imidazole, benzimidazole, furan, thiophene, pyrrole, triazole, pyridine, quinoline, isoquinoline, etc. or aliphatic rings such as pyrrolidine, tetrahydrofuran, tetrahydrothiophene, imidazolidine, oxazolidine, etc. A plethora of the heterocyclic receptors synthesized so far has different elements of chirality and possesses special characteristic features to influence the stability of host-guest complex and enantioselective sensing. The key features of these hosts are summarized as follows:

1. Heterocycles have unshared electron pairs present on the heteroatoms useful for the three points hydrogen bond formation, especially when chiral ammonium cations are studied, with the chiral guest molecule.
2. Heterocycles possess a permanent dipole responsible for the charge-dipole electrostatic interactions.
3. The aromatic heterocycles have  $\pi$  electrons to facilitate the corresponding  $\pi$ - $\pi$  stacking interaction and cation- $\pi$  binding with a chiral aromatic guest molecule.
4. The conformational rigidity is increased by the presence of heterocyclic ring, which imparts a good deal of preorganization of the chiral host suiting a guest molecule.
5. The aliphatic heterocyclic ring system may assist the hydrophobic interaction with a chiral guest molecule.
6. The heterocyclic ring may additionally influence the steric interaction responsible for chiral discrimination.

#### 5. Chiral Hosts with Six Member Heterocycle/s

Six-membered cyclic structures are most abundant in nature. One of the primary reasons being conformational and hence such structures are thermodynamically stable. Aromatic rings have advantage of presence of ring current which very strongly influence the NMR signals of the analyte. Pyridine ring has found wide-spread use in the reported receptors so far.



### 5.1. Nitrogen Containing Six Member Heterocycle/s

#### Pyridine Ring

Pyridine is one of the six membered aromatic heterocycles which has been extensively used in chiral organocatalysis [55], chiral metal-based catalysis [56], chiral resolving agents [57,58] etc. Reports reveal that inclusion of symmetrical, 2,6-disubstituted pyridine motifs in the host architecture, offers enhanced binding properties to it. The strikingly common unit found in pyridine containing hosts are the presence of one or more 2,6-disubstituted pyridines, with pyridine nitrogen pointing inwardly, in the structural construct of the macrocycle or the molecular cleft. (Chart 1, part A). Another class of pyridine containing receptors include one or more 4,4'-bipyridine motif giving rise to rigid molecular clefts or cyclophanes (Chart 1, part B).

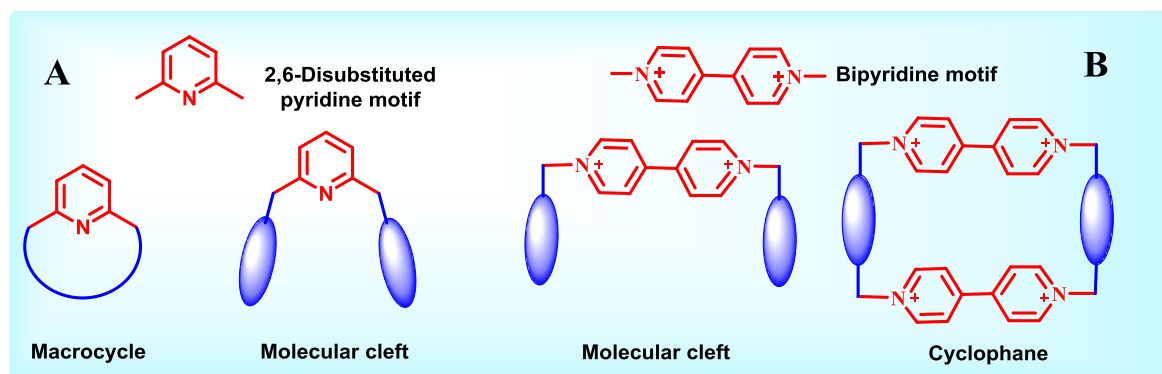


Chart 1. 2,6-disubstituted pyridine (A) and 4,4'-Bipyridine (B) containing hosts.

Incorporation of a pyridine unit provides proton acceptors at the pyridyl nitrogens which are important for the tripod hydrogen bonding, while the aromatic system contributes via  $\pi$ - $\pi$  stacking interaction, along with imparting increased rigidity to form thermodynamically stable complexes with guest molecules. Owing to the aforementioned special features of the pyridine ring, Izatt and group have designed various macrocyclic hosts, particularly chiral crowns ethers containing pyridine units [18], which enable these hosts to recognize specific guests such as chiral organic ammonium salts. It was one of the first extensive recognition studies using chiral macrocycles (Figure 2) and enantiopure alkylammonium salts. Several experimental techniques such as temperature-dependent  $^1\text{H}$  NMR spectroscopy, titration calorimetry, Fourier transform ion cyclotron resonance mass spectrometry, and selective crystallization have been employed to establish the corresponding host-guest chiral recognition in the given systems and to report the  $K$ ,  $\Delta H$ , and  $\Delta S$  values for the interactions, thus quantitating the binding processes. Additionally, the X-ray crystallographic results provided a structural basis for the recognition.

The parameters and supramolecular interactions that are involved in these chiral systems have been studied exhaustively and several [18,59,60] reviews on this and similar works have been summarized by the group. Their systematic investigations revealed the effect of substituents on the crown ether, guest type and solvent on the extent of enantiomeric recognition.

In continuation of the research on chiral recognition, the authors [61] have developed a gas-phase ion-molecule host-guest system, based on (*S,S*)-dimethyldiketopyridino-18-crown-6 (*S,S*-8) macrocycle for the enantioselective recognition of *R* and *S* enantiomers of  $\alpha$ -(1-naphthyl)ethylammonium ( $\text{NapEt}^+$ ) cation (Figure 3) using mass spectrometry (Reaction 1). It was demonstrated that the *S,S*-8-*R*- $\text{NapEt}^+$  complex was more stable than the *S,S*-8-*S*- $\text{NapEt}^+$  complex with the equilibrium constant  $K$  obtained for *S*- $\text{NapEt}^+$  being larger than that for *R*- $\text{NapEt}^+$  by a factor of 4. These results confirmed considerable recognition, which was measured by using the FT-ICR/MS techniques. However, no recognition was observed for the same host-guest interaction in the solution phase, indicating that the stabilization of

the complex formed is entirely dependent on the cation- $\pi$ interactions between the hydrogen-bonded ammonium ion and aromatic ring of the host.

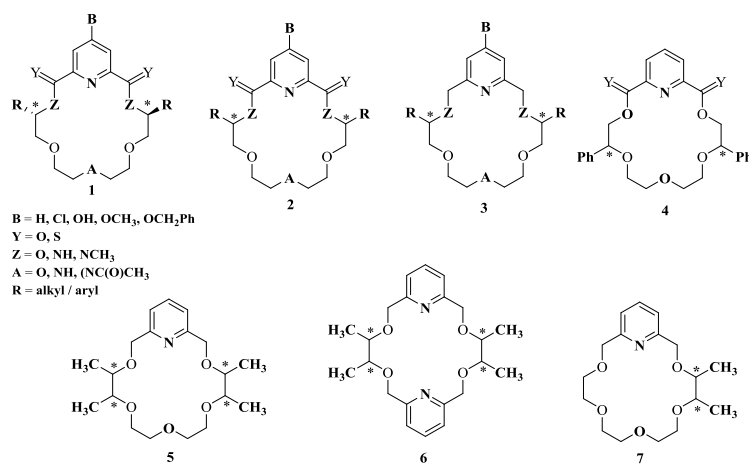


**Figure 2.** Chiral pyridine containing crown ether ligands.

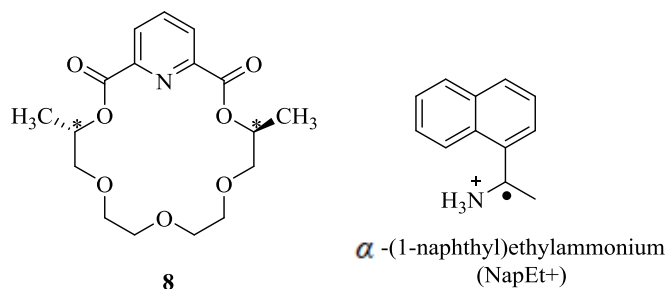
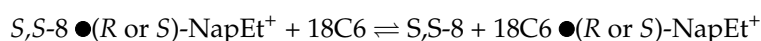


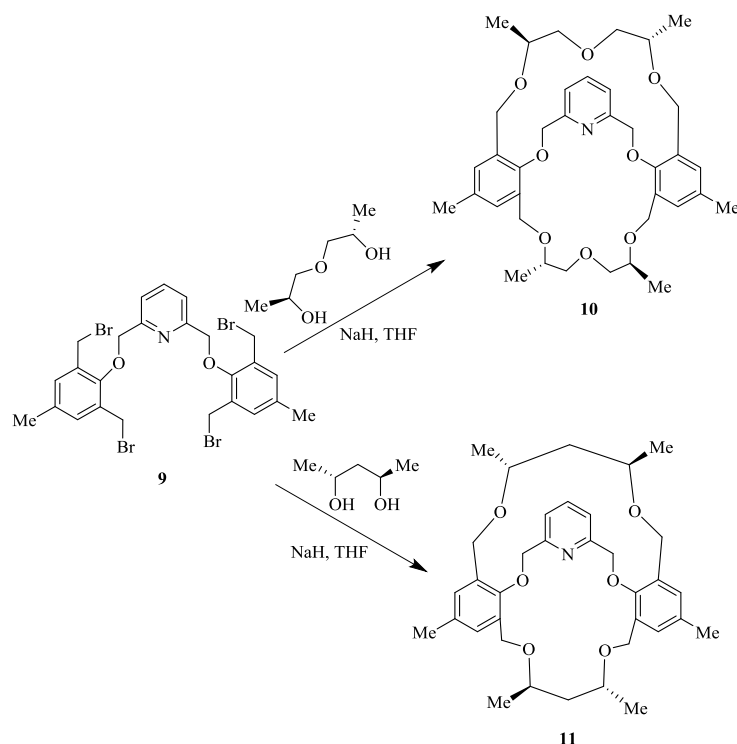
**Figure 3.** (*S,S*)-dimethyldiketopyridino-18-crown-6 (*S,S*-8) and  $\alpha$ -(1-naphthyl)ethylammonium (NapEt<sup>+</sup>).



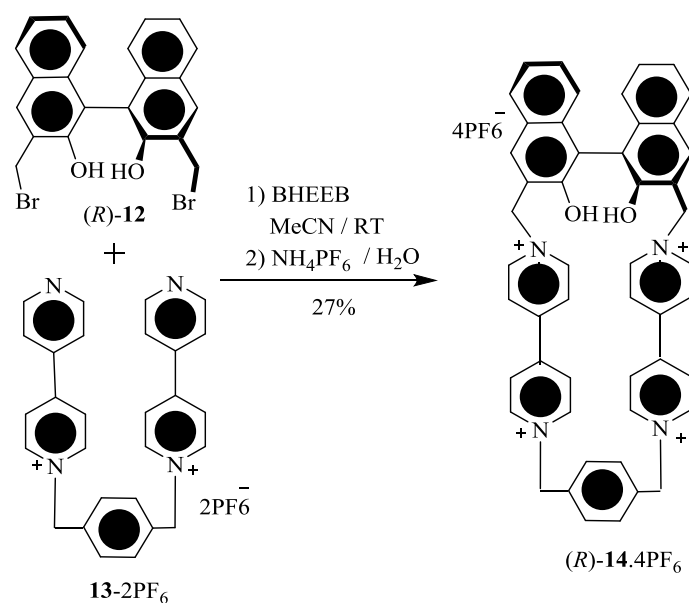
In their continuing efforts, same group then synthesized two chiral macrobicyclic cleft compounds containing a pyridine ring [62] as it possesses a three-dimensional cavity which might be useful for the recognition process. Treatment of pyridine-bridged tetrabromide **9** with the respective chiral glycols, chiral methyl-substituted diethylene glycol, (1*S*,5*S*)-3-oxapentane-1,5-diol or the (2*R*,4*R*)-pentanediol furnished the chiral tetramethyl-substituted macrobicyclic **10** and macrocycle **11**, respectively (Scheme 1). <sup>1</sup>H NMR spectroscopy has been used to determine the chiral recognition behavior of the synthesized compounds **10** and **11**. Indeed, (*S,S,S,S*)-**10**, as a chiral host demonstrated a high degree of the enantiomeric discrimination for (*S*)-enantiomers of  $\alpha$ -(1-naphthyl)-ethylammonium perchlorate (NapEt) and phenyl ethyl ammonium perchlorate (PhEt) over their (*R*)-forms. However, a reverse sequence of the recognition was observed for the (*S,S*)-**8** host wherein it recognizes the corresponding (*R*) forms of NapEt and PhEt over their (*S*) forms. This high recognition ability of cleft compound was observed owing to its increased molecular rigidity after introduction of a second macro ring on the monocyclic pyridine-crown ligand. The chiral discrimination behavior was studied using binary solvent system, lower enantiomeric recognition was observed for MeOH/CHCl<sub>3</sub> in comparison with Ethanol:Dichloroethane (2:8) which revealed the effect of solvent.

Stoddart et al. [63] have developed new axially-chiral tetracationic cyclophanes, (*R*)-**14**.4PF<sub>6</sub> and (*R,R*)-**16**.4PF<sub>6</sub> (Scheme 2). Tetracationic cyclophane, (*R*)-**14**.4PF<sub>6</sub> was obtained by the reaction of (*R*)-**12** and **13**.2PF<sub>6</sub> and similarly D<sub>2</sub> symmetric tetracationic cyclophane, (*R,R*)-**16**.4PF<sub>6</sub> was synthesized using the treatment of (*R*)-**12** and (*R*)-**15**.2PF<sub>6</sub>. These tetracationic cyclophane receptors were found to be effective for the chiral recognition in the case of several chiral amino acids, such as L- and

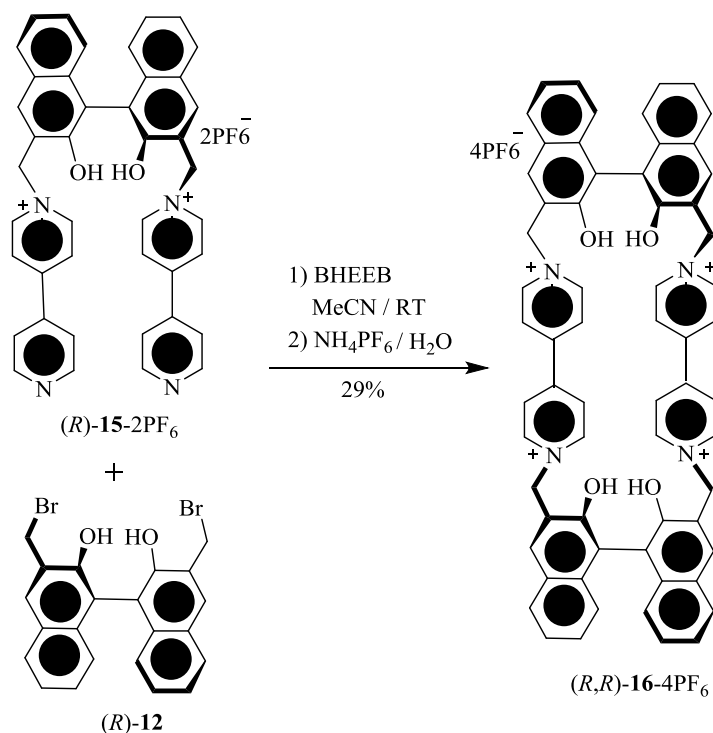
D-enantiomers of phenylalanine (Phe), tyrosine (Tyr), and tryptophane (Trp) as free forms, or methyl esters, or *N*-acetyls in H<sub>2</sub>O and organic solvents, as determined by using UV-Vis titration. The binding constant and free energies of 1:1 host-guest complexation are provided in Table 1. As one can see, the enantioselective recognition ability decreases from *N*-acetyl-Trp to *N*-acetyl-Tyr (Table 1, entries 7 and 8) and further to less  $\pi$ -electron-rich *N*-acetyl-Phe (Table 1, entries 9 and 10). These results revealed a greater extent of the secondary stereoelectronic interactions between the functional groups of  $\pi$ -electron rich guest and bulky optically-active binaphthol spacer(s) of cyclophane(s), which can be attributed to the  $\pi$ -electron rich nature of guest (primary mode of binding).



**Scheme 1.** Synthesis of macrobicyclic cleft compounds **10** and **11**.



**Scheme 2.** Cont.



**Scheme 2.** Synthesis of axially-chiral tetracationic cyclophanes  $(R)\text{-14.4PF}_6$  and  $(R,R)\text{-16.4PF}_6$ .

**Table 1.** Binding constants ( $K_a$ ) and free energies of complexation ( $-\Delta G_0$ ) for the 1:1 complexes between cyclophanes  $(R)\text{-14.X}$  ( $X = \text{PF}_6$  or  $\text{Cl}$ ) and  $(R,R)\text{-16.4 PF}_6$  and  $\pi$ -electron-rich amino acids <sup>a</sup>.

Entry	Substrate	Solvent	$K_2 \text{ (M}^{-1}\text{)}$		$K_a(\text{L})/K_a(\text{D})$		$-\Delta G_0 \text{ (kcal/mol)}$		$\Delta\Delta G_0 \text{ (kcal/mol)}^b$	
			$(R)\text{-14}$	$(R,R)\text{-16}$	$(R)\text{-14}$	$(R,R)\text{-16}$	$(R)\text{-14}$	$(R,R)\text{-16}$	$(R)\text{-14}$	$(R,R)\text{-16}$
1	L-Trp	H <sub>2</sub> O <sup>c</sup>	2470	ND <sup>d</sup>			4.63			
2	D-Trp	H <sub>2</sub> O <sup>c</sup>	5860	ND <sup>d</sup>	0.42		5.14		−0.51	
3	L-Trp OMe.HCl	H <sub>2</sub> O <sup>c</sup>	753	ND <sup>d</sup>			3.92			
4	D-Trp OMe.HCl	H <sub>2</sub> O <sup>c</sup>	803	ND <sup>d</sup>	0.94		3.96		−0.04	
5	N-Ac-L-Trp	A <sup>e</sup>	20700	4280			5.89	4.95		
6	N-Ac-D-Trp	A <sup>e</sup>	2670	1080	7.75	3.96	4.67	4.14	1.22	0.81
7	N-Ac-L-Tyr	B <sup>e</sup>	10060	2340			5.45			
8	N-Ac-D-Tyr	B <sup>e</sup>	2125	1047	4.73	2.23	4.53	4.12	0.92	0.48
9	N-Ac-L-Phe	A <sup>e</sup>	1220	219			4.21	3.19		
10	N-Ac-D-Phe	A <sup>e</sup>	2260	137	0.54	1.60	4.57	2.91	−0.36	0.28

<sup>a</sup> All binding constants were determined by UV/vis titration at 25 °C. <sup>b</sup>  $\Delta\Delta G_0 = \Delta G_0(\text{L}) - \Delta G_0(\text{D})$ . <sup>c</sup> In H<sub>2</sub>O as solvent.

<sup>d</sup> Not determined. <sup>e</sup> Solvent mixture A: MeCN 90% DMF 10%; solvent mixture B: MeCN 90% DMSO 10%.

Hollosi et al. [64] have established the applicability of CD spectroscopy as an effective tool for the enantioselective discrimination of aryl alkyl ammonium salts **19–21** by pyridine-18-crown-6 type ligands, **17** and **18** (Figure 4). Furthermore, the stoichiometry and relative stability of host-guest complexes have been determined. Intriguingly, the study revealed that the heterochiral complexation of  $(R,R)\text{-17}$  with  $(S)$ -arylalkyl ammonium salts **19** and **20** or  $(S,S)\text{-18}$  with  $(R)$ -salts **19** and **20** exhibited additional spectral effects in the spectral region  $^1\text{L}_b$  and  $^1\text{L}_a$  in the form of high amplitude of CD than homochiral complexation.

Mallouk et al. [65] have synthesized the  $(S)$ -valine-leucine-alanine cyclophane, **26** (Scheme 3). The bipyridine fragment, **23** of **26** was prepared by the reaction of 4, 4'-bipyridine with 4-(chloromethyl)benzoic acid followed by the treatment with 4-(bromomethyl)benzylamine hydrobromide. The standard solid phase synthesis was employed to produce the N-*t*-BOC-protected tripeptide unit, **24**. Finally, the bipyridine and N-*t*-BOC-protected tripeptide units **24** were coupled to obtain the required  $(S)$ -valine-leucine-alanine cyclophane, **26**.  $^1\text{H}$  NMR titration for the complexation of chiral cyclophane host **26** in an aqueous media with diverse pharmaceutically interesting chiral

and racemic  $\pi$ -donor guest molecules, such as Non-steroidal Anti-inflammatory Drugs (NSAIDs),  $\beta$ -blockers, amino acids, and amino acid derivatives were performed confirming weak binding abilities in the range of  $1\text{--}39\text{ M}^{-1}$  (Table 2). Out of the studied guest molecules, racemic nandanol and DOPA exhibited the substantial binding with **26**. Interestingly, the (*R*)/(*S*) enantioselectivity ratio of  $13 \pm 5$  was found for dihydroxyphenylalanine (DOPA), indicating a strong  $\pi$ -electron donor cationic guest. Two-dimensional NOESY  $^1\text{H}$  NMR spectra revealed the corresponding multiple intermolecular NOE's signals for (*R*)-DOPA and the host, **26** in the host-guest complex. This result unambiguously confirmed a strong and enantioselective binding of (*R*)-DOPA inside the cavity of **26**, while no measurable interaction was detected for (*S*)-DOPA under the same conditions.

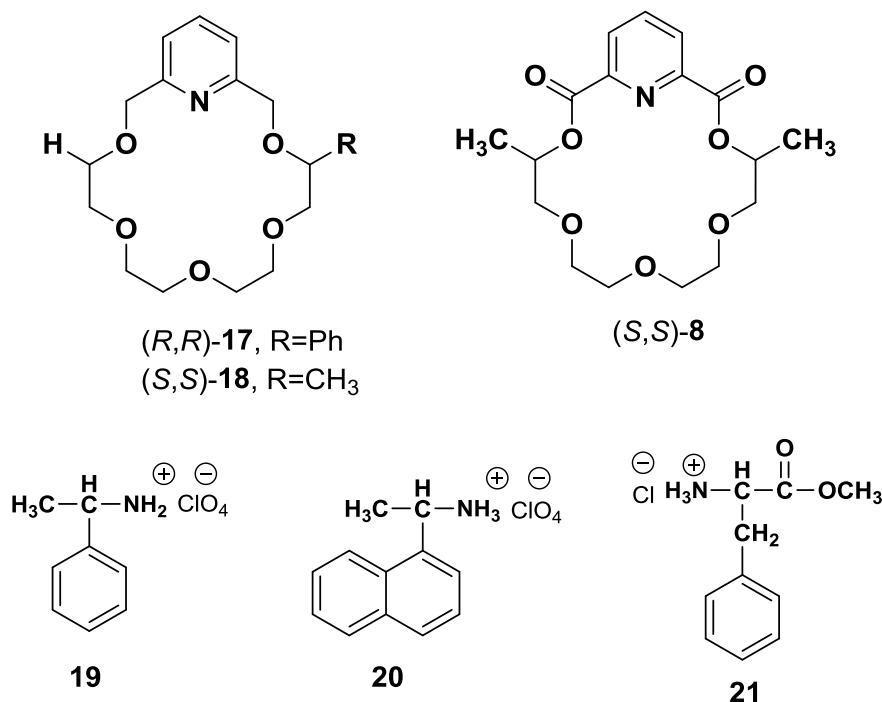


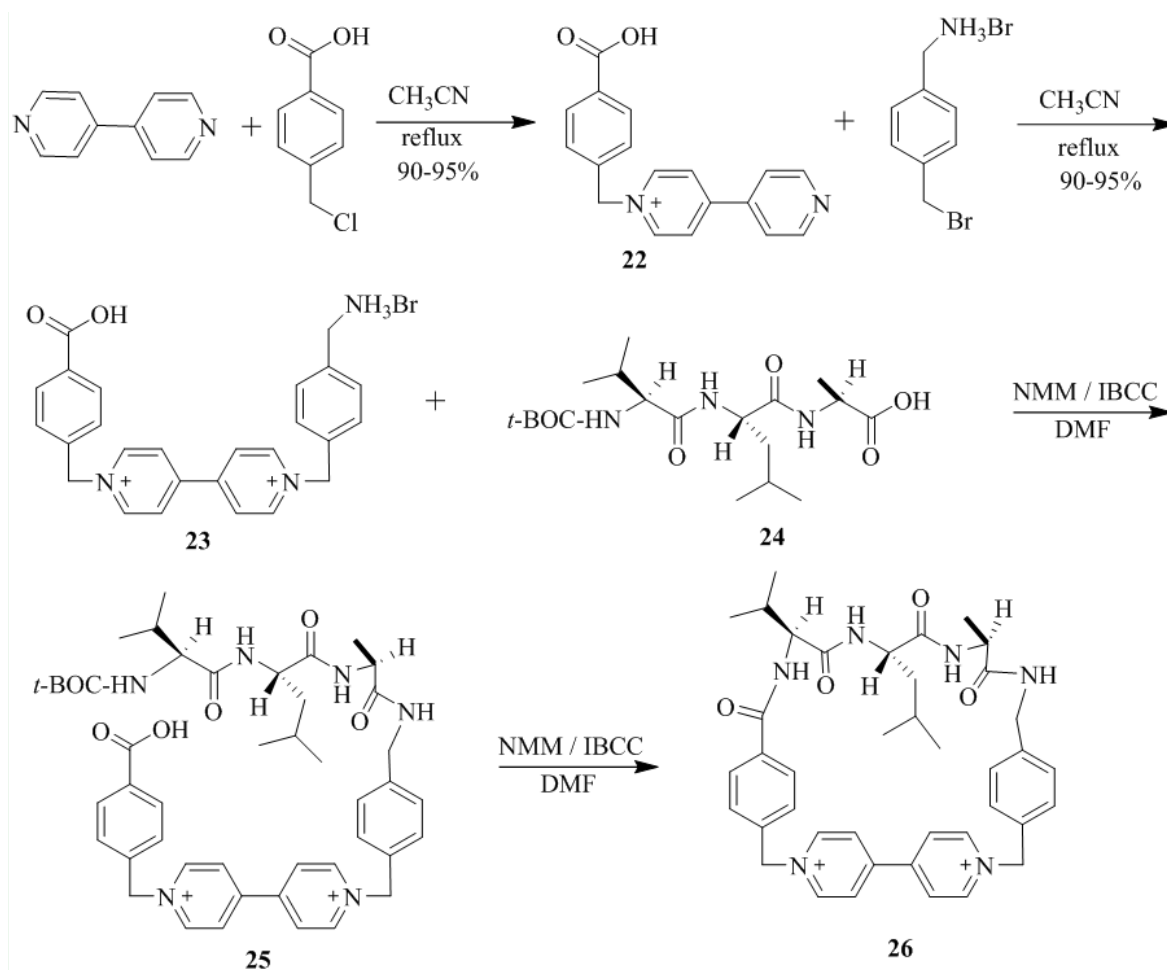
**Figure 4.** Pyridine-18-crown-6 (**17**, **18**) type ligands host for enantioselective recognition of aryl alkyl ammonium salts **19–21**.

Hua et al. [30] reported the synthesis of five pyridine-based macrocyclic receptors, **29a–e** (Schemes 4 and 5) by simple acylation of the chiral diamine dihydrobromide intermediates, **28a–c** with 2,6-pyridinedicarbonyl dichloride in a highly diluted solution. However, the acylation of chiral diamine dihydrobromides, **28a–b** with 2,6-pyridinedicarbonyl dichloride simultaneously afforded the [1 + 1] cyclization products, **29a–b** and [2 + 2] cyclization products **29c–d**. More importantly, under similar reaction condition, the acylation reaction of **28c** and 2,6-pyridinedicarbonyl dichloride, afforded the only [1 + 1] product **29e**, while the [2 + 2] product was not formed. The enantioselective interaction of synthesized chiral macrocyclic receptors, **29a–e** with D- and L-amino acid methyl ester hydrochlorides was evaluated by using fluorescence spectroscopy and the difference of fluorescence intensity confirmed significant chiral molecular recognition (Table 3).

As seen in Table 3, macrocycles, **29c,e** exhibit the better enantiomeric recognition for D- and L-Ala methyl ester hydrochlorides as compared to other chiral macrocycles, **29a,b,d**. Chiral macrocycles, **29a,c,e** all show excellent chiral discrimination for Phe methyl ester hydrochloride, whereas **29b,d** do not. In the case of D- and L-His methyl ester dihydrochloride, only **29b** displayed recognition.

Suh et al. [53] synthesized new pyridine-based chiral crown ether, **34** (Scheme 6) as follows. Diol, **30** obtained from the known five step methodology, was coupled with diiodide, **37** prepared from chelidamic acid (**35**) to furnish **32**. The reduction of cyano group of **32**, followed by the treatment

with ethyl isocyanate provided the required chiral host, **34**. The authors also synthesized chiral bis-pyridino-18-crown-6, **31** with the diphenyl substituent by similar methodology in order to compare it with the chiral host, **34**. These hosts exhibited chiral molecular recognition for the enantiomers of methyl ester hydrochlorides of Leu, Gly(Ph), and Phe, which was determined by enantiomer labeled (EL) guest method using fast atom bombardment mass spectrometry (FAB-MS). For host, **34** the IRIS values obtained are in the range of 1.12 to 1.44 indicating that the (*R*)-enantiomer of amino acids showed binding preference over the (*S*)-enantiomer. However, for the host, **31** the IRIS values for chiral recognition were found to be lower than for the chiral host, **34**.



**Scheme 3.** Synthetic of (*S*)-valine-leucine-alanine cyclophane, **26**.

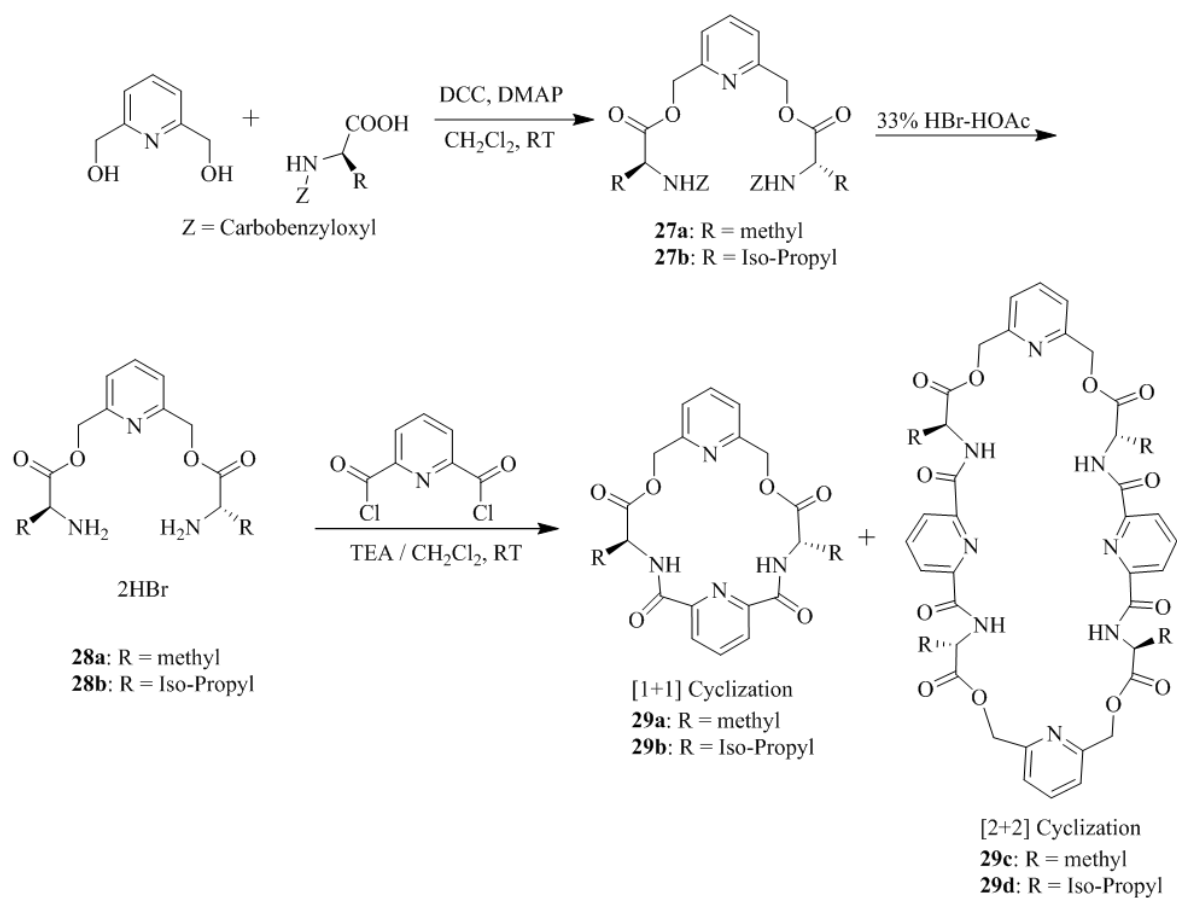
**Table 2.** Results of NMR titrations using the dibromide salt of **26**. Association constants ( $K_a$ ) represent the average of two or more proton chemical shifts.

Guest	$K_a$ ( $M^{-1}$ )	Solvent System	Structure
( <i>R</i> )-DOPA ( <i>S</i> )-DOPA	$39 \pm 6$ $3 \pm 1$	$17D_2O:1acetone-d_6:1DCI$	
( <i>R</i> )-Tryptophan ( <i>S</i> )-Tryptophan	$5 \pm 1$ $6 \pm 1$	$17D_2O:1acetone-d_6:1DCI$	

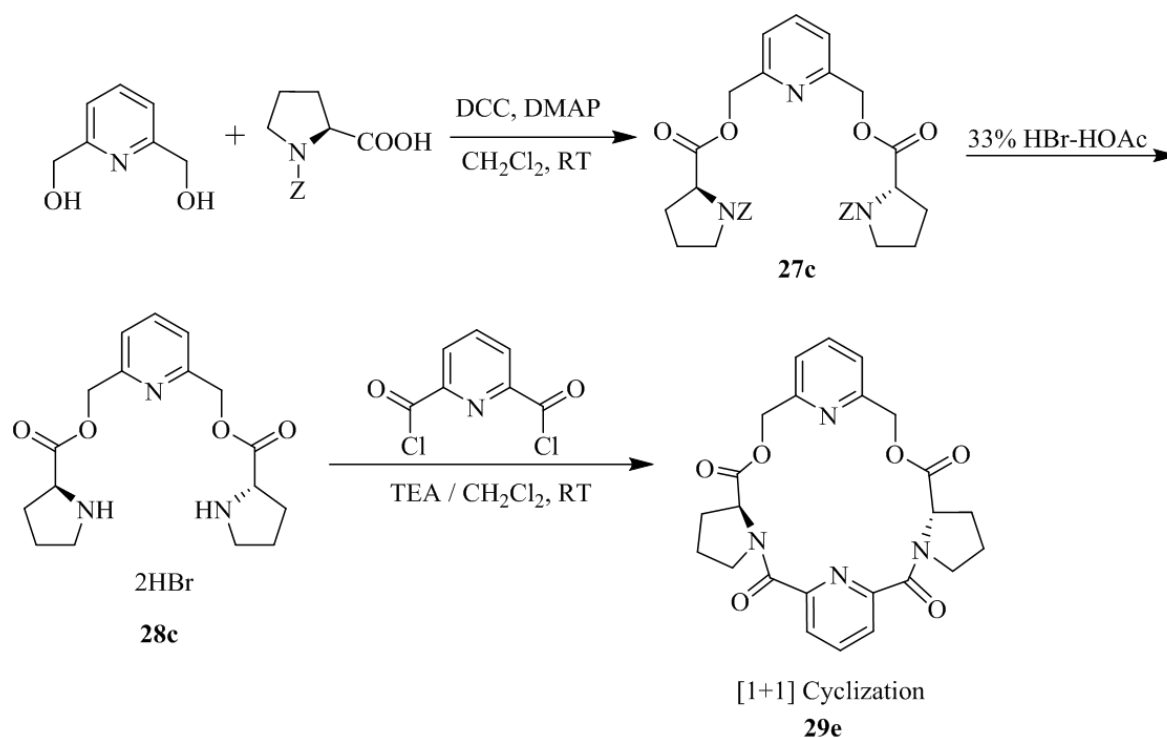


Table 2. Cont.

Guest	$K_a$ ( $M^{-1}$ )	Solvent System	Structure
Pindalol	$6 \pm 1$	$17D_2O:1acetone-d_6:1DCI$	
Nandolol	$23 \pm 3$	$10acetone-d_6:3D_2O$	
(R)-(-)-α-Methoxy Phenylacetic acid (S)-(+)-α-Methoxy Phenylacetic acid	$5 \pm 1$ $8 \pm 6$	$1acetone-d_6:1D_2O$	
N-(2-naphthyl)alaninate	$10 \pm 1$	$9acetone-d_6:4D_2O$	
(S)-6-methoxy-α-methyl-2-naphthalene acetic acid	$9 \pm 1$	$29D_2O:11acetone-d_6:1MeOD$	



Scheme 4. Preparation of chiral macrocycles 29a–d.



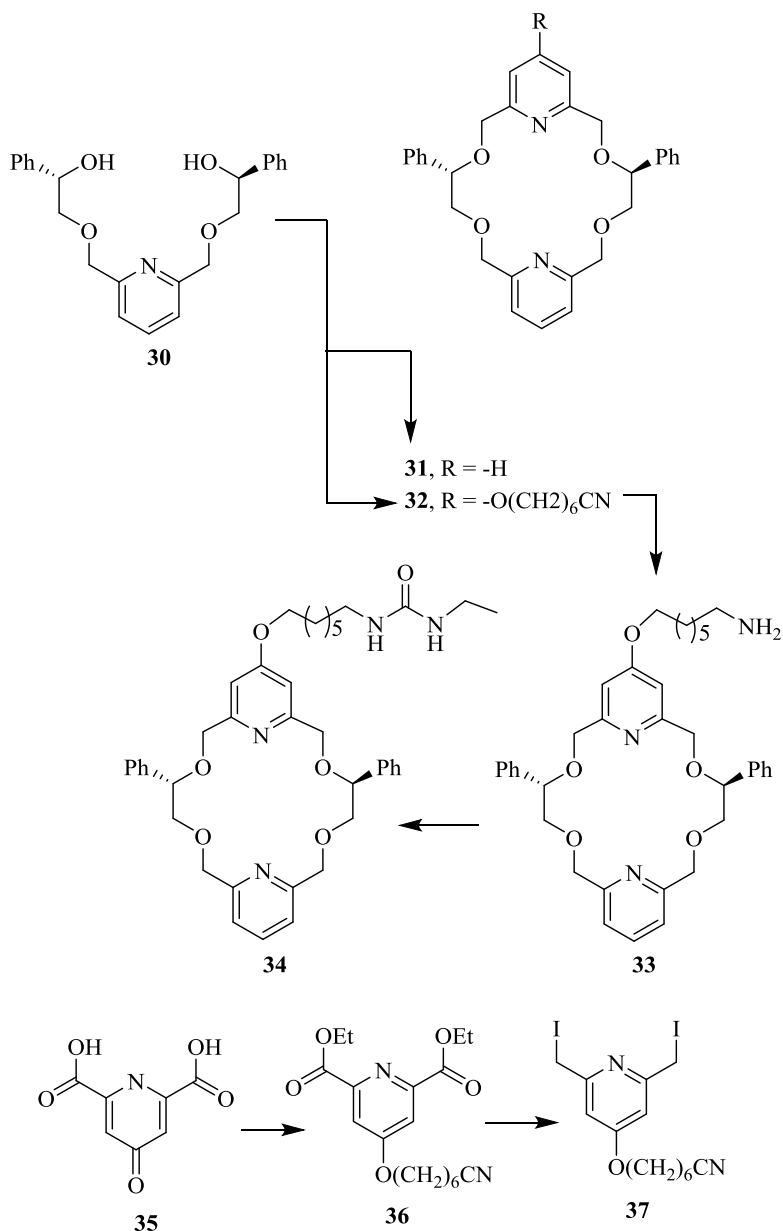
Scheme 5. Preparation of Chiral Macrocycle 29e.

**Table 3.** Chiral recognition data determined by fluorescence spectra for the interactions of pyridine-containing chiral ligands with enantiomers of amino acid methyl ester hydrochlorides.

Ligand	Amino Acid Methyl Ester Hydrochlorides, Cation	$\lambda_{\max}$ (nm)	$\Delta\lambda$ (nm)	I/I <sub>0</sub> (Rel. Intensity)
<b>29a</b>	D-Ala	350	8	0.68
	L-Ala	342		
	D-Phe	350	50	0.84
	L-Phe	400		
	D-His	350	0	0.67
	L-His	350		
<b>29b</b>	D-Ala	392	12	1.08
	L-Ala	362		
	D-Phe	374	10	1.32
	L-Phe	360		
	D-His	350	38	0.91
	L-His	400		
<b>29c</b>	D-Ala	348	52	0.37
	L-Ala	400		
	D-Phe	348	48	0.85
	L-Phe	352		
	D-His	400	1	1.50
	L-His	352		
<b>29d</b>	D-Ala	351		0.72
	L-Ala	392		
	D-Phe	354	12	1.19
	L-Phe	366		
	D-His	380	14	0.96
	L-His	366		
		350	16	1.01
		364		
				1.19
				1.96
				0.82

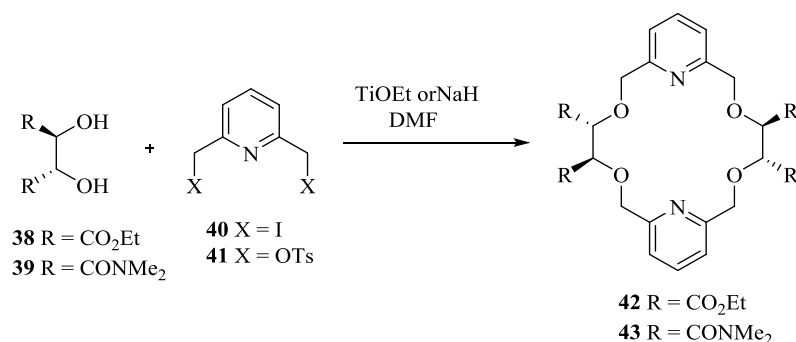
Table 3. Cont.

Ligand	Amino Acid Methyl Ester Hydrochlorides, Cation	$\lambda_{\max}$ (nm)	$\Delta\lambda$ (nm)	I/I <sub>0</sub> (Rel. Intensity)
29e		350		
	D-Ala	400	50	0.78
	L-Ala	450		4.69
	D-Phe	350	50	0.84
	L-Phe	400		1.25
	D-His	348	8	1.05
	L-His	340		0.99



Scheme 6. Synthesis of chiral macrocycles, 31 and 34.

The same group [23] has prepared *C*<sub>2</sub>-symmetric chiral bis-pyridino-18-crown-6, (*R,R,R,R*)-**42** and **43** (Scheme 7) with tetraethyl tetracarboxylate and tetramethyl tetracarboxamide groups as chiral barriers in 2008. The synthesis was carried out by a simple alkylation of diethyl-*L*-tartarate (**38**) or *N,N,N',N'*-tetramethyl tartaramide (**38**) with 2,6-bis(iodomethyl)pyridine (**40**).



**Scheme 7.** Synthetic routes for chiral bis-pyridino-18-crown-6 ethers **42** and **43**.

In this case, the authors used electrospray ionization mass spectrometry (ESI-MS) as a detection tool to evaluate the enantiomeric recognition of amino acid methyl ester hydrochlorides, **44–53** (Figure 5) by macrocycles, (*R,R,R,R*)-**42** and **43**. The *IRIS* values obtained by ESI-MS (Table 4) for the (*R,R,R,R*)-**42** with the chiral amino acid methyl ester hydrochlorides guest in the range from 1.30 to 7.66, revealed more stable complexes with the (*R*)-enantiomer preference. However, *IRIS* values for chiral recognition of (*R,R,R,R*)-**43** found in the range of 0.22 to 2.31 demonstrated the inconsistent preference in comparison with (*R,R,R,R*)-**42**.

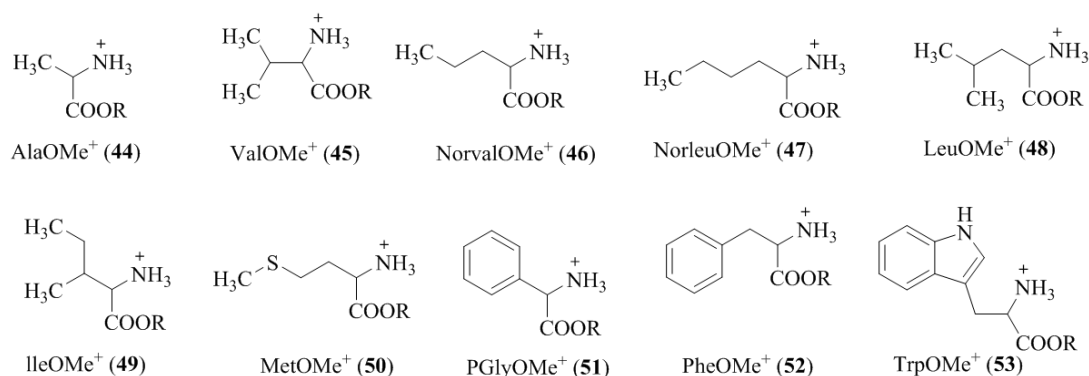


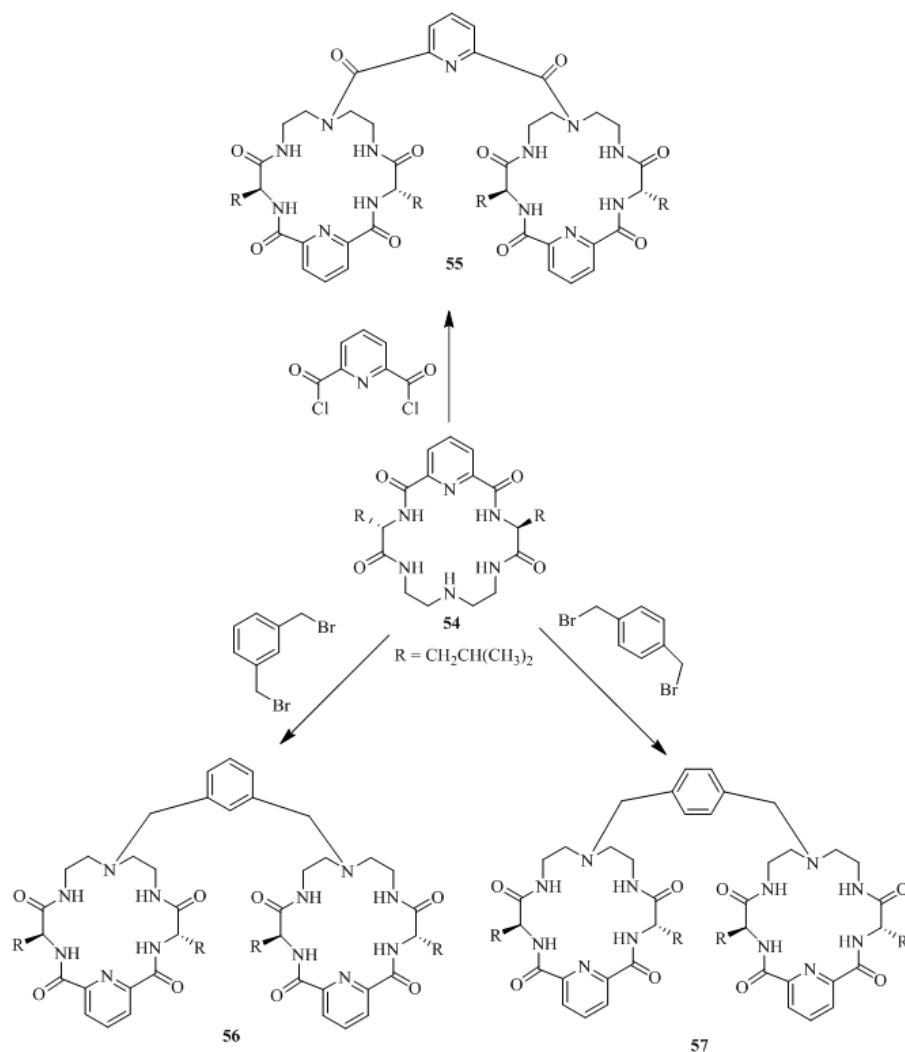
**Figure 5.** The chemical structures of amino acid methyl ester hydrochlorides (CH<sub>3</sub> and CD<sub>3</sub> esters) (**44–53**) used for the chiral recognition.

**Table 4.** *IRIS* Values using the ESI-MS guest method.

Host/Guest	44	45	46	47	48	49	50	51	52	53
<b>42</b>	7.66	1.65	3.41	2.36	5.59	1.30	1.94	4.17	1.80	3.44
<b>43</b>	0.22	0.82	2.27	0.52	1.06	2.31	0.81	0.52	1.68	2.23

Xie et al. [66] developed the first examples of bis-macrocyclic oxo-polyamine type molecular tweezers as the corresponding chiral recognition hosts (Scheme 8). The tweezers, **55–57** were prepared through a simple condensation of pyridine ring containing macrocyclic polyamide **54** with 2,6-bis(chlorocarbonyl)pyridine,  $\alpha$ ,  $\alpha'$ -dibromo-*m*-xylene and  $\alpha$ ,  $\alpha'$ -dibromo-*p*-xylene respectively.

These tweezer-like receptors, **54–57** showed significant chiral molecular recognition for amino acid esters as determined by using the differential UV spectrometry. The association constants, free energy changes and enantioselectivities,  $K_L/K_D$  are shown in Table 5. It was revealed that the extent of enantioselective recognition for the amino acid derivatives depends on diverse parameters such as the tweezers' shape, steric effects, structural rigidity, hydrogen bond, and  $\pi$ - $\pi$  stacking between the aromatic groups.



**Scheme 8.** Synthesis of bis-macrocytic oxo-polyamine type molecular tweezers (55–57).

**Table 5.** Binding constants ( $K_a$ ), the Gibbs free energy changes ( $-\Delta G_0$ ), enantioselectivities  $K_L/K_D$  and  $\Delta\Delta G_0$  calculated from  $-\Delta G_0$  for the complexation of L/D-amino acid esters with the chiral receptors 54–57 in  $\text{CHCl}_3$  at 25 °C <sup>a</sup>.

Entry	Host	Guest <sup>b</sup>	$K_a$ ( $\text{dm}^3 \text{mol}^{-1}$ )	$K_L/K_D$	$-\Delta G_0$ ( $\text{kJ mol}^{-1}$ )	$\Delta\Delta G_0$ ( $\text{kJ mol}^{-1}$ ) <sup>c</sup>
1	54	L-Phe-OMe	46.3	0.75	9.50	0.73
2	54	D-Phe-OMe	62.0		10.23	
3	54	L-Trp-OMe	58.0	0.67	10.06	0.98
4	54	D-Trp-OMe	86.1		11.04	
5	55	L-Ala-OMe	74.1	1.21	10.67	−0.48
6	55	D-Ala-OMe	61.2		10.19	
7	55	L-Leu-OMe	68.0	2.70	10.45	−2.46
8	55	D-Leu-OMe	25.2		7.99	
9	55	L-Phe-OMe	213	3.92	13.28	−3.38
10	55	D-Phe-OMe	54.4		9.90	
11	55	L-Trp-OMe	1280	7.90	17.72	−5.12
12	55	D-Trp-OMe	162		12.60	
13	56	L-Leu-OMe	59.9	2.0	10.14	−1.71
14	56	D-Leu-OMe	30.0		8.43	
15	57	L-Leu-OMe	36.8	1.33	8.93	−0.72
16	57	D-Leu-OMe	27.7		8.23	

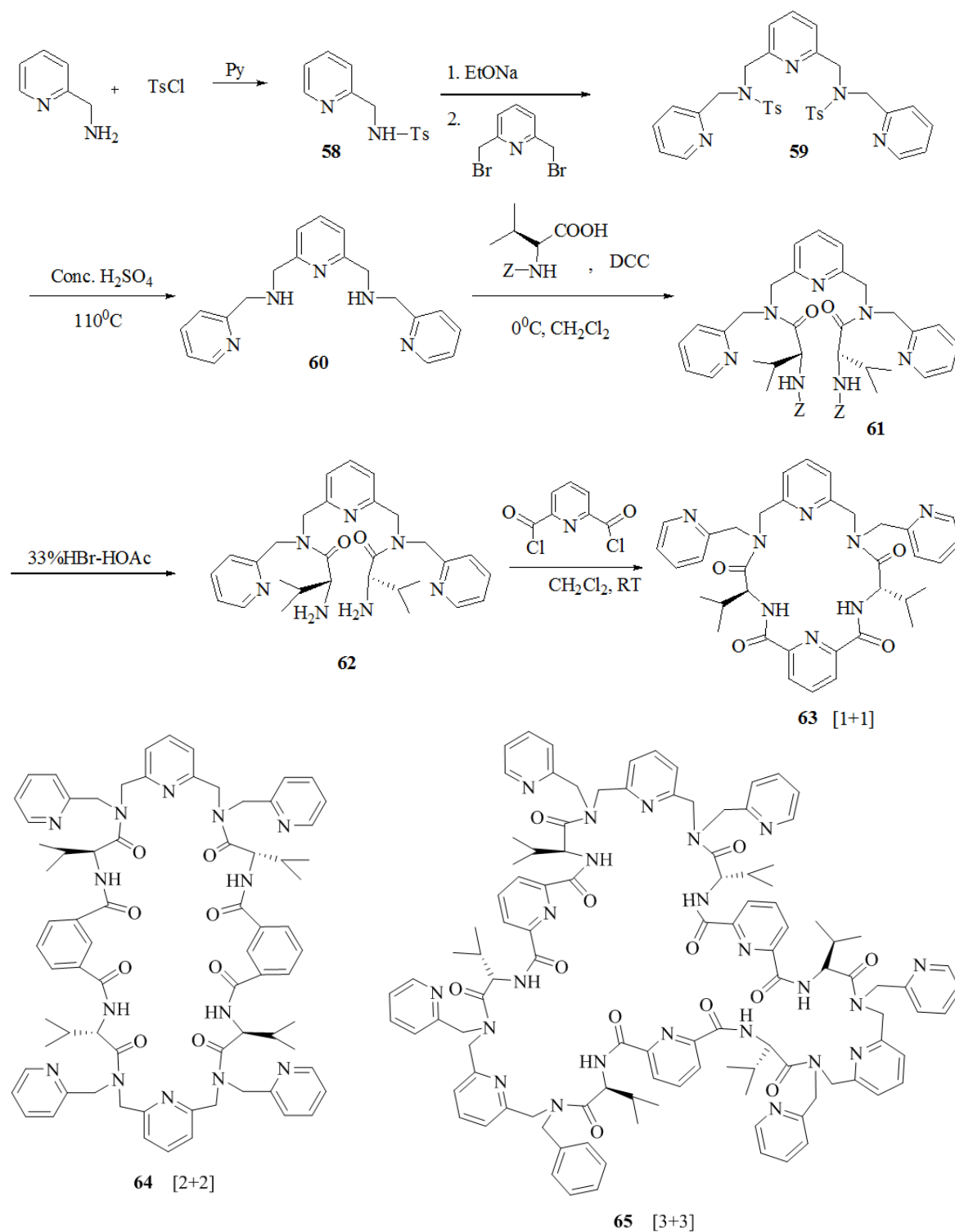
<sup>a</sup> The concentration of the receptors:  $2.0 \times 10^{-4} \text{ mol dm}^{-3}$ . <sup>b</sup> Ala-OMe: alanine methyl ester; Leu-OMe: leucine methyl ester; Phe-OMe: phenylalanine methyl ester; Trp-OMe: tryptophane methyl ester. <sup>c</sup>  $\Delta\Delta G_0 = \Delta G_0 - \Delta G_0$ .

Hua et al. [67] prepared seven  $C_2$ -symmetrical pyridyl unit containing macrocycles. The tosylamine, **58** was reacted with 2,6-bis(bromomethyl)pyridine to afford compound, **59**. Further detosylation gave 2,6-bis(*N*-picolylaminomethyl)-pyridine, **60** followed by condensation with *Z*-protected Val to furnish **61**, while subsequent deprotection yielded **62**. Finally, all three chiral macrocycles, **63**, **64** and **65** were synthesized by acylation of the chiral diamine dihydrobromide intermediate, **62** with 2,6-pyridinedicarbonyl dichloride at high dilution (Scheme 9). These macrocycles, **63**, **64** and **65** were obtained by the [1 + 1], [2 + 2] and [3 + 3] cyclization in 15.6%, 5.1% and 3.7% yields, respectively. By following a similar methodology, the macrocycles, **66**, **67**, **68** and **69** (Figure 6) were synthesized from the respective acids. Macrocycle, **63** was investigated for the chiral molecular recognition of amino acid derivatives by using several spectroscopic techniques such as IR, FAB-MS, fluorescence and UV-vis. Macrocycle **63** showed significant enantiomeric discrimination by IR spectroscopy, wherein the IR frequency shift values of D-amino acid methyl esterhydrochlorides were greater than that of L-isomers. Furthermore, the FAB-MS data showed host-guest 1 + 1 molecular ion peaks for macrocycles **63** and **69** with benzene ring containing amino acid methyl ester hydrochlorides owing to  $\pi$ - $\pi$  interactions with pyridine ring of the macrocycles showed excellent enantioselective binding. The fluorescence data demonstrated that the when macrocycles **63** and **66** mixed with guest amino acids, Ala-OMe and Ph-OMe, the fluorescence intensity increases. However, in the case of macrocycles **67** and **69** fluorescence intensity decreases probably because nitrogen in the pyridine ring as a binding site interacts with proton by static force.

Sakai et al. [68] designed and synthesized a series of the pyridine incorporated chiral bifunctional macrocyclic hosts, **70–74** (Figure 7) using two 2,6-diacylaminopyridine as binding units, chiral BINOL to provide an anisotropic ring-current effect, and amides giving rise to a V-shaped arrangement in **70–72**, while a parallel alignment in **73**. Out of the five chiral receptors, **70** was evaluated for the chiral discrimination ability using  $^1\text{H}$  or  $^{19}\text{F}$  NMR and was found to be an excellent versatile chiral solvating agent for a wide range of the chiral compounds (Figure 8) having the following functionalities: carboxylic acid, oxazolidinone, lactone, alcohol, sulfoxide, sulfoximine, isocyanate, or epoxide. In particular, **70**, having the  $\text{NO}_2$  group, influenced the binding capacity as well as the degree of enantioselectivity and further host exhibited special characteristic features such as versatility, signal sharpness, high splitting ability, high sensitivity, wide detection window, and easy synthetic accessibility.

Wilhelm et al. [69] synthesized a series of the (–)-nicotine-based chiral ionic liquid as follows. (Schemes 10–12). (–)-Nicotine, **75** was treated with one equivalent of methyl iodide to furnish **79**, (Scheme 10) subsequently the anion metathesis was carried out and iodide was replaced by  $\text{PF}_6$ ,  $\text{BF}_4$ , and  $\text{NTf}_2$ , respectively to obtain the chiral ionic liquids (Scheme 11). In order to produce the desired salt, **78**, **75** was reacted with ethyl bromide, however, the product, **83a** was isolated instead of **78**. As **83b** was not suitable, a different anion was then converted to *N*-ethyl nicotinium bromide **83a**, which upon the anion metathesis resulted in the chiral ionic liquids, **83b–d** (Scheme 12). The newly developed enantiopure ionic liquids were evaluated as chiral solvating agents using  $^{19}\text{F}$  NMR spectroscopy. In the case of **79b** the best result was observed with Mosher's acid in the  $^{19}\text{F}$  NMR and with mandelic acid in the  $^1\text{H}$  NMR (Table 6, entry 3).





Scheme 9. Preparation of macrocycles 63–65.

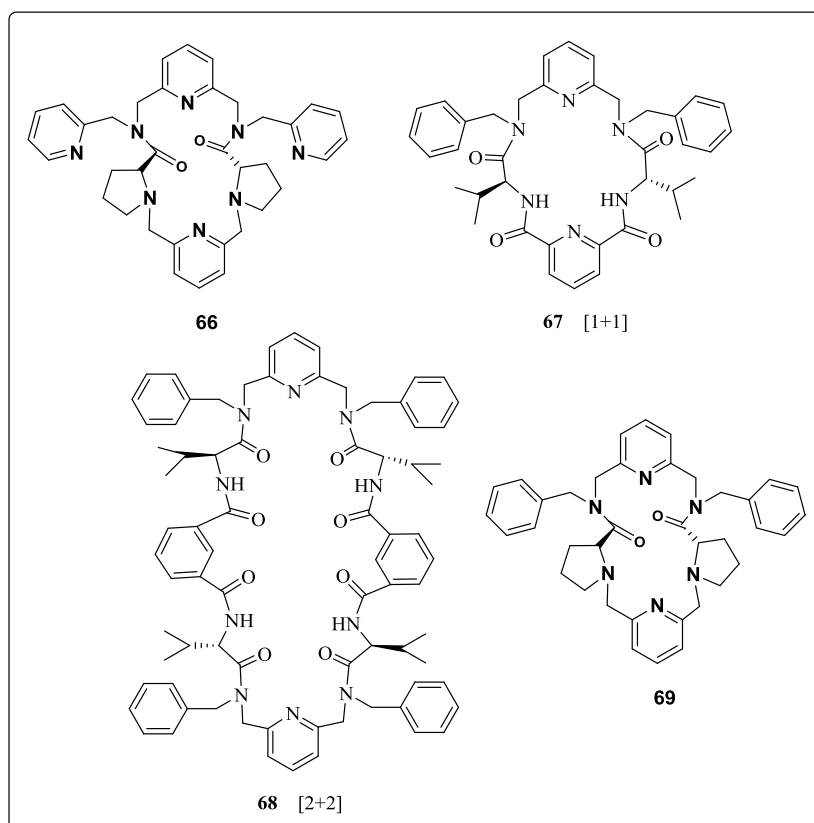


Figure 6. Macrocycle 66–69.

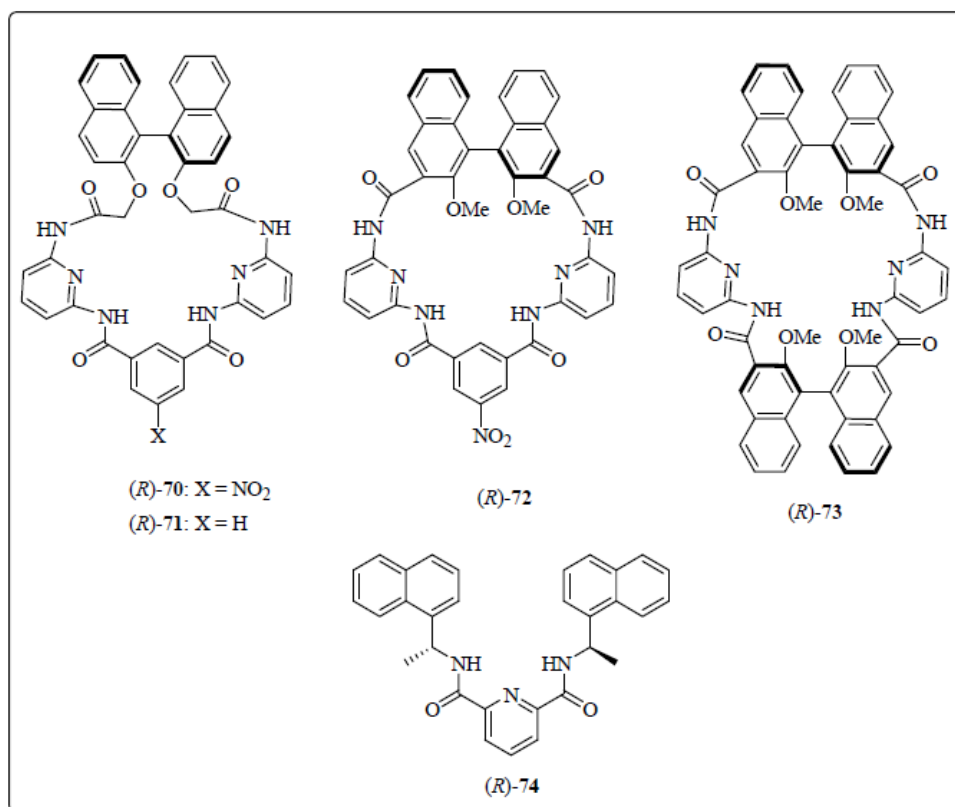


Figure 7. Chiral solvating agents, 70–74.

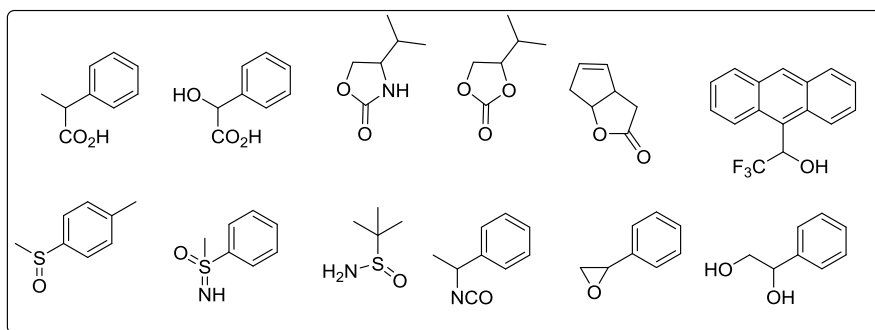
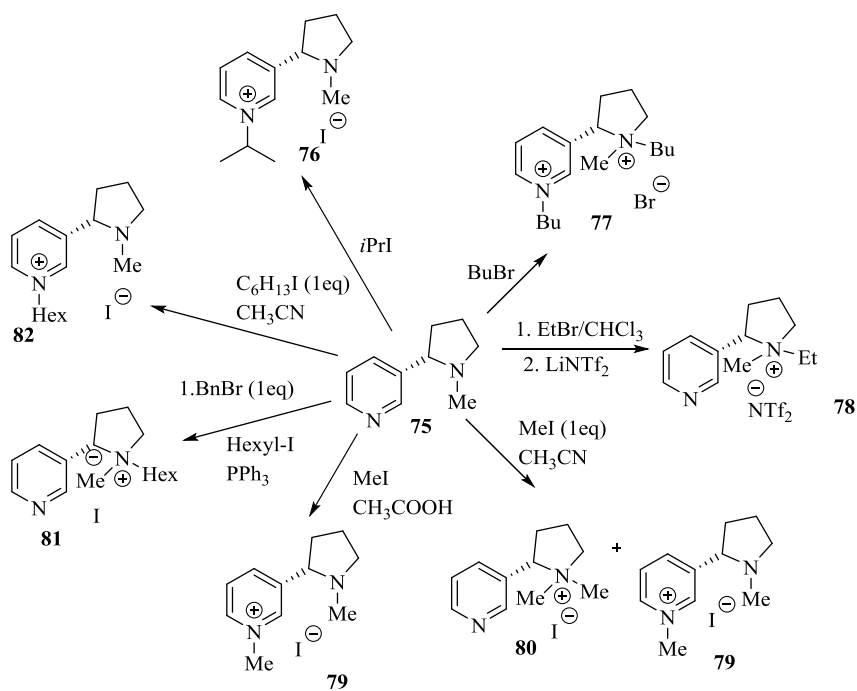
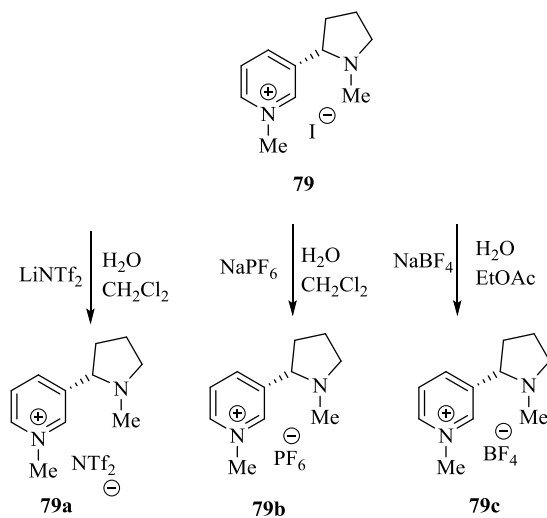


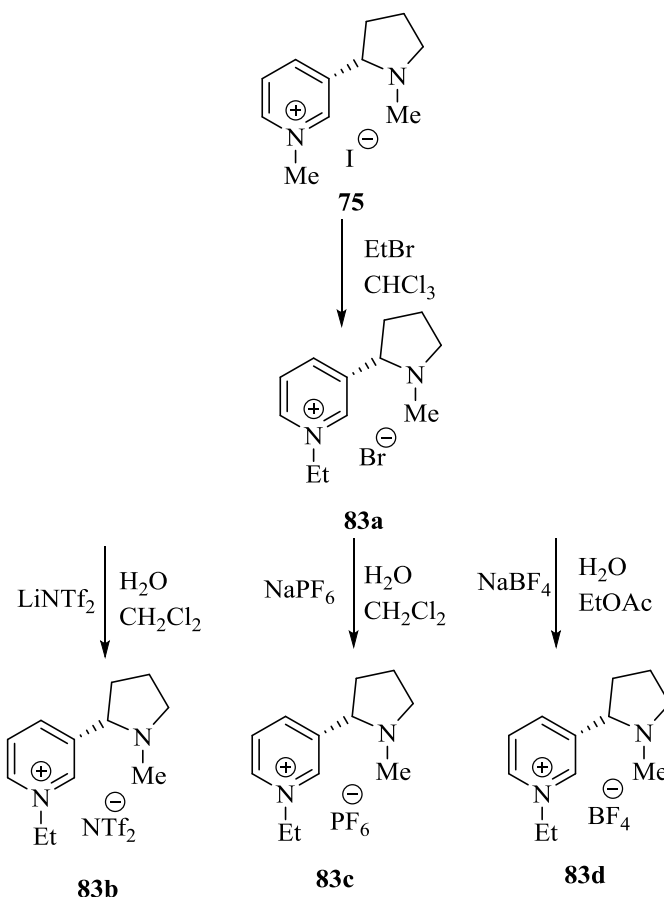
Figure 8. Chiral guests used for chiral recognition by (R)-70.



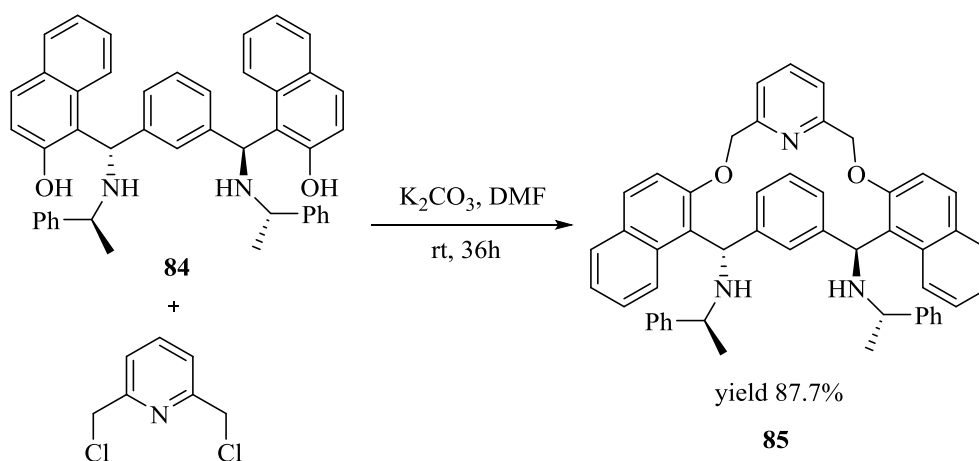
Scheme 10. Synthesis of Ionic liquid 76–82.



Scheme 11. Synthesis of Ionic liquid 79a–c.

Scheme 12. Synthesis of Ionic liquid **83b**–**d**.

Zhang et al. [70] developed a chiral shift reagent, macrocyclic compound, **85** (Scheme 13) by the simple alkylation of  $C_2$ -symmetric aminonaphthol, **84** with pyridyl chloride in a high yield. Enantiomeric acids gave large nonequivalent chemical shifts (upto 0.80 ppm) in the presence of **85** in  $^1\text{H}$  NMR (500 MHz) spectra. The quantitative analysis of mandelic acid with a different enantiomeric purity showed that the host, **85** is an excellent chemical shift reagent for chiral carboxylic acids. Indeed, **85** exhibited an excellent ability to discriminate (Table 7) the enantiomers of a broad variety of carboxylic acids (Figure 9) by  $^1\text{H}$  NMR spectroscopy.

Scheme 13. Synthesis of **85**.

**Table 6.**  $^{19}\text{F}$  NMR chemical shifts ( $\delta$ ) of Mosher's acid or mandelic acid in ppm and resolution of  $\Delta\delta$  values in Hz (282 MHz  $^{19}\text{F}$  NMR), (500 MHz  $^1\text{H}$  NMR).

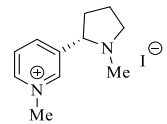
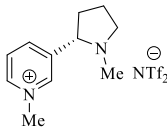
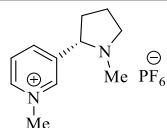
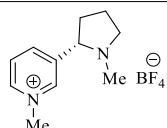
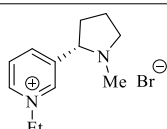
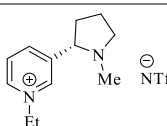
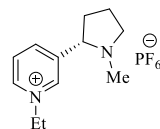
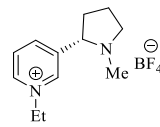
Entry	Salts	CDCl <sub>3</sub>						CD <sub>3</sub> OD			
		<sup>19</sup> Fδ Mosher's Acid	Δδ	<sup>1</sup> H δ Mosher's Acid	Δ δ	<sup>1</sup> H δ Mandelic Acid	Δ δ	<sup>19</sup> Fδ Mosher's Acid	Δ δ	<sup>1</sup> HδMosher's Acid	Δ δ
1	-	-71.0	-	3.56q	-	5.25	-	-73.17	-	3.57q	-
2		-70.61/-70.63	5.9	3.51/3.50	7.5	4.99/5.01	5.7	-	-	-	-
3		-70.86/-70.89	9.0	3.44/3.40	20.0	4.96/4.98	10.0	-71.26/-71.29	9.1	3.55q/3.56q	4.0
4		-71.09	0	3.54/3.53	6.5	5.19	0	-71.11/-71.13	6.6	3.56q/3.57q	5.0
5		-70.90/-70.92	7.2	3.49/3.47	10.0	4.95/4.96	5.4	-71.20	0	3.56q	0
6		-71.02/-71.04	5.0	3.47/3.46	5.5	5.01/5.03	6.8	-71.18	0	3.57q	0
7		-69.90/-70.57	7.5	3.45/3.42	17.0	5.20	0	-71.64/-71.65	4.3	3.55q/3.56q	2.0

Table 6. Cont.

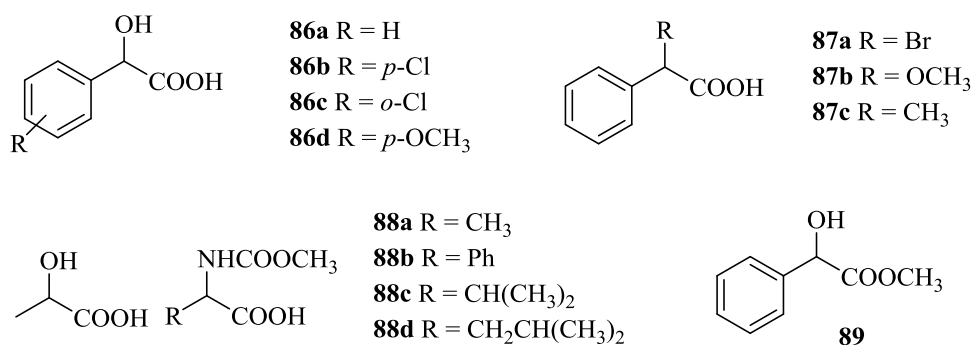
Entry	Salts	CDCl <sub>3</sub>				CD <sub>3</sub> OD					
		<sup>19</sup> Fδ Mosher's Acid	Δ δ	<sup>1</sup> H δ Mosher's Acid	Δ δ	<sup>1</sup> H δ Mandelic Acid	Δ δ	<sup>19</sup> Fδ Mosher's Acid	Δ δ	<sup>1</sup> HδMosher's Acid	Δ δ
8		−70.67/−70.68	4.5	3.54/3.53	4.5	4.99/5.00	5.0	−70.85/−70.88	8.1	3.58q/3.57q	4.5
9		−71.10	0	3.50/3.48	8.0	5.24/5.26	7.8	−71.69/−71.70	5.5	3.57q/3.56q	3.0

0.5 equiv. of Mosher's acid and mandelic acid with different salts in CDCl<sub>3</sub> and Mosher's acid with different salts in deuterated methanol.

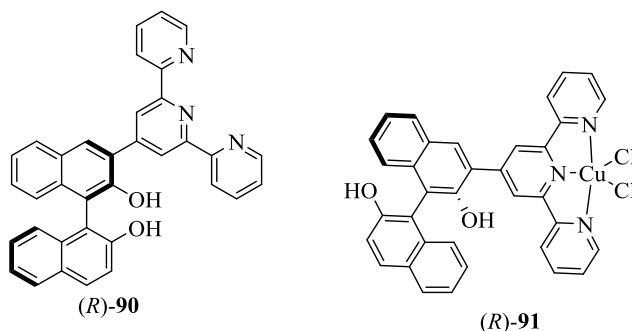


**Table 7.** Measurements of  $^1\text{H}$  Chemical Shift Inequivalencies  $\Delta\Delta\delta$  of **86a** and **88b** in the presence of **85** by  $^1\text{H}$  NMR Spectroscopy (500 MHz) in different solvents at 25 °C.

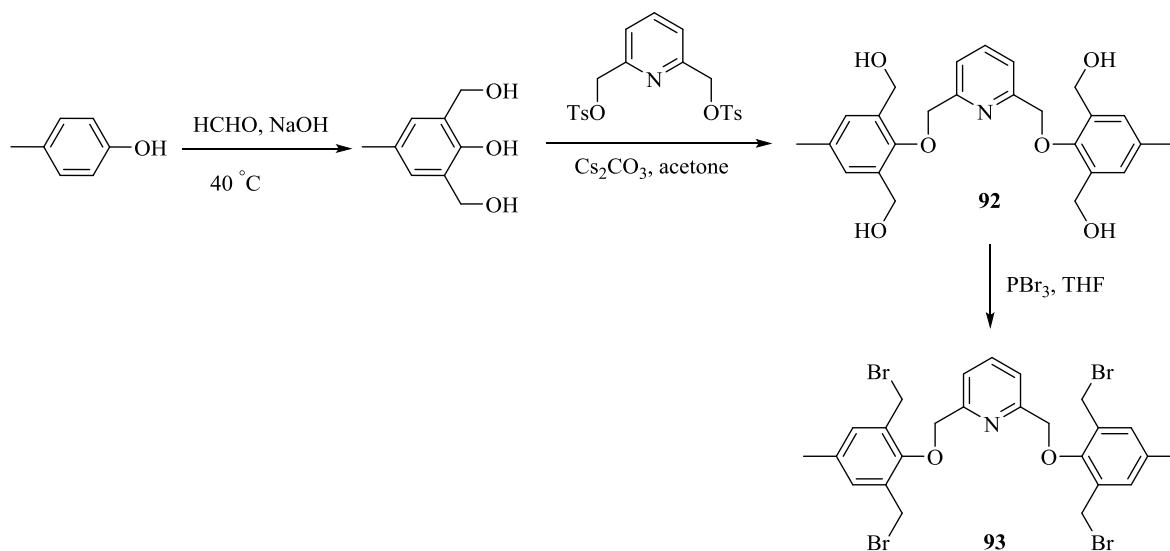
Entry	Solvent	$\Delta\Delta\delta$ (ppm)	
		4	13
1	$\text{CDCl}_3$	0.62	0.39
2	$\text{CDCl}_3/\text{C}_6\text{D}_6$ (10%)	0.62	0.39
3	$\text{CDCl}_3/\text{Acetone-}d_6$ (10%)	0.53	0.27
4	$\text{CDCl}_3/\text{CD}_3\text{OD}$ (10%)	0.43	0.21
5	$\text{CDCl}_3/\text{DMSO-}d_6$ (10%)	0.13	0.04

**Figure 9.** Structures of the guests studied.

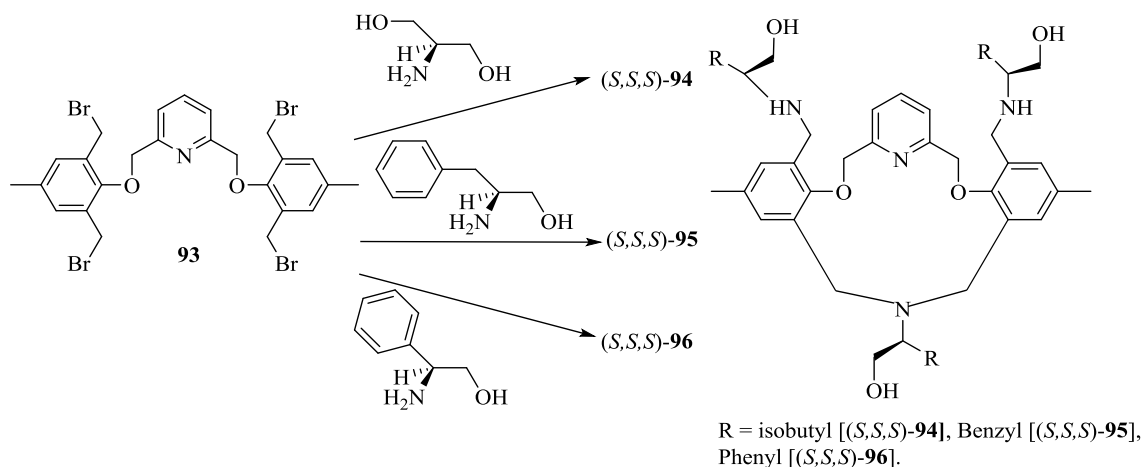
Pu et al. [71] reported the first example of enantioselective gel collapsing as a new means of the visual chiral sensing (Figure 10). The BINOL-terpyridine-Cu(II) complex, (*R*)-**91** was obtained as a green solid by reaction between the terpyridine conjugate, (*R*)-**90** and  $\text{CuCl}_2 \cdot 2\text{H}_2\text{O}$ . The enantioselective sensing of gel, (*R*)-**91** was studied upon interaction with chiral amino alcohols. It was observed that (*R*)-**91** in chloroform when mixed with (*R*)-phenylglycinol remained stable, whereas when mixed with (*S*)-phenylglycinol collapsed. This confirmed the enantioselective nature of gel towards chiral amino alcohols. This result was compared to the fluorescence response of (*R*)-**91** towards (*R*)- and (*S*)-phenyl glycinol in solution. Intriguingly, enhancement in the fluorescence intensity was observed when (*R*)-**91** was treated with an excess of (*S*)-phenylglycinol. In contrast, weaker fluorescence was observed in the case of (*R*)-phenylglycinol. This difference is due to displacement of the Cu(II) ion in (*R*)-**91** by the chiral amino alcohol, which is enantioselective. Indeed, the reaction of (*R*)-**91** with (*S*)-phenylglycinol is more favorable than that with (*R*)-phenylglycinol. Moreover, other chiral amino alcohols including prolinol, valinol, phenylalaninol, leucinol, and 1-amino-2-propanol also exhibited significant fluorescent enhancement in the presence of (*R*)-**91**.

**Figure 10.** First example of enantioselective gel, **91** and its precursor, **90**.

Togrul et al. [27] synthesized a series of pyridine-macrocycles bearing amino alcohol subunits. A tetra-bromide building block, **93** was prepared for the macrocycle synthesis (Scheme 14) starting from 4-methylphenol, which was converted to 2,5-dihydroxymethyl-4-methylphenol followed by the reaction with pyridine ditosylate to give **92** and final bromination using  $\text{PBr}_3$ . The chiral macrocycles, (*S,S,S*)-**94**, (*S,S,S*)-**95** and (*S,S,S*)-**96** (Scheme 15) were obtained by the treatment of **93** with respective amino alcohols and their enantiomeric recognition properties towards alkyl ammonium salts were investigated by UV-vis spectroscopy (Figure 11). The association constants are summarized in Table 8, demonstrated that the complex host bearing phenyl, (*S,S,S*)-**94** and isobutyl, (*S,S,S*)-**94** are more stable with an (*S*)-configuration of the enantiomer of guests of both **98** and **97**; over the (*R*)-configuration because the phenyl and cyclohexyl groups in the (*S*)-enantiomers are placed opposite to the isobutyl and phenyl side chains in the cavity of the host, whereas in opposite enantiomers, these groups are located in the same face, causing unfavorable steric interactions.



Scheme 14. Synthesis of compound, **93**.



Scheme 15. Synthesis of compound, **94**.

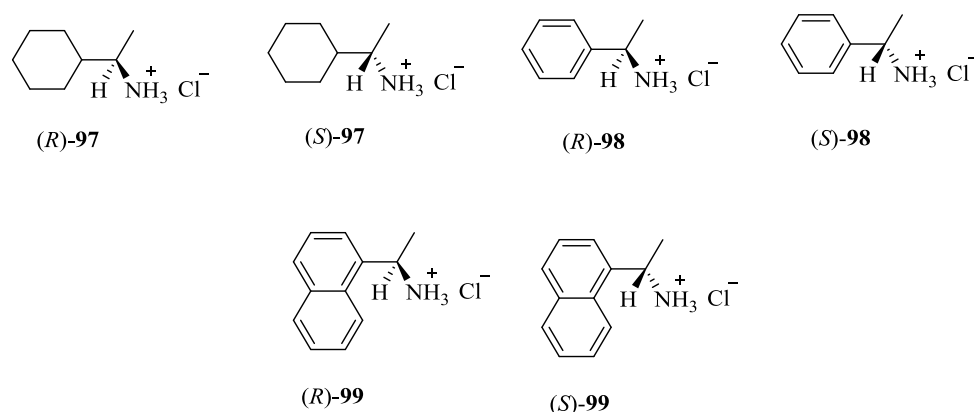
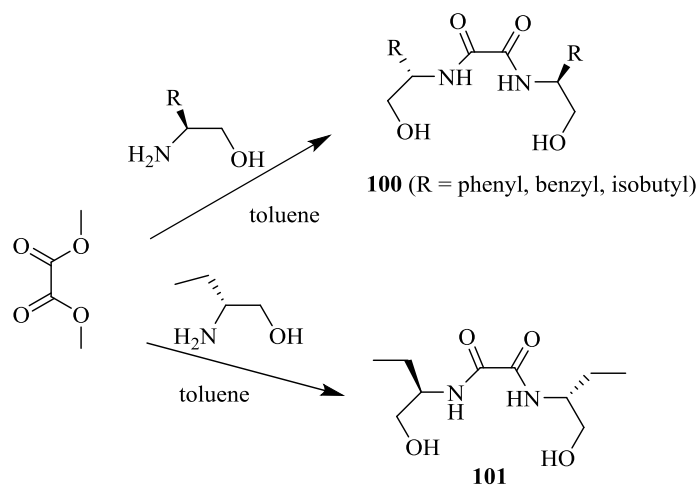


**Figure 11.** Ammonium hydrochloride salts used as guests.

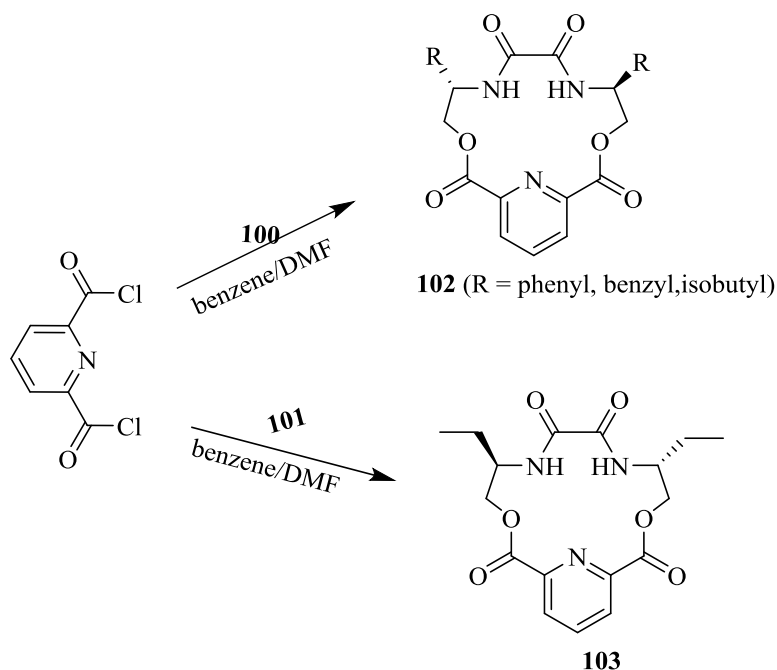
**Table 8.** Binding constant ( $K_a$ ), the Gibbs free energy changes ( $-\Delta G_0$ ), enantioselectivities  $K_S/K_R$  or  $\Delta\Delta G_0$  for including the *R/S* guest with the chiral host macrocycles in  $\text{CHCl}_3$  at 25 °C.

Host	Guest	$K_a$ ( $\text{M}^{-1}$ )	$K_S/K_R$	$-\Delta G_0$ ( $\text{kJ mol}^{-1}$ )	$\Delta\Delta G_0$ ( $\text{kJ mol}^{-1}$ )
<i>(S,S,S)</i> -94	<i>(R)</i> -98	$(2.0 \pm 0.23) \times 10^4$	2.0	24.62	1.63
	<i>(S)</i> -98	$(4.0 \pm 0.34) \times 10^4$		26.25	
	<i>(R)</i> -97	$(1.0 \pm 0.42) \times 10^4$	5.0	22.82	3.99
	<i>(S)</i> -97	$(5.0 \pm 0.36) \times 10^4$		26.81	
<i>(S,S,S)</i> -95	<i>(R)</i> -98	$(2.0 \pm 0.31) \times 10^5$	0.9	30.24	−0.26
	<i>(S)</i> -98	$(1.8 \pm 0.38) \times 10^5$		29.98	
	<i>(R)</i> -97	$(1.67 \pm 0.19) \times 10^4$	2.4	24.09	2.16
	<i>(S)</i> -97	$(4.0 \pm 0.43) \times 10^4$		26.25	
<i>(S,S,S)</i> -96	<i>(R)</i> -98	$(1.5 \pm 0.26) \times 10^4$	2.1	23.82	1.80
	<i>(S)</i> -98	$(3.1 \pm 0.18) \times 10^4$		25.62	
	<i>(R)</i> -97	$(1.0 \pm 0.34) \times 10^4$	5.0	22.82	3.99
	<i>(S)</i> -97	$(5.0 \pm 0.46) \times 10^4$		26.81	

The same group [72] has developed a series of the  $C_2$ -symmetric, pyridine and diamide–diester groups containing lactone type macrocycles (**102**, **103**) with different side arms by reacting chiral bis(aminoalcohol)oxalamides with acyl pyridine (Schemes 16 and 17).



**Scheme 16.** Synthesis of bis(aminoalcohol)oxalamides.



**Scheme 17.** Synthesis of pyridine-15-crown-5 type macrocycles.

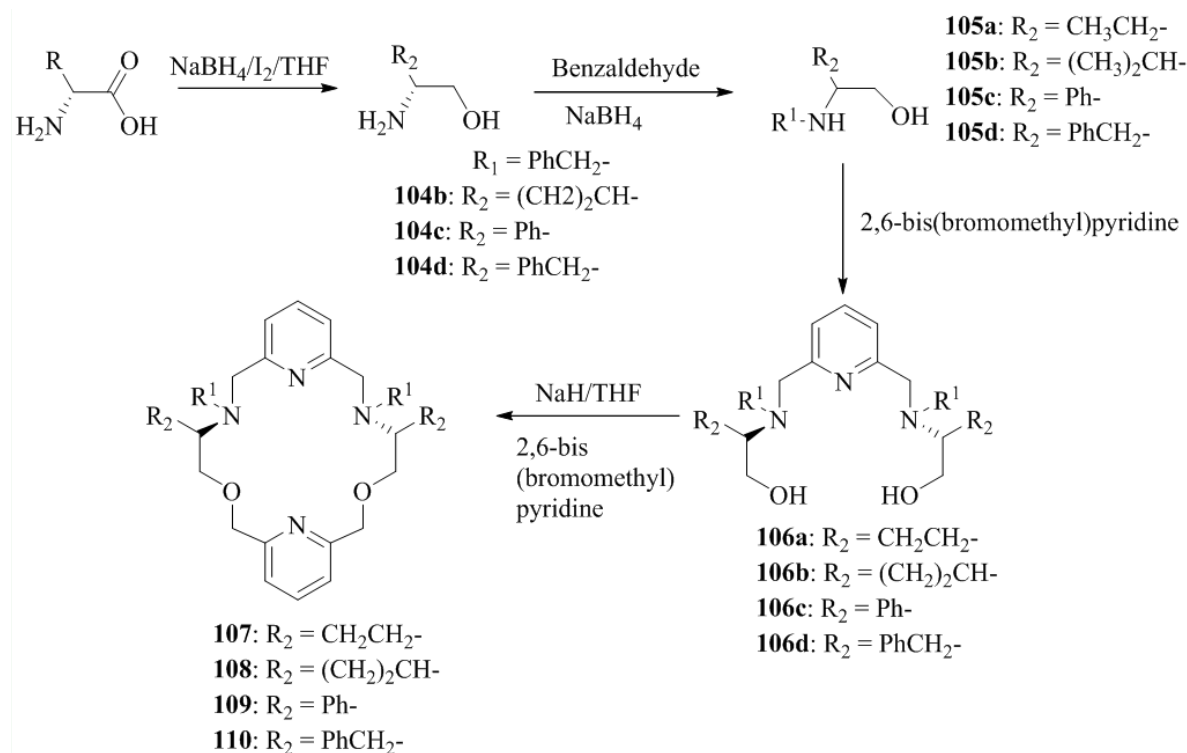
The standard  $^1\text{H}$  NMR titration experiments were carried out in order to investigate the chiral discrimination ability and complex stability of **102** and **103** with enantiomeric perchlorate salts **98** and **99**. The detailed results are summarized in Table 9. The host **102** formed stable complexes with (*S*)-enantiomers of **98** and **99** whereas host **103** formed the stable complexes with (*R*)-enantiomers of guest as host **103** contains the inverted stereogenic center compared to host **102**. Interestingly, replacing the phenyl group with benzyl ring in the host **102b**, reversed discrimination observed and formed the more stable complexes with (*R*)-enantiomers of **98** and **99**.

**Table 9.** Binding constant ( $K_a$ ), the Gibbs free energy changes ( $\Delta G_0$ ), enantioselectivities  $K_R/K_S$  or  $\Delta\Delta G_0$  for including the *R/S* guest with the chiral host macrocycles in  $\text{DMSO-d}_6$  at  $25^\circ\text{C}$ .

Entry	Host	Guest <sup>a</sup>	$K_a$ ( $\text{M}^{-1}$ ) <sup>b</sup>	$K_a^S/K_a^R$ <sup>c</sup>	$-\Delta G_0$ ( $\text{kJ mol}^{-1}$ ) <sup>d</sup>	$\Delta\Delta G_0$ ( $\text{kJ mol}^{-1}$ ) <sup>e</sup>	ED <sup>f</sup>
1	( <i>S,S</i> )- <b>102a</b>	( <i>R</i> )- <b>98</b>	$33.6 \pm 0.3$	3.86	8.71	3.34	59( <i>S</i> )
2	( <i>S,S</i> )- <b>102a</b>	( <i>S</i> )- <b>98</b>	$129.6 \pm 0.5$		12.05		
3	( <i>S,S</i> )- <b>102a</b>	( <i>R</i> )- <b>99</b>	$327.1 \pm 0.2$	31.0	14.35	8.50	94( <i>S</i> )
4	( <i>S,S</i> )- <b>102a</b>	( <i>S</i> )- <b>99</b>	$10,138 \pm 71$		22.85		
5	( <i>S,S</i> )- <b>102b</b>	( <i>R</i> )- <b>98</b>	$1852 \pm 17$	1.44	18.64	0.91	18( <i>S</i> )
6	( <i>S,S</i> )- <b>102b</b>	( <i>S</i> )- <b>98</b>	$2668 \pm 10$		19.55		
7	( <i>S,S</i> )- <b>102b</b>	( <i>R</i> )- <b>99</b>	$721.4 \pm 3.1$	0.36	16.31	−2.51	47( <i>R</i> )
8	( <i>S,S</i> )- <b>102b</b>	( <i>S</i> )- <b>99</b>	$262.6 \pm 2.6$		13.80		
9	( <i>S,S</i> )- <b>102c</b>	( <i>R</i> )- <b>98</b>	$2559 \pm 7$	1.05	19.44	0.20	2( <i>S</i> )
10	( <i>S,S</i> )- <b>102c</b>	( <i>S</i> )- <b>98</b>	$2681 \pm 5$		19.56		
11	( <i>S,S</i> )- <b>102c</b>	( <i>R</i> )- <b>99</b>	$1126 \pm 4$	1.34	17.41	0.73	30( <i>S</i> )
12	( <i>S,S</i> )- <b>102c</b>	( <i>S</i> )- <b>99</b>	$1511 \pm 4$		18.14		
13	( <i>R,R</i> )- <b>103</b>	( <i>R</i> )- <b>98</b>	$5412 \pm 17$		21.30		
14	( <i>R,R</i> )- <b>103</b>	( <i>S</i> )- <b>98</b>	nd <sup>g</sup>		nd <sup>g</sup>		
15	( <i>R,R</i> )- <b>103</b>	( <i>R</i> )- <b>99</b>	$4719 \pm 9$	0.60	20.96	−1.27	25( <i>R</i> )
16	( <i>R,R</i> )- <b>103</b>	( <i>S</i> )- <b>99</b>	$2833 \pm 7$		19.69		

<sup>a</sup> **98**:  $\alpha$ -phenylethylammonium perchlorate salts; **99**:  $\alpha$ -(1-naphthyl)ethylammonium perchlorate salts. <sup>b</sup> The binding constants between the hosts and the guests observed by  $^1\text{H}$  NMR titration. <sup>c</sup> The ratios of binding constants for each enantiomer. <sup>d</sup> The binding free energy change for the complexes, calculated by  $\Delta G_0 = -RT \ln K_a$ . <sup>e</sup>  $\Delta\Delta G_0 = -(\Delta G_{0(R)} - \Delta G_{0(S)})$ . <sup>f</sup> Enantiomeric discrimination factor. <sup>g</sup> Not determined.

Yilmaz Turgut et al. [73] synthesized four  $C_2$ -symmetric chiral pyridine containing 18-crown-6 macrocycles, each containing pairs of the following substituents: ethyl (**107**), isopropyl (**108**), phenyl (**109**), and benzyl (**110**). The synthetic strategy adopted was as follows: firstly, as a chiral source, D-Val, D-Phgly and D-Phe were reduced to the corresponding amino alcohols, D-valinol, **104b**, D-Phenyl glycinol **104c** and D-phenylalaninol, **104d**. The compound, **104a** and the reduced products, **104b–d** were reacted with benzaldehyde to give imines, which subsequently were converted to the corresponding N-benzyl derivatives, **105a**, **105b**, and **105c** (Scheme 18) followed by the treatment with 2,6-bis(bromomethyl) pyridine to afford **106a–d**. The pyridine containing  $C_2$ -symmetric **106a–d** having ethyl-, isopropyl-, phenyl-, and benzyl-moieties in their side arms were cyclized in a 1:1 ratio with 2,6-bis(bromomethyl)pyridine to the desired chiral macrocycles, **107**, **108**, **109** and **110** possessing the dipyridine units (Scheme 18). The chiral recognition of macrocycles towards the D-, L-amino acid methyl ester derivatives was determined by the  $^1\text{H}$  NMR titration method (Table 10). The compounds, **107** and **108** with the ethyl and isopropyl substituents at the stereogenic center, respectively, demonstrated the highest enantioselectivity and stable complexes, whereas the compounds, **109** and **110** with the corresponding phenyl and benzyl substituents possess a low-to-medium level of these properties. This inefficiency is a result of the fact that the phenyl and benzyl moieties prevent the guest cations from approaching the host.



**Scheme 18.** Synthesis of chiral amino alcohols and chiral macrocycles.

Kumares Ghosh et al. [74] prepared a series of pyridinium-based chiral compounds, **112–114**, **119** and **122**. The synthesis proceeds (Schemes 19 and 20) with the reaction of Boc-protected L-amino acids like Val (**111a**), Ala (**111b**) and Phgly (**111c**) and 3-aminopyridine to furnish the coupled products, **112a–c**, respectively. Further removal of the Boc-groups in **112a–c** yielded the corresponding amines, **113a–c**, which upon reaction with 1-naphthyl isocyanate afforded the respective urea derivatives, **114a–c**. The compounds, **114a–c** reacted with the corresponding chloroamides, **119a–c** to produce the chloride salts. Further, the anion exchange reactions with  $\text{NH}_4\text{PF}_6$  yielded the desired compounds, **115**, **116** and **117**. On the other hand, reaction of **114a** with benzyl bromide followed by the  $\text{Br}^-$  exchange with  $\text{PF}_6^-$  gave **118**.

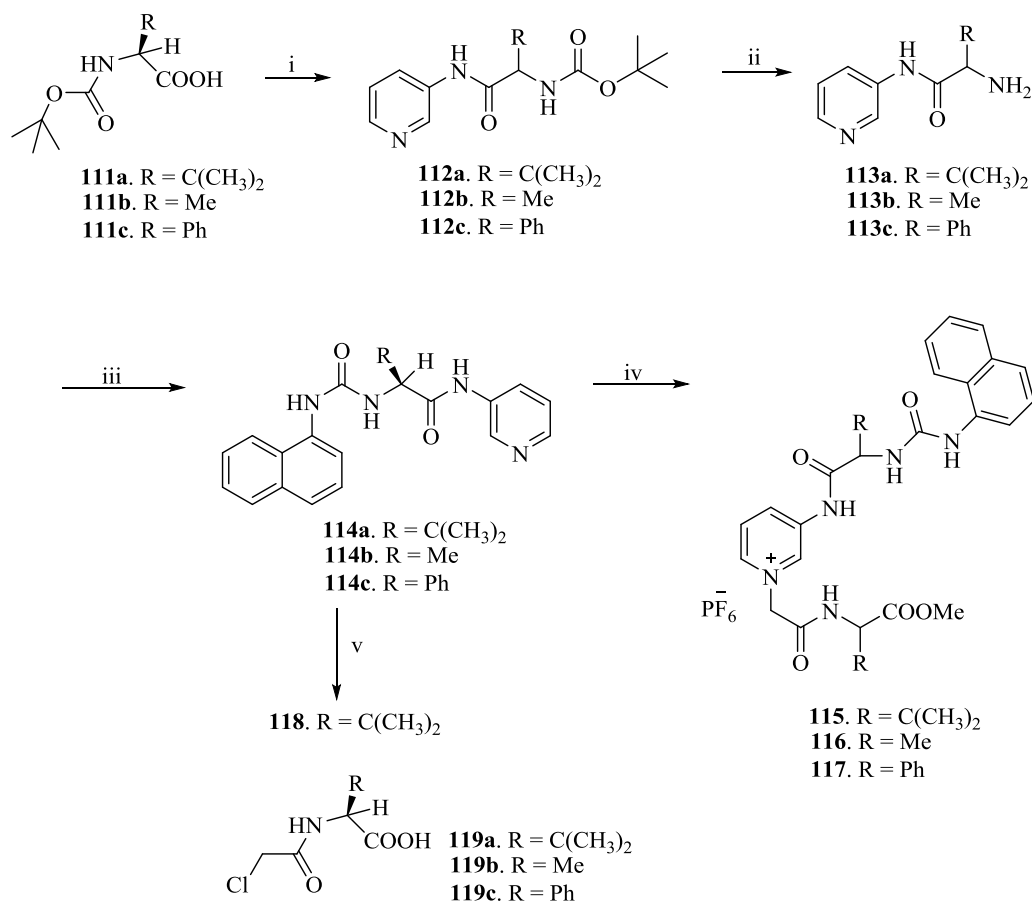
**Table 10.** Association constant ( $K_a$ ), the Gibbs free energy changes ( $-\Delta G_0$ ), enantioselectivities  $K_D/K_L$  for the complexation of D-/L-guest with the **107**, **108**, **109**, and **110** in  $CDCl_3$  with 0.25%  $CD_3OD$ .

Entry	Host	Guests	$K_{ass}$ ( $M^{-1}$ )	$K_D/K_L$	$-\Delta G_0$ ( $kJ\ mol^{-1}$ ) <sup>a</sup>	$-\Delta\Delta G_0$ ( $kJ\ mol^{-1}$ ) <sup>b</sup>
1	<b>107</b>	D-PheOMe.HCl	1785	2.04	18.3	1.80
2	<b>107</b>	L-PheOMe.HCl	875		16.5	
3	<b>107</b>	D-ValOMe.HCl	2325	2.63	18.9	2.30
4	<b>107</b>	L-ValOMe.HCl	885		16.6	
5	<b>108</b>	D-PheOMe.HCl	2580	1.22	1.2	0.5
6	<b>108</b>	L-PheOMe.HCl	2105		18.7	
7	<b>108</b>	D-ValOMe.HCl	13,590	5.08	23.3	4.00
8	<b>108</b>	L-ValOMe.HCl	2675		19.3	
9	<b>109</b>	D-PheOMe.HCl	395	0.77 ( $K_L/K_D = 1.29$ )	14.6	0.60
10	<b>109</b>	L-PheOMe.HCl	510		15.2	
11	<b>109</b>	D-ValOMe.HCl	32	0.33 ( $K_L/K_D = 3.00$ )	8.5	2.80
12	<b>109</b>	L-ValOMe.HCl	96		11.3	
13	<b>110</b>	D-PheOMe.HCl	1190	1.21	17.3	0.50
14	<b>110</b>	L-PheOMe.HCl	983		16.8	
15	<b>110</b>	D-ValOMe.HCl	660	0.72 ( $K_L/K_D = 1.38$ )	15.8	0.8
16	<b>110</b>	L-ValOMe.HCl	914		16.6	

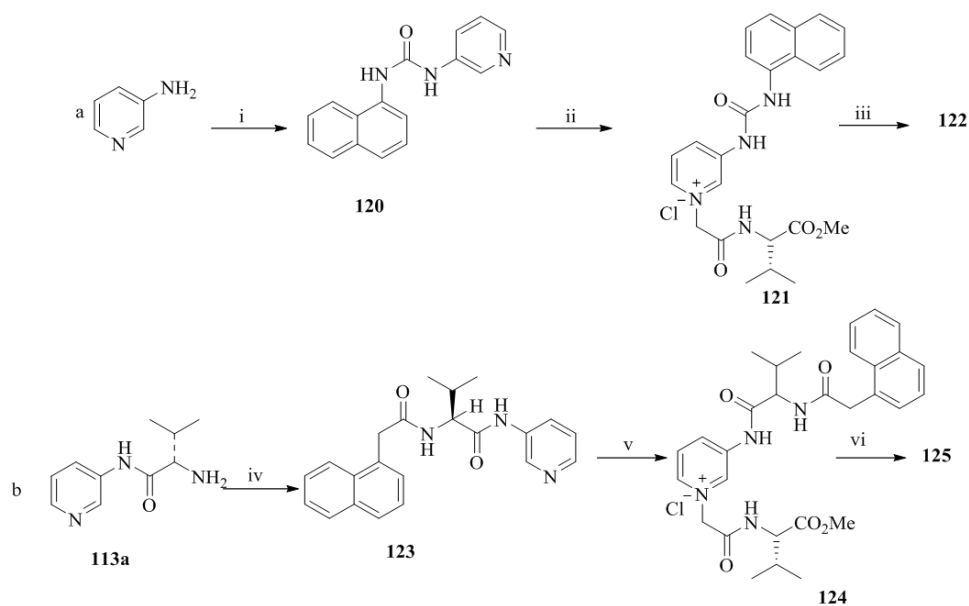
The treatment of 3-aminopyridine with 1-naphthylamine and phosgene afforded the urea, **120**, (Scheme 20) followed by the reaction with the chloroamide, **119a**, to give the chloride salt, **121**. Then the chloride exchange of **121** by using  $NH_4PF_6$  gave the desired compound, **122**. Next, the amine, **113a** was coupled with 1-naphthylacetyl chloride to obtain the amide derivative, **123**, which, subsequently reacted with **119a** to yield the chloride salt, **124** followed by the ion exchange with  $NH_4PF_6$  to furnish the desired compound, **122**. Among the synthesized compounds, **115–117**, **122**, and **125**, the structures, **115** and **125** have been established as effective fluorescent chiral receptors for the selective enantioselective recognition of D-lactate over L-lactate.

Bedekar et al. [75] synthesized two diastereomers of the optically active N, O-containing macrocycles, **129** and **130**. First, the ring opening reaction of cyclohexene oxide, **126** with (S)-2-phenylethyl amine afforded two diastereomers of aminocyclohexanol, **127a,b**, (Scheme 21) which after separation and subsequent condensation with m-xylene dibromide furnished the respective diols, **128a,b** (Scheme 22). The final transesterification with dimethyl 2, 6-pyridinedicarboxylate afforded the desired eighteen membered macrocycles, (S,S,S)-**129** and (R,R,S)-**130**. Using  $^{31}P$  NMR as a detection tool, the macrocycles (S,S,S)-**129** and (R,R,S)-**130** were tested for the chiral discrimination of chiral BINOL-based phosphoric acid derivatives by measuring the corresponding chemical shifts (Table 11). The macrocycle, (R,R,S)-**130** showed better discrimination, while (S,S,S)-**129** was found to be ineffective. Further, the discrimination of chiral phosphoric acid **131a** was corroborated by fluorescence, where the quenching was observed with the interaction of chiral host molecules **129** and **130**. The fluorescence quenching efficiency, ratio of  $K^{R-131a}_{sv} / K^{S-131a}_{sv}$  was observed to be 1.05 and 1.40 respectively for **129** and **130**.

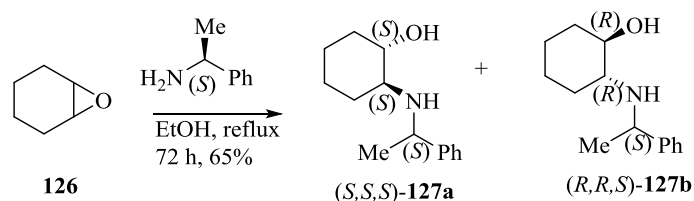
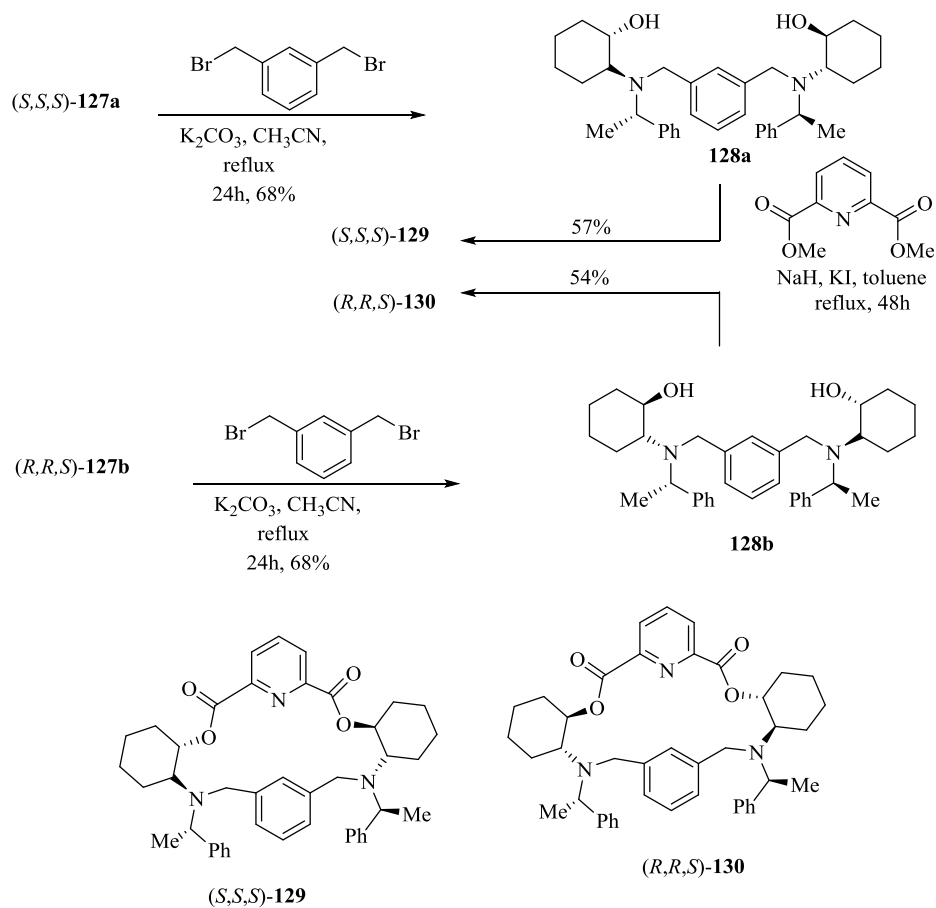
Interestingly, for the same set of macrocyclic chiral solvating agents (CSAs) **129** and **130**, interaction with the second group of analytes, such as  $\alpha$ -substituted phosphonic acids (**132** to **136**) gave a reverse trend (Table 12). The authors proposed that these analytes being smaller in size were better accommodated in the partially closed cavity of macrocycle (S,S,S)-**129**. The formation of H-bond between the phosphonic acid analyte and H-bond acceptor sites of macrocyclic CSA is apparently favored by the partially closed cavity of (S,S,S)-**129**.

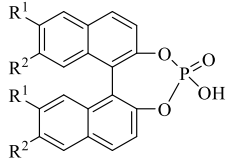


**Scheme 19.** (i) 3-Aminopyridine, DCC, CH<sub>2</sub>Cl<sub>2</sub>, 20 h; (ii) TFA, CH<sub>2</sub>Cl<sub>2</sub>, 3 h; (iii) 1-naphthylamine, triphosgene, Et<sub>3</sub>N, CH<sub>2</sub>Cl<sub>2</sub>, 16 h; (iv) (a) **119a–c**, CH<sub>3</sub>CN, reflux, 4 days; (b) NH<sub>4</sub>PF<sub>6</sub>, CH<sub>3</sub>OH–H<sub>2</sub>O; (v) (a) benzyl bromide, CH<sub>3</sub>CN, reflux, 18 h; (b) NH<sub>4</sub>PF<sub>6</sub>, CH<sub>3</sub>OH–H<sub>2</sub>O.



**Scheme 20.** (a) (i) 1-Naphthylamine, triphosgene, Et<sub>3</sub>N, CH<sub>2</sub>Cl<sub>2</sub>, 18 h; (ii) **119a**, CH<sub>3</sub>CN, reflux, 4 days; (iii) NH<sub>4</sub>PF<sub>6</sub>, CH<sub>3</sub>OH–H<sub>2</sub>O; (iv) (b) (iv) 1-naphthylacetyl chloride, CH<sub>2</sub>Cl<sub>2</sub>, Et<sub>3</sub>N, 12 h; (v) **119a** CH<sub>3</sub>CN, reflux, 3 days; (vi) NH<sub>4</sub>PF<sub>6</sub>, CH<sub>3</sub>OH–H<sub>2</sub>O.

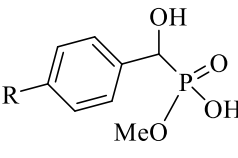
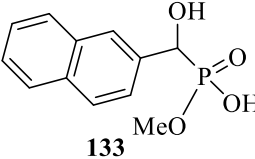
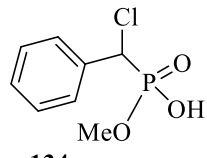
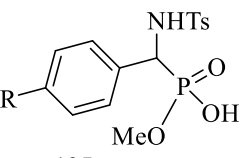
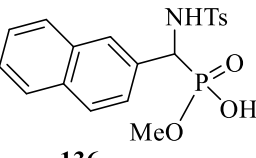
**Scheme 21.** Preparation of amino alcohols from cyclohexeneoxide.**Scheme 22.** Synthesis of macrocycles, **129** and **130**.**Table 11.** Discrimination of binaphthyl phosphoric acids **131**<sup>a</sup>.

					
<b>131</b>					
No.	Comp. No.	R <sub>1</sub>	R <sub>2</sub>	(S,S,S)-129	(R,R,S)-130
1	<b>131a</b>	H	H	0.03	0.74
2	<b>131b</b>	H	Ome	_b	0.68
3	<b>131c</b>	H	i-Pr	_b	0.76
4	<b>131d</b>	NO <sub>2</sub>	H	_b	0.81
5	<b>131e</b>	Br	H	_b	0.40

<sup>a</sup> In CDCl<sub>3</sub> (20 mM), 162 MHz (<sup>31</sup>P NMR), ratio of 5:1 (2:1). \_b Not resolved.



**Table 12.** Discrimination of monomethyl esters of substituted phosphoric acids **132** to **136** <sup>a</sup>.

<div style="display: flex; justify-content: space-around; align-items: flex-end;"> <div style="text-align: center;">  <p><b>132</b></p> </div> <div style="text-align: center;">  <p><b>133</b></p> </div> <div style="text-align: center;">  <p><b>134</b></p> </div> </div>				
<div style="display: flex; justify-content: space-around; align-items: flex-end;"> <div style="text-align: center;">  <p><b>135</b></p> </div> <div style="text-align: center;">  <p><b>136</b></p> </div> </div>				
No.	Comp. No.	R	( <i>S,S,S</i> )-129	( <i>R,R,S</i> )-130
1	<b>132a</b>	H	0.17	0.04
2	<b>132b</b>	Me	0.19	_b
3	<b>133c</b>	Cl	0.16	_b
4	<b>133</b>	-	0.17	_b
5	<b>134</b>	-	_b	_b
6	<b>135a</b>	H	0.40	_b
7	<b>135b</b>	Me	0.42	_b
8	<b>135c</b>	Cl	0.45	0.10
9	<b>135d</b>	OMe	0.43	_b
10	<b>135e</b>	NO <sub>2</sub>	0.40	0.12
11	<b>136</b>	-	0.37	_b

<sup>a</sup> In CD<sub>3</sub>OD (5%), in CDCl<sub>3</sub> (20 mM), 162 MHz (<sup>31</sup>P NMR), ratio of A to 10:4 (2:1). \_b Not resolved.

## 5.2. Oxygen Containing Six Member Heterocycle

Oxygen containing six member heterocycles is another class of motif found as structural core in several natural and synthetic compounds. Oxygen atom in the heterocyclic ring has two unshared pairs of electrons and hence can effectively participate in many types of the non-bonded interactions mentioned above. Six-membered carbohydrate unit has been very widely used in commercially popular chiral chromatographic columns. It is also a harder Lewis base than nitrogen and consequently different types of ligands can be probed with these heterocycle containing receptors. The particularly chromene heterocycle is a well-known significant core unit in the molecular recognition [32]. Chromenone core has exclusively placed oxygen atoms in 1,4-arrangement in conjugation with a double bond which facilitates brisk electron movement upon change in the electronic environment and hence quick detection under spectroscopic techniques, while studying host-guest interactions (Chart 2). Hence chromenone becomes a molecule of choice for receptor construction. The general design of chromenone based hosts discussed here, contain one or more chromenone motifs present in the receptor backbone, of molecular cleft or macrocycles.

Moran et al. [33] for the first time synthesized the chromenone and Spiro-bifluorene containing chiral macrocyclic receptor, **141** by reaction of the bis-aminomethylspirobifluorene unit **137** with nitrochromenone 2-carboxylic acid chloride, subsequent reduction of the nitro groups, treatment with phosgene, and slow hydrolysis of the intermediate isocyanates (Scheme 23). Significant chiral recognition of hydroxycarboxylates such as lactic or mandelic acids has been achieved with the macrocyclic receptor, **141** by using <sup>1</sup>H NMR. Thus, the receptors **141** showed a good association of the carboxylate group owing to four efficient hydrogen bonds for the syn- and anti-lone pairs of oxo-anion. The resolution of racemic receptor, **141** was achieved on a TLC plate by taking the advantage of its complexing properties with (*R*)-mandelic acid tetramethylammonium salt.

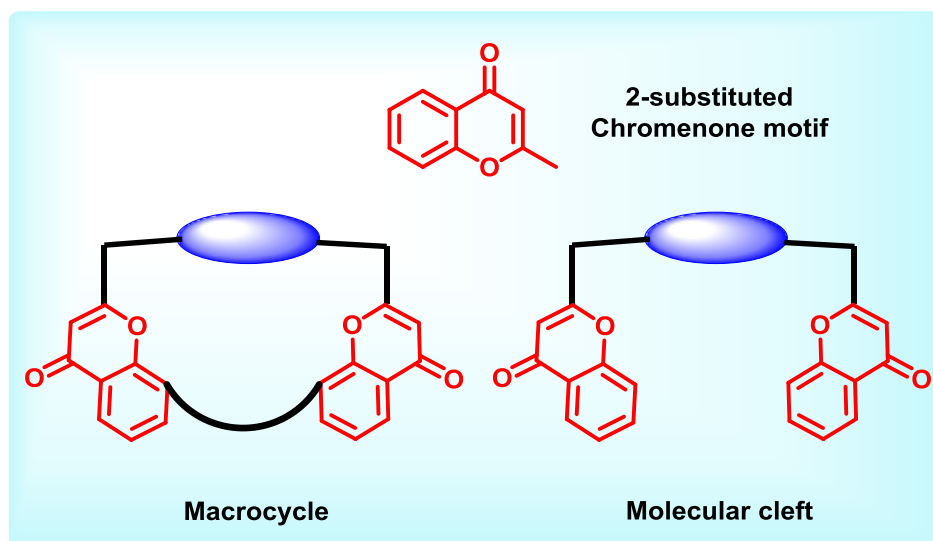
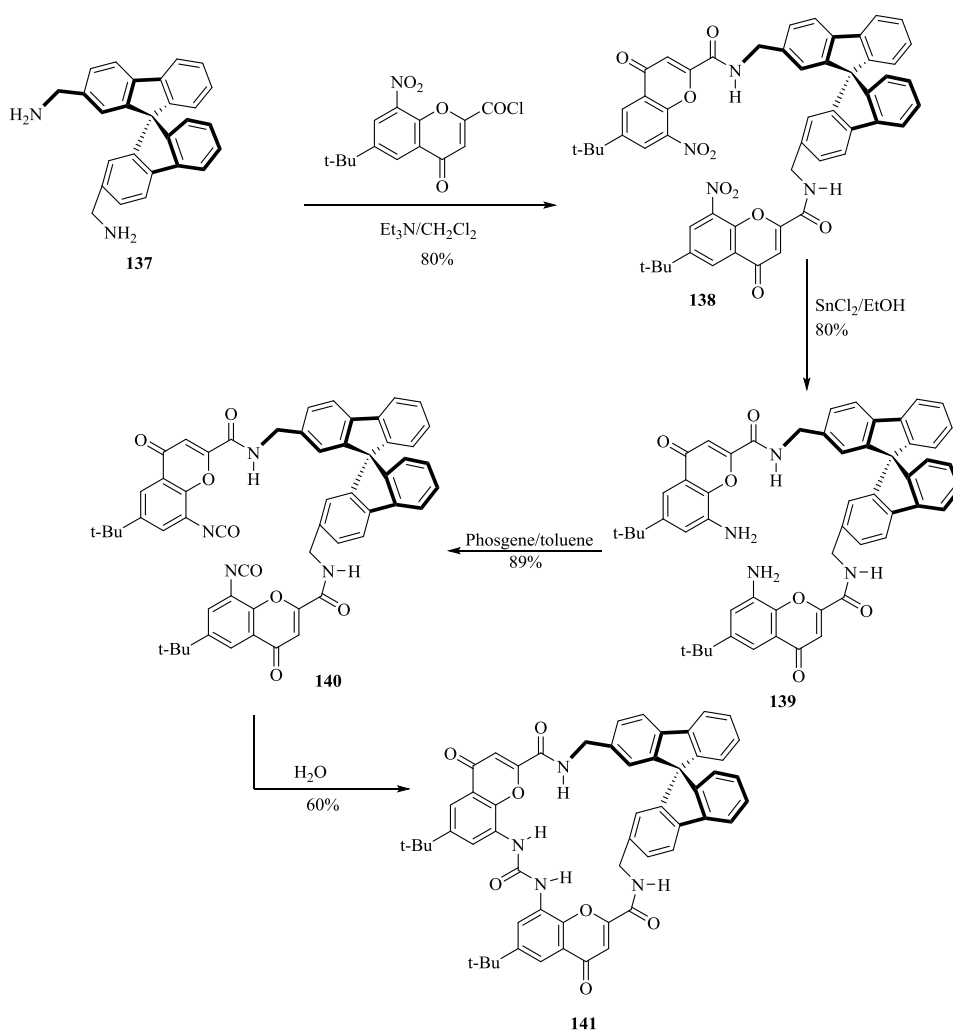


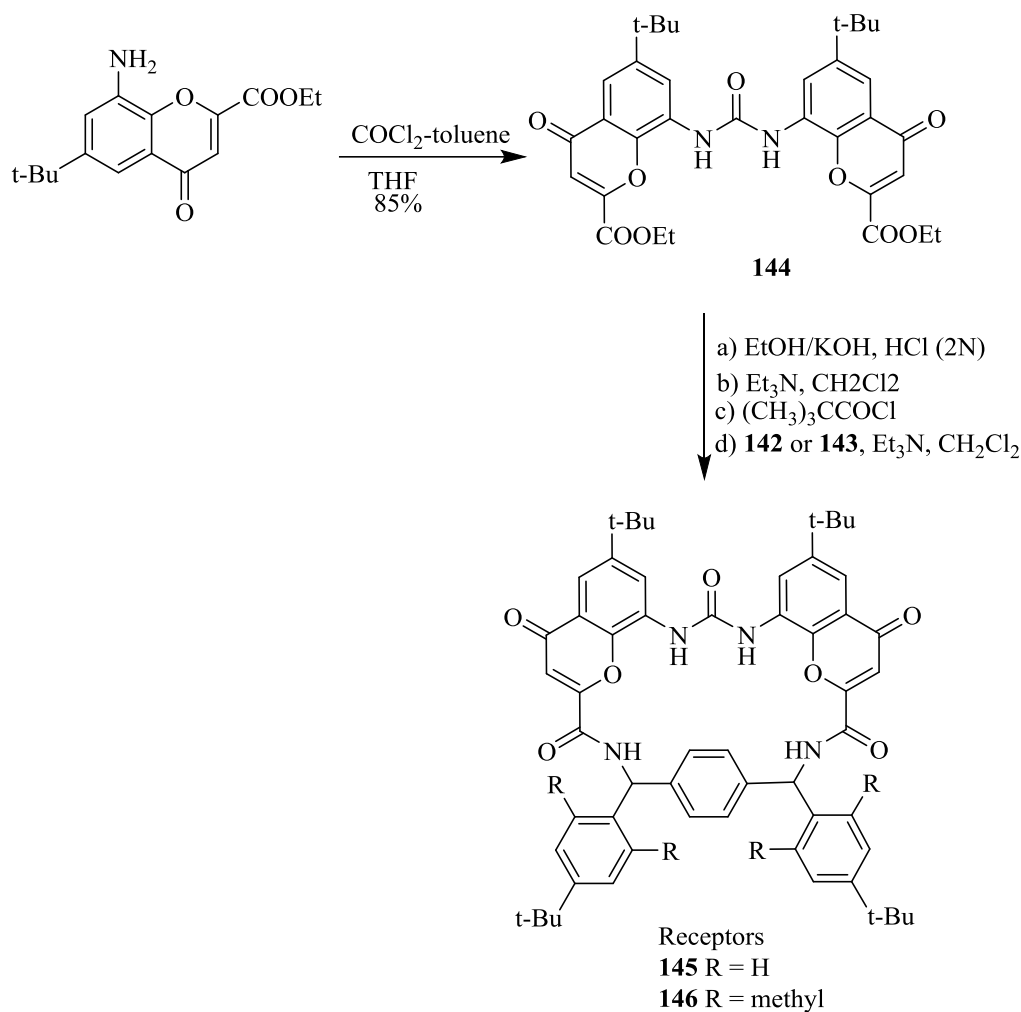
Chart 2. General design of chromenone containing hosts.



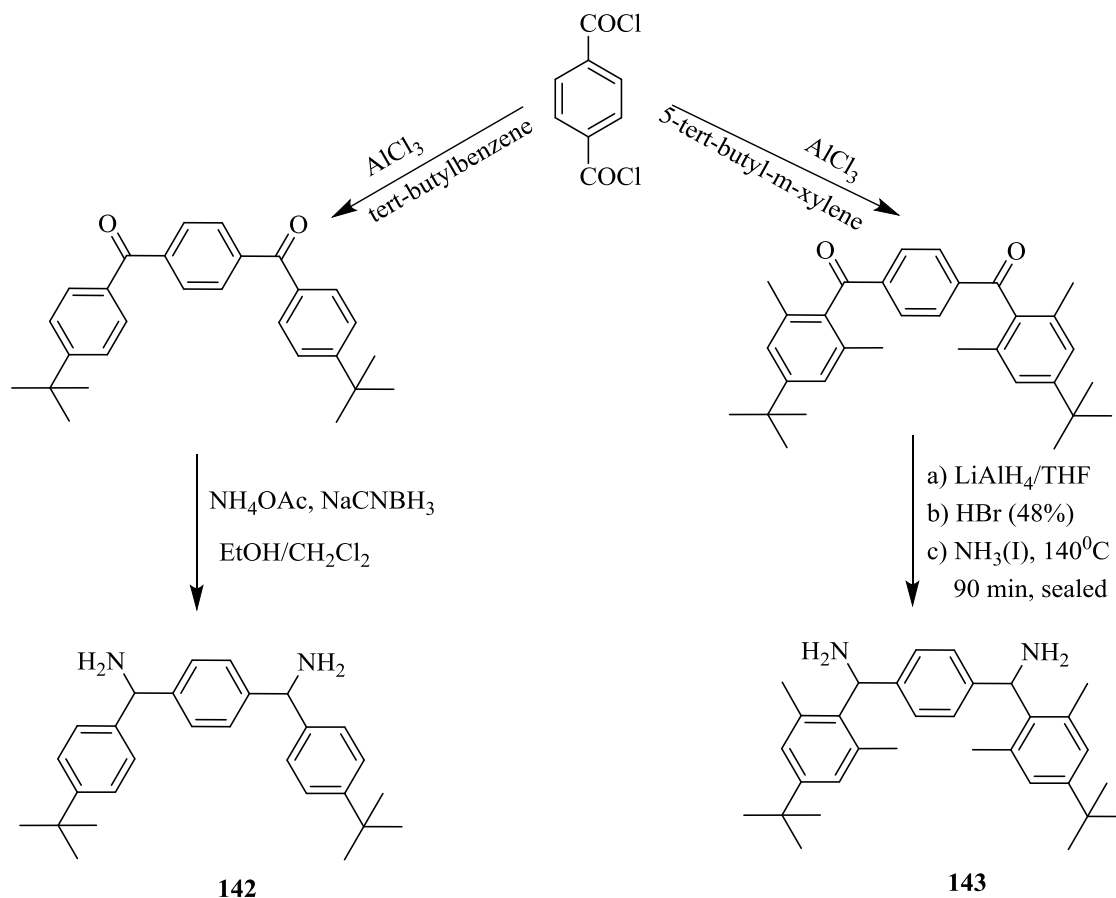
Scheme 23. Preparation of Receptor 141.

With the excellent recognition ability of bischromenylurea skeleton-based receptor **141** for chiral acids, this strategy was further extended [76]. Hence, bischromenylurea and  $\alpha,\alpha'$ -(*o,o'*-dialkyl)diphenyl-*p*-xylylenediamine spacer-based receptors (**145**, **146**) (Scheme 24) were prepared by a simple synthetic approach involving the hydrolysis of ethoxy carbonyl amino chromenone, **144** to give a dicarboxylic acid, which was subsequently coupled with the diamine, **142** or **143** (Scheme 25).

The chiral recognition behavior of racemic receptors, **145** and **146** has been tested with the enantiomers of naproxen by using  $^1\text{H}$  NMR. However, only a slight chiral discrimination (ratio 1.2:1) was observed for the receptor **145** and (*S*)-naproxen. Intriguingly, high enantioselectivity of 7.2:1 was obtained for the racemic receptor, **146** and (*S*)-naproxen. Apparently this is because **146** possesses a rigid and hindered cavity, where the host-guest binding takes place without disturbing the required complementary geometry.



**Scheme 24.** Synthesis of receptors, **145** and **146**.

Scheme 25. Synthesis of diamines, **142** and **143**.

## 6. Five Member Heterocycles Containing Receptors

Five member heterocycles such as imidazole, thiophene, furan, oxazole and oxazoline-based chiral compounds have attracted a widespread interest in the asymmetric synthesis and molecular recognition of metal ion, anion and chiral guests, owing to their striking structural features discussed in the Section 4. In the contemporary days several chiral receptors with five membered heterocycles have been developed and explored for the selective detection of chiral acids, chiral alcohols, chiral diamines and chiral amines. However, further chiral recognition using such receptors is used for the determination of concentration and enantiomeric excess of chiral analytes by high throughput methods. In this section, the recent developments in the receptor with five member heterocycles for chiral discrimination processes are presented.

### 6.1. Imidazole Ring Containing Receptors

Imidazole core has profound existence in nature, undoubtedly the synthetic community is inspired to construct receptors containing imidazole motifs. Imidazole moiety is bestowed with unique properties like basicity, nucleophilicity, and coordination ability. Acidity of the NH proton present in the imidazole ring can be tuned by changing the electronic properties of the imidazole substituents which is useful in anion binding. On the other hand, the presence of a donor pyridine-like nitrogen atom within the ring enables the imidazole ring towards selectivity in binding cationic species, thus making imidazole derivatives excellent metal ion sensors. The general receptor design of imidazole containing receptors discussed here, contain one or more imidazole motifs either separated by a chiral spacer to form a molecular cleft or 2,2'-linked bisimidazole motif as spacer itself with suitably placed terminal chiral arms (Chart 3).

Xie et al. [34] synthesized the chiral imidazole containing cyclophanes, **149–152** by highly selective *N*-alkylation of the imidazolyl 1*N*-position of **148** with the corresponding dibromides (Scheme 26).

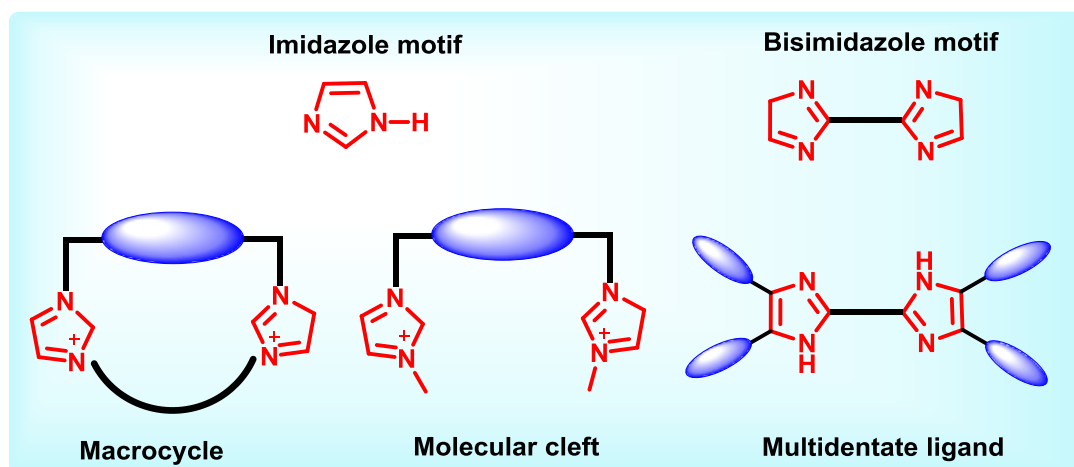
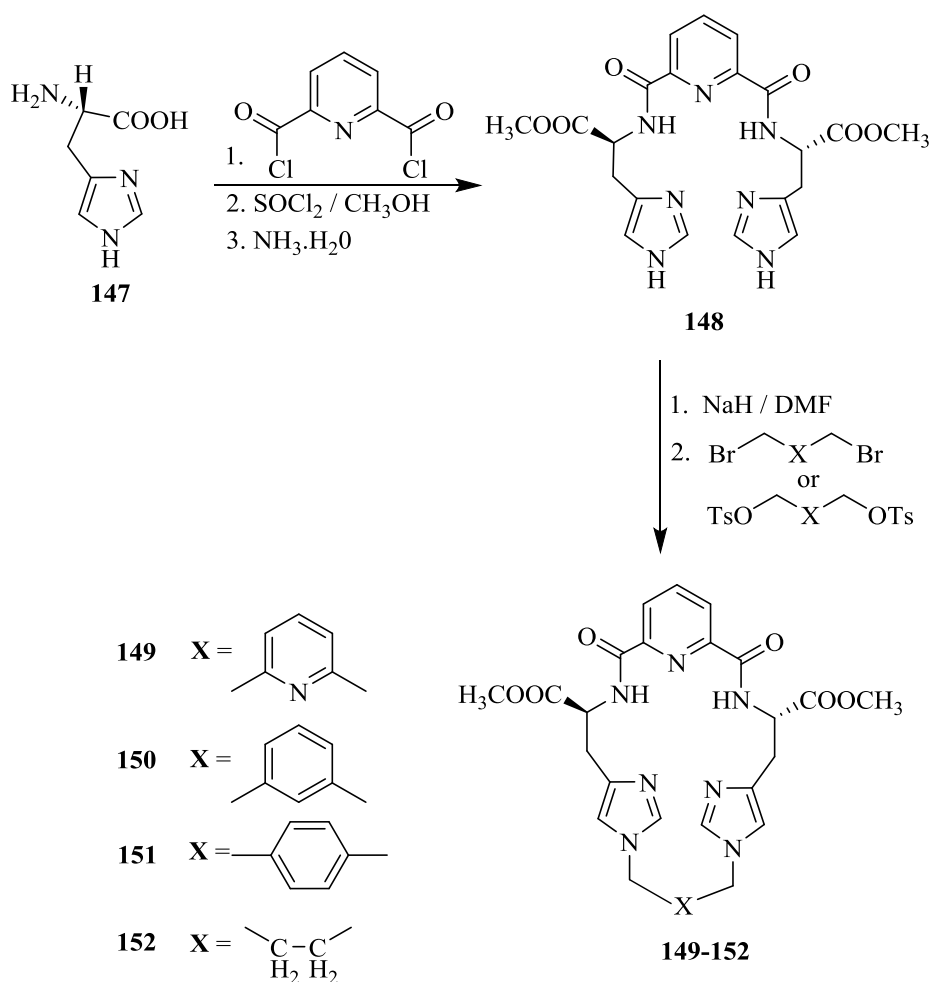


Chart 3. General design of imidazole containing hosts.



Scheme 26. Synthesis of chiral imidazole cyclophanes, **149–152**.

On the basis of differential UV spectroscopic studies, the association constants ( $K_a$ ) of inclusion complexes of the chiral imidazole cyclophane receptors with amino acid esters along with the free

energy change ( $G_0$ ) were determined (Table 13). The  $K_D$  values of **149** and **152** for D-Phe-OMe with the  $-(CH_2)_4-$  moiety were found to be 1063 and 208  $\text{dm}^3 \text{mol}^{-1}$ , respectively, which corresponds to the D/L-selectivity ( $K_D/K_L$ ) of 3.33 and 1.40. The enantioselective recognition ability of **149** with  $\alpha$ -amino acid esters and their hydrochlorides gave  $K_D/K_L$  in the range of 1.45–3.52 and  $G_0$  from 20.93 to 23.11  $\text{kJ mol}^{-1}$ . However, **149** gave fairly poor recognition ability for amino acid esters with the aliphatic side chain (Table 13, entries 3–8) due to absence of  $\pi$ - $\pi$  stacking interactions with receptor.

**Table 13.** Association constants ( $K_a$ ), the Gibbs free energy changes ( $-\Delta G_0$ ), enantioselectivities  $K_D/K_L$  or  $\Delta\Delta G_0$  calculated from  $-\Delta G_0$  for the including complexation of L/D-amino acid esters with **148–152** in  $\text{CHCl}_3$  at 25 °C <sup>a</sup>.

Entry	Host	Guests	$K_a$ ( $\text{M}^{-1}$ )	$K_D/K_L$	$-\Delta G_0$ ( $\text{kJ mol}^{-1}$ ) <sup>a</sup>	$-\Delta\Delta G_0$ ( $\text{kJ mol}^{-1}$ ) <sup>b</sup>
1	<b>148</b>	L-Phe-OMe	89.4	1.12	11.13	−0.27
2	<b>148</b>	D-Phe-OMe	99.8		11.40	
3	<b>149</b>	L-Ala-OMe	437	1.45	15.06	−0.93
4	<b>149</b>	D-Ala-OMe	634		15.99	
5	<b>149</b>	L-Val-OMe	299	2.05	14.12	−1.78
6	<b>149</b>	D-Val-OMe	613		15.90	
7	<b>149</b>	L-Leu-OMe	260	2.24	13.78	−2.00
8	<b>149</b>	D-Leu-OMe	583		15.78	
9	<b>149</b>	L-Phe-OMe	319	3.33	14.28	−2.99
10	<b>149</b>	D-Phe-OMe	1063		17.27	
11	<b>149</b>	L-Trp-OMe	1238	2.68	17.64	−2.44
12	<b>149</b>	D-Trp-OMe	3314		20.08	
13	<b>149</b>	L-Ala-OMe.HCl	471	2.80	15.25	−2.55
14	<b>149</b>	D-Ala-OMe.HCl	1319		17.80	
15	<b>149</b>	L-Leu-OMe.HCl	327	3.52	14.35	−3.11
16	<b>149</b>	D-Leu-OMe.HCl	1150		17.46	
17	<b>150</b>	L-Phe-OMe	224	2.33	13.41	−2.10
18	<b>150</b>	D-Phe-OMe	523		15.51	
19	<b>151</b>	L-Phe-OMe	217	2.00	13.33	−1.71
20	<b>151</b>	D-Phe-OMe	433		15.40	
21	<b>152</b>	L-Phe-OMe	149	1.40	12.40	−0.82
22	<b>152</b>	D-Phe-OMe	208		13.22	

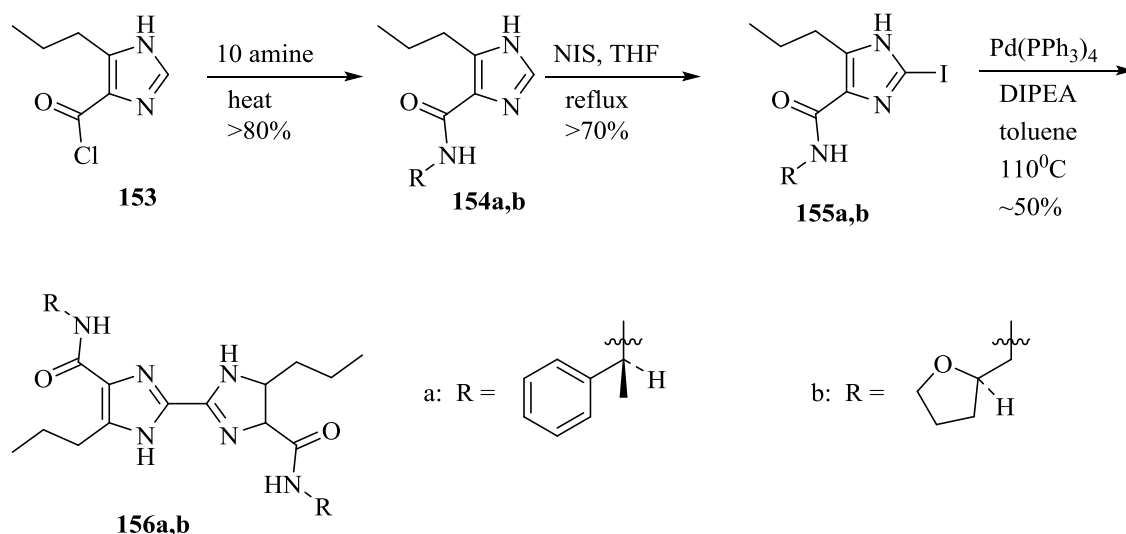
<sup>a</sup> The concentration of the receptors:  $2.0 \times 10^{-4} \text{ mol dm}^{-3}$ . <sup>b</sup> Ala-OMe: alanine methyl ester; Val-OMe: valine methyl ester; Leu-OMe: leucine methyl ester; Phe-OMe: phenylalanine methyl ester; Trp-OMe: tryptophan methyl ester; Ala-OMe.HCl: alanine methyl ester hydrochloride; Leu-OMe.HCl: leucine methyl ester hydrochloride.

Allen et al. [77] prepared chiral 4,4'-diamido-2,2'-biimidazoles, **156a,b** (Scheme 27) by the treatment of acid chloride, **153** with (*S*)- $\alpha$ -methylbenzylamine and (*R*)-tetrahydrofurfurylamine to afford **154a,b**, followed by the corresponding iodination and coupling. The macromolecules, **156a,b** were found to be beneficial for the chiral recognition of *N*-protected amino acids as revealed by the NMR titration methods. In particular, **156a** discriminates the enantiomers of *N*-Boc-Phe, while **156b** discriminates the enantiomers of *N*-Boc-Ser (Table 14).

**Table 14.** Binding constants  $K_a$  ( $\text{M}^{-1}$ ) <sup>a</sup> for chiral biimidazoles with amino acid derivatives in  $\text{CDCl}_3$  at 23 °C.

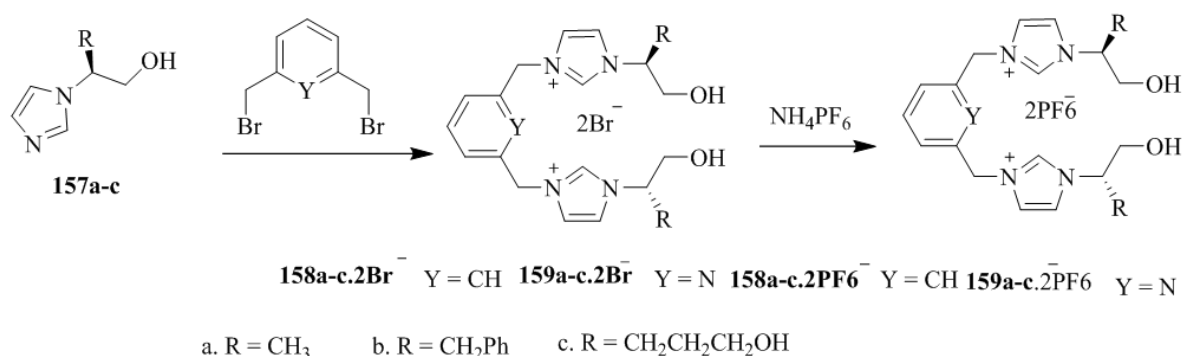
Complex	$K_a$
<b>156a</b> . <i>N</i> -Boc-L-Phe, -D-Phe	100,65
<b>156b</b> . <i>N</i> -Boc-L-Ser, -D-Ser	<6065
<b>156a</b> . <i>N</i> -Boc-L-Phe, -D-Phe	6565
<b>156b</b> . <i>N</i> -Boc-L-Ser, -D-Ser	120,270

<sup>a</sup> Values represent averages of at least two replicate titrations, rounded to the nearest  $\pm 5 \text{ M}^{-1}$ . Errors in individual fits were  $\leq 15\%$ .



**Scheme 27.** Synthesis of chiral 4,4'-diamido-2,2'-biimidazoles, **156a,b**.

Later Xie and coworkers [78,79] synthesized the imidazole-based chiral molecular tweezers (Scheme 28) spaced by 2,6-di(bromomethyl)-4-chlorophenol, 1,3-phenylenebis(methylene) and 2,6-pyridylenebis(methylene). The dibromide salts, **158a–c.2Br<sup>−</sup>** and **159a–c.2Br<sup>−</sup>** were obtained by the direct quaternization of **157a–c** with 2,6-di(bromomethyl)-4-chlorophenol or 1,3-bis(bromomethyl)benzene or 2,6-bis(bromomethyl)pyridine while the hexafluorophosphate salts **158a–c.2PF<sub>6</sub><sup>−</sup>** and **159a–c.2PF<sub>6</sub><sup>−</sup>** were prepared by the treatment with a saturated aqueous solution of  $\text{NH}_4\text{PF}_6$ . The chiral discrimination of chiral molecular tweezers for amino acids or their derivatives (Tables 15 and 16) were evaluated by the UV-vis titration method.



**Scheme 28.** Synthesis of chiral molecular tweezers.

**Table 15.** Binding constants ( $K_a$ ), Gibbs free energy changes ( $-\Delta G_0$ ), enantioselectivities  $K_L/K_D$  or  $\Delta\Delta G$  calculated from  $-\Delta G$  for the including complexation of L/D-amino acids or their derivatives with hosts at 27 °C in water or acetonitrile.

Entry	Host <sup>a,b</sup>	Guest	K/dm <sup>3</sup> mol	$K_L/K_D$	$-\Delta G_0/\text{KJ mol}^{-1}$	$-\Delta\Delta G_0/\text{KJ mol}^{-1}$
1	<b>158a2Br<sup>−</sup></b>	L-Phe	10,328	1.29	23.05	0.63
2	<b>158a2Br<sup>−</sup></b>	D-Phe	8012		22.42	
3	<b>158a2Br<sup>−</sup></b>	L-Thr	766	1.82	16.56	1.49
4	<b>158a2Br<sup>−</sup></b>	D-Thr	421		15.07	
5	<b>158b2Br<sup>−</sup></b>	L-Phe	19,518	1.89	24.64	1.59
6	<b>158b2Br<sup>−</sup></b>	D-Phe	10,324		23.05	

Table 15. Cont.

Entry	Host <sup>a,b</sup>	Guest	K/dm <sup>3</sup> mol	K <sub>L</sub> /K <sub>D</sub>	−ΔG <sub>0</sub> /KJ mol <sup>−1</sup>	−ΔΔG <sub>0</sub> /KJ mol <sup>−1</sup>
7	158b2Br <sup>−</sup>	L-His	7627	2.03	22.30	1.77
8	158b2Br <sup>−</sup>	D-His	3761		20.53	
9	158c2Br <sup>−</sup>	L-Phe	14,026	1.71	23.82	1.34
10	158b2Br <sup>−</sup>	D-Phe	8222		22.48	
11	159a2Br <sup>−</sup>	L-Ala	820	1.61	16.73	1.19
12	159a2Br <sup>−</sup>	D-Ala	509		15.54	
13	159a2Br <sup>−</sup>	L-Thr	1901	2.10	18.83	1.85
14	159a2Br <sup>−</sup>	D-Thr	904		16.98	
15	159a2Br <sup>−</sup>	L-Phe	13,053	2.51	23.64	2.75
16	159a2Br <sup>−</sup>	D-Phe	5196		20.89	
17	159a2Br <sup>−</sup>	L-His	11,639	3.03	23.35	2.76
18	159a2Br <sup>−</sup>	D-His	3841		20.59	
19	159a2Br <sup>−</sup>	L-Phe	28,321	3.35	25.57	3.02
20	159a2Br <sup>−</sup>	D-Phe	8458		22.55	
21	159a2Br <sup>−</sup>	L-His	12,031	3.20	23.43	2.91
22	159a2Br <sup>−</sup>	D-His	3741		20.52	
23	159c2Br <sup>−</sup>	L-Phe	14,733	2.14	23.94	1.90
24	159c2Br <sup>−</sup>	D-Phe	6899		22.04	
25	158a2PF <sub>6</sub> <sup>−</sup>	BOC-L-His-Ome	870	3.50	16.88	3.13
26	158a2PF <sub>6</sub> <sup>−</sup>	BOC-D-His-Ome	248		13.75	
27	158b2PF <sub>6</sub> <sup>−</sup>	BOC-L-His-Ome	1001	4.07	17.23	3.50
28	158b2PF <sub>6</sub> <sup>−</sup>	BOC-D-His-Ome	246		13.73	
29	159a2PF <sub>6</sub> <sup>−</sup>	L-Ala-Ome	610	1.72	16.00	1.50
30	159a2PF <sub>6</sub> <sup>−</sup>	D-Ala-Ome	355		14.50	
31	159a2PF <sub>6</sub> <sup>−</sup>	L-Phe-Ome	9294	2.72	22.79	2.49
32	159a2PF <sub>6</sub> <sup>−</sup>	L-Phe-Ome	3421		20.30	
33	159a2PF <sub>6</sub> <sup>−</sup>	BOC-L-Phe-Ome	9166	3.34	22.76	3.01
34	159a2PF <sub>6</sub> <sup>−</sup>	BOC-D-Phe-Ome	2741		19.74	
35	159b2PF <sub>6</sub> <sup>−</sup>	L-Phe-Ome	10,720	3.14	23.15	2.86
36	159b2PF <sub>6</sub> <sup>−</sup>	D-Phe-Ome	3412		20.29	
37	159b2PF <sub>6</sub> <sup>−</sup>	BOC-L-Phe-Ome	13,903	4.03	23.79	3.47
38	159b2PF <sub>6</sub> <sup>−</sup>	BOC-L-Phe-Ome	3446		20.32	
39	159b2PF <sub>6</sub> <sup>−</sup>	BOC-L-His-Ome	1284	5.10	17.48	3.69
40	159b2PF <sub>6</sub> <sup>−</sup>	BOC-D-His-Ome	252		13.79	

<sup>a</sup> 158a-c2Br<sup>−</sup> and 159a-c2Br<sup>−</sup> in water, 158a-c2PF<sub>6</sub><sup>−</sup> and 159a2PF<sub>6</sub><sup>−</sup> in acetonitrile. <sup>b</sup> the concentration of hosts 5.0 × 10<sup>−5</sup> mol dm<sup>−3</sup>.

**Table 16.** Binding constants (*K<sub>a</sub>*), Gibbs free energy changes (−Δ*G*<sub>0</sub>), enantioselectivities *K<sub>L</sub>*/*K<sub>D</sub>* or ΔΔ*G* calculated from −Δ*G* for the complexation of L/D-amino acids or their methyl esters with 158a–159b at 27 ± 0.1 °C in water or acetonitrile.

Entry	Host <sup>a,b</sup>	Guest <sup>c</sup>	K/dm <sup>3</sup> mol	K <sub>L</sub> /K <sub>D</sub>	−ΔG <sub>0</sub> /Kj mol <sup>−1</sup>	−ΔΔG <sub>0</sub> /Kj mol <sup>−1</sup> <sup>d</sup>
1	158a	L-Ala D-Ala	1623 897	1.81	18.44 16.95	1.49
2	158a	L-Phe D-Phe	33,748 19,241	1.75	26.01 24.60	1.41
3	158a	L-His D-His	7458 3876	1.92	22.24 20.61	1.63
4	159a	L-Phe-Ome D-Phe-Ome	4099 2515	1.59	20.99 19.83	1.16



Table 16. Cont.

Entry	Host <sup>a,b</sup>	Guest <sup>c</sup>	K/dm <sup>3</sup> mol	K <sub>L</sub> /K <sub>D</sub>	−ΔG <sub>0</sub> /Kj mol <sup>−1</sup>	−ΔΔG <sub>0</sub> /Kj mol <sup>−1</sup> <sup>d</sup>
5	158b	L-Ala D-Ala	1682 921	1.82	18.53 17.02	1.51
6	158b	L-Phe D-Phe	68,274 20,310	3.36	27.76 24.74	3.02
7	158b	L-His D-His	9510 3129	3.04	22.85 20.07	2.78
8	159b	L-Ala-OMe D-Ala-OMe	1704 874	1.95	18.55 16.69	1.86
9	159b	BOC-L-Ala-OMe BOC-D-Ala-OMe	1453 690	2.10	18.16 16.30	1.86
10	159b	L-Phe-OMe D-Phe-OMe	6882 3105	2.22	22.04 20.06	1.98
11	159b	BOC-L-Phe-OMe BOC-D-Phe-OMe	6736 2510	2.68	21.99 19.52	2.47
12	159b	BOC-L-His-OMe BOC-D-His-OMe	2941 717	4.10	19.92 16.40	3.52

<sup>a</sup> 158a,b in water; 159a,b in acetonitrile. <sup>b</sup> the concentration of hosts  $5.0 \times 10^{-5}$  mol dm<sup>−3</sup>; <sup>c</sup> Phe-OMe: phenylalanine methyl ester; BOC-Phe-OMe: BOC-phenylalanine methyl ester; BOC-Ala-OMe: BOC-alanine methyl ester; BOC-His-OMe: BOC-Histidine methyl ester. <sup>d</sup>  $\Delta\Delta G_0 = -(\Delta G_{0(L)} - \Delta G_{0(D)})$ .

Yu et al. [29] designed and synthesized the imidazolium-functionalized BINOLs, (*R*)-160, (*S*)-161 and (*S*)-162 (Figure 12). These hosts were evaluated for chiral recognition with various amino acid derivatives, tetrabutylammonium salts of *t*-Boc-amino acids, such as Ala, Ser, Leu, and Phe. However, *R*-160 exhibited a noteworthy binding ability only for *t*-BOC alanine anion with the high enantioselectivity ( $K_D/K_L$ ) of 4.5, while (*S*)-161, bearing imidazolium rings attached to a flexible methylene linker, showed the higher association constant but furnished moderate enantioselectivity,  $K_L/K_D$  value of 2.9 for the same chiral guest. This is a result of the reduction of the steric factor between the BINOL unit and imidazolium due to the flexible methylene linker.

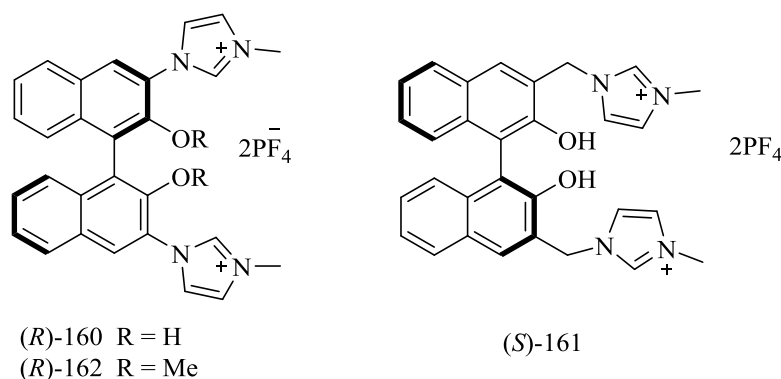
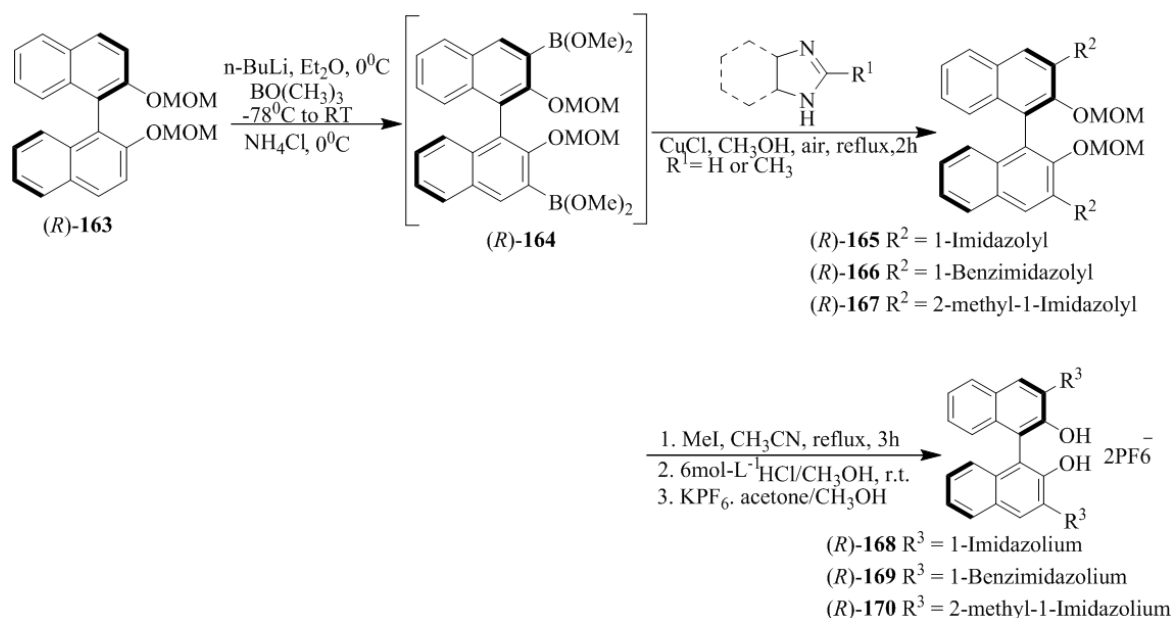


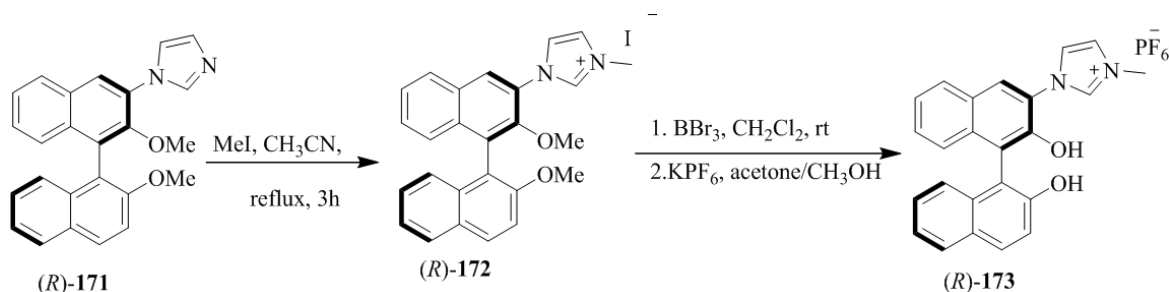
Figure 12. Imidazolium-functionalized anion-binding receptors.

Yu et al. [24] developed the imidazolium/benzimidazolium-containing receptors, (*R*)-168, (*R*)-169, (*R*)-170, (*R*)-173, and (*R*)-176. At first, MOM-protected boronic acid ester, (*R*)-164 upon the *N*-arylation with imidazole derivative or benzimidazole yielded the respective coupled products (165–167) followed by methylation to give the desired hosts, 168–170 (Scheme 29). Further, (*R*)-171 and (*R*)-174 (Schemes 30 and 31) were converted to (*R*)-173 and (*R*)-176, respectively. The synthesized compounds were then evaluated for the chiral discrimination of amino acid derivatives, such as Ala, Ser, Leu, and Phe, and tetrabutylammonium salts of *t*-Boc-amino acids studied by using fluorescence spectroscopy. The association constants of (*R*)-178 with L- and D-Boc alanine were found to be  $4.55 \times 10^5$  and

$1.02 \times 10^5 \text{ L mol}^{-1}$ , respectively, with the  $K_L/K_D$  value of 4.5. While (*R*)-**176** displayed larger association constants with both L- and D- *t*-Boc alanines, the enantioselectivity was very similar ( $K_L/K_D = 4.1$ ). However, when (*R*)-**173** containing only one 3-imidazolium substituent was tested with two enantiomers of *t*-Boc-alanine, the enantioselectivity was as low as 1.1. Thus, the  $C_2$  symmetric sensors, (*R*)-**168** and (*R*)-**176** were more efficient than the  $C_1$  symmetric (*R*)-**173** in the chiral recognition.

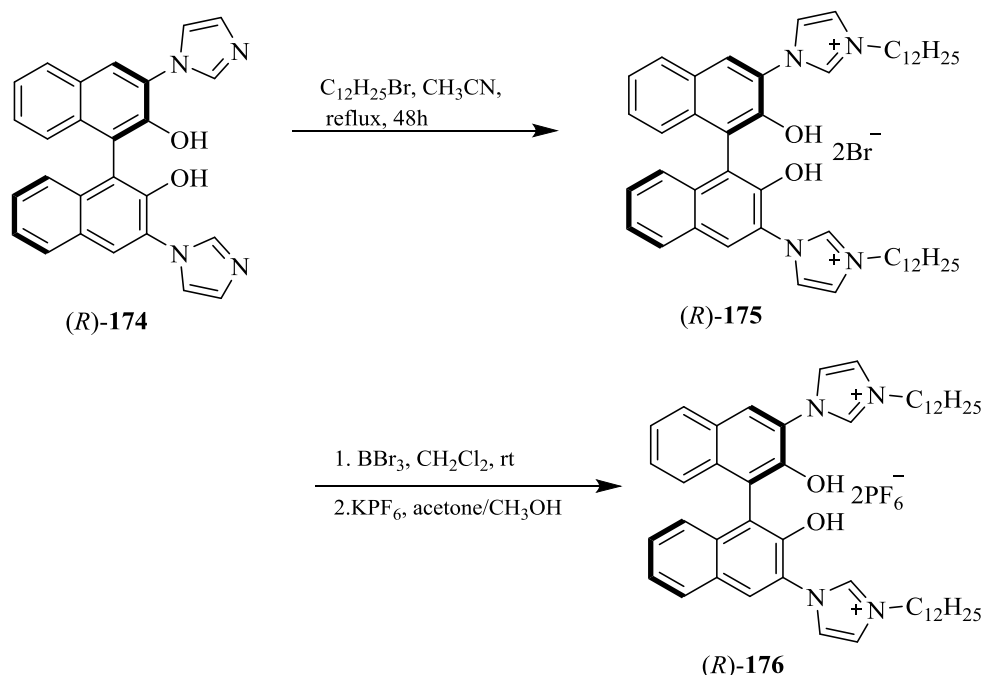


**Scheme 29.** Synthesis of receptors, (*R*)-**168**, (*R*)-**169** and (*R*)-**170**.

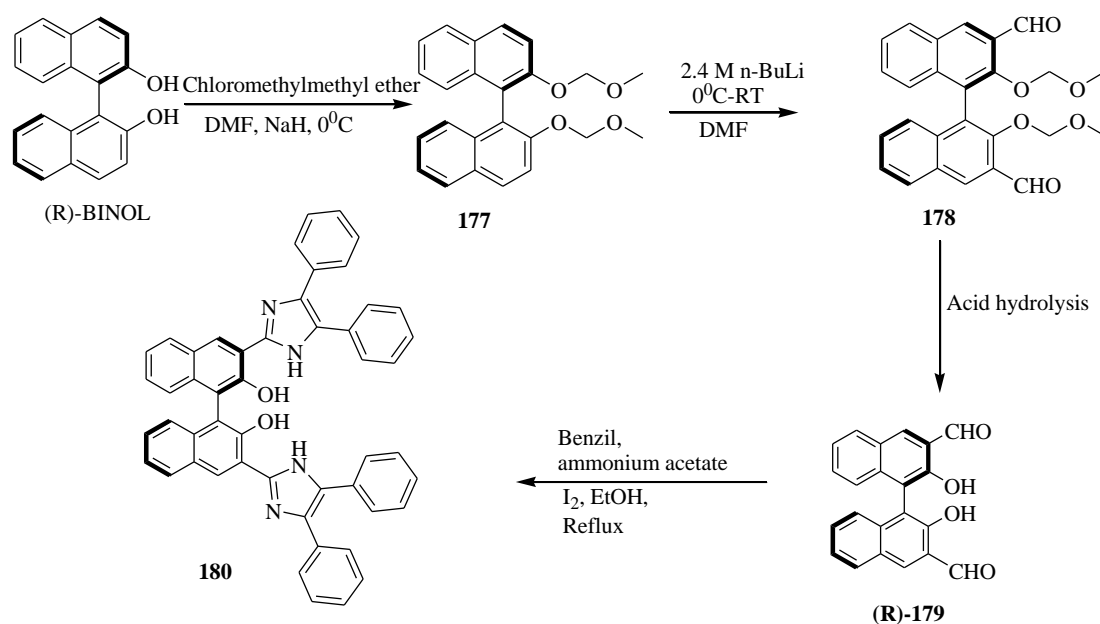


**Scheme 30.** Synthesis of the mono-imidazolium substituted receptor, (*R*)-**173**.

Iyer et al. [80] developed the BINOL-imidazole-based fluorescent sensor, **180** (Scheme 32). It was synthesized by the first formylation of MOM-protected BINOL, **177** followed by the deprotection of MOM and treatment with benzil in the presence of iodine to afford the desired product. This compound was found to be useful as a fluorescent sensor for Cu(II). Furthermore, the in situ generated complex, Cu(II)-**180** was studied for the fluorescent enantioselective recognition of unmodified amino acids (Table 17). L-ala displayed a large enhancement in the fluorescence intensity; whereas D-enantiomer has a small influence under the similar experimental conditions with an enantiomeric fluorescence difference ratio [ $\text{ef} = I_L - I_0 / I_D - I_0$ ] of 1.52 at the 1:50 molar ratio.



Scheme 31. Synthesis of (R)-176.



Scheme 32. Synthesis procedure of the sensor, 180.

## 6.2. Benzimidazole Ring Containing Receptors

Benzimidazole is a member of benzo-fused heterocycles. It has received more attention compared to the other members of the same class is possibly because generation of chiral benzimidazoles by easy synthetic protocol. A chiral center can be easily incorporated in the heterocycle and this has led to use of these molecules as a chiral organo-catalyst or as a metal atom containing catalysts [9]. Several such reports have appeared periodically. The use of this molecule in chiral molecular recognition has not received the attention it deserved. Endowed with aromatic electron cloud and almost rigid conformation for the small sized macrocycles can be good structural features for use of chiral benzimidazoles in chiral molecular recognition. Due to the synthetic ease and freedom in

structural tuning that benzimidazole core offers, it is a popular structural motif to be included in chiral ligand design. Our group has been exploring the benzimidazole core in an effective manner for over two decades and very recently we were successful in using it as a chiral host for enantiomeric guests. The Chart 4 ahead, depicts the various manners in which 2-substituted chiral benzimidazole cores can be included in ligand design. Several open chained molecular clefts with benzimidazole motif as end groups can be created using the general receptor design. Using the benzimidazole core, we have successfully synthesized few unsymmetrical macrocycles. Symmetrical macrocycles can also be prepared using various spacer (Chart 4).

**Table 17.** Amino acids employed in enantioselective sensing studies and their respective enantiomeric fluorescent difference ratio.

Amino Acid <sup>a</sup>	( $\Delta I/I_0$ )max	Ef
Ala	1.50	1.52
Phe	1.58	1.68
Pro	1.44	1.61
Ser	2.60	4.04
Met	1.44	1.33

<sup>a</sup> Methionine (Met), Proline (Pro).

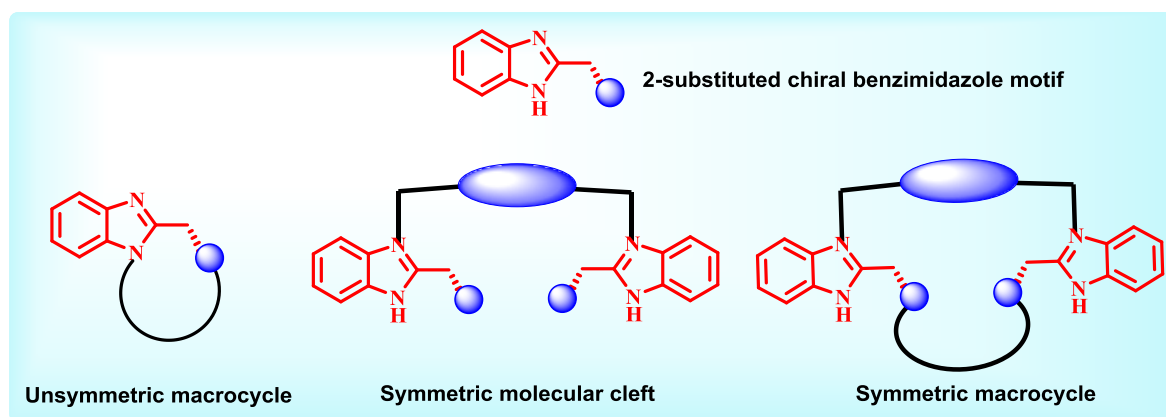


**Chart 4.** General design of benzimidazole containing hosts.

Recently, our group [36] has synthesized the chiral benzimidazole-based receptors (Figure 13), mono aza-15-crown-5 **181**, monoaza-[18]crown-6 (*S,R*)-**182**, (*S,S*)-**183**, and [18]crown-6-sized aza-crown **184**.

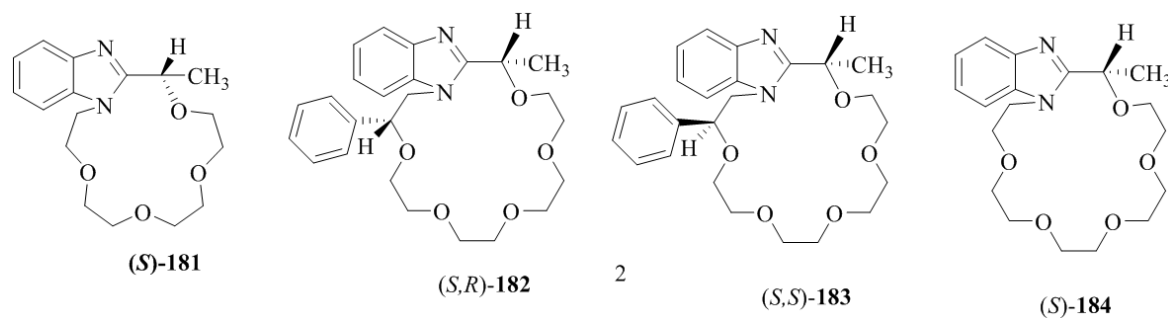


**Figure 13.** Chiral benzimidazole-based receptors **181**–**184**.

Supramolecular interactions between the aza-crown host, **181** and enantiomerically pure amine guests in the ionic and neutral forms displayed the enantio-discrimination ability for phenylethyl

amine and naphthylethyl amine. However, the reversed enantioselective binding was observed for [18]crown-6, aza-crowns (*S,R*)-**182**, (*S,S*)-**183** and (*S*)-**184**.

This was the first report which revealed the opposite steric preferences in chiral supramolecular systems. The experimental study was supported by single-crystal XRD data (Figures 14 and 15) and DFT studies. Size-dependent pre-organization effects leading to the corresponding molecular models was invoked to explain the origins of size-dependent enantioselective binding in aza-crowns (*S,R*)-**182**, (*S,S*)-**183** and (*S*)-**184** and (*S*)-**181**. It was established that these effects influence the preferences for guests with the opposite absolute configuration. Numerous known components, in particular nonbonding interactions responsible for the effective enantioselective binding are known, such as ligating size, hydrogen bonding, dipole-dipole interaction, pi-stacking etc. With these findings, an additional component of size-dependent pre-organization effects for the effective binding of enantiomeric guests was introduced.

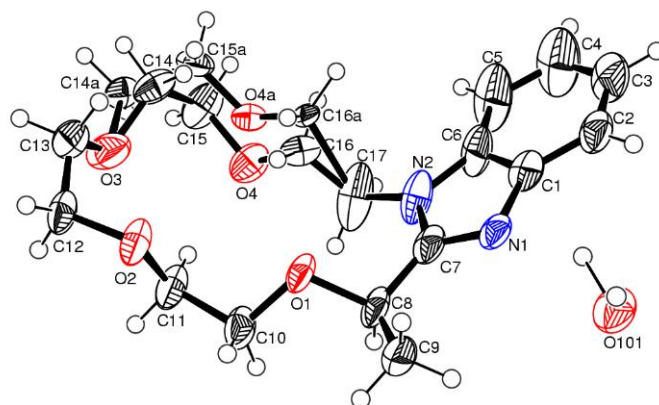


Figure 14. ORTEP representation of the X-ray crystal structure of **181**.

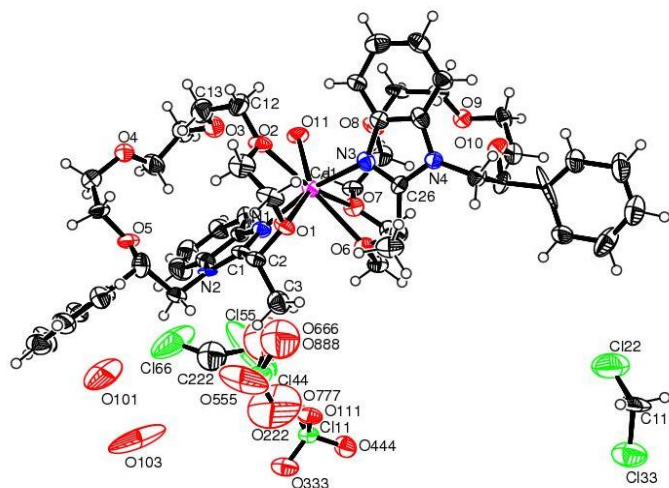
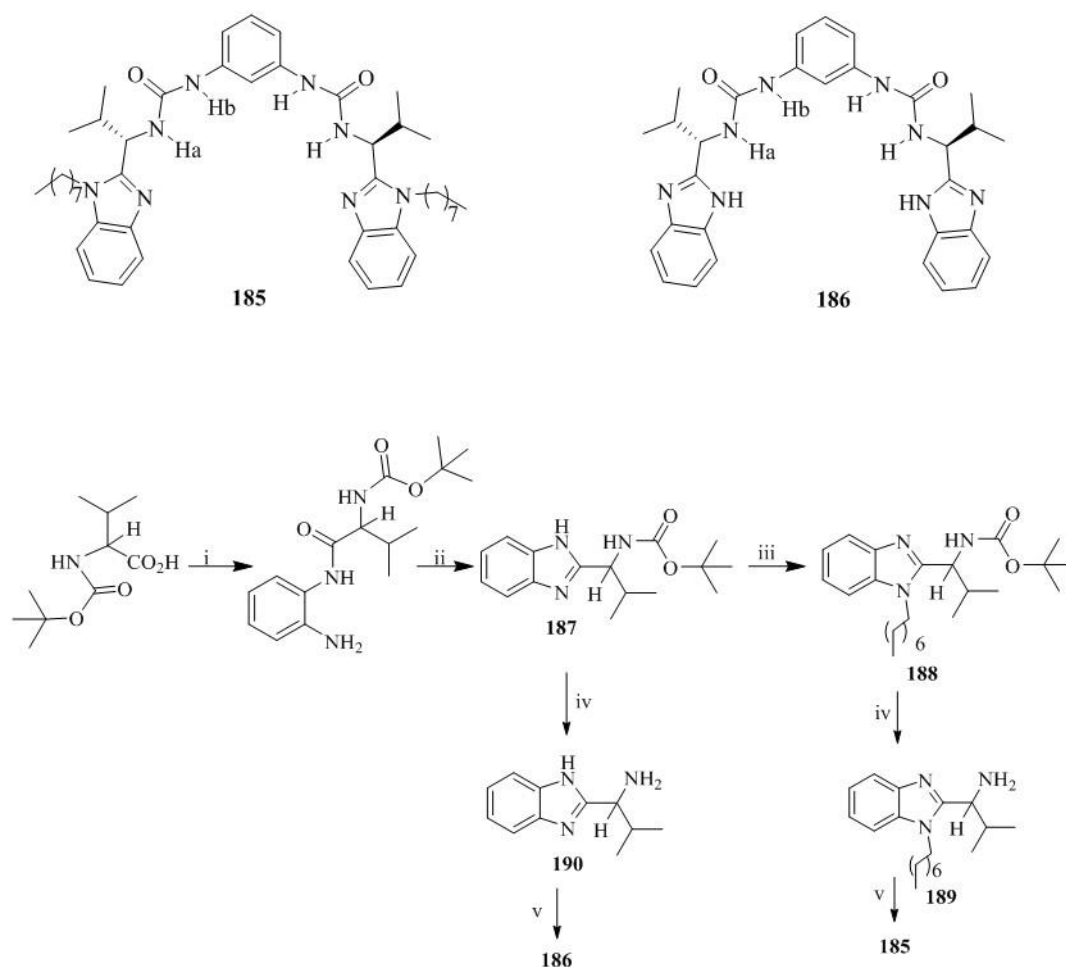


Figure 15. ORTEP diagram of the  $\text{Cd}^{2+}$  complex of (*S,R*)-**182**. Ellipsoids are given at the 50% probability level.

Ghosh et al. [81] prepared the L-Valine derived benzimidazole-based bis-ureas, **185** and **186**, according to the procedure illustrated in Scheme 33. Alkylation of the ring nitrogen of chiral benzimidazole, **187** yielded **188** and subsequent deprotection afforded the **189**. Coupling of **189** with 1,3-diisocyanatobenzene furnished the desired compound, **185**, whereas deprotection of **187** gave **190** followed by the treatment with 1,3-diisocyanatobenzene to obtain compound **186**.



**Scheme 33.** Reagents and conditions (i) *o*-phenylenediamine, DCC, DMAP, stirred in  $\text{CH}_2\text{Cl}_2$  for 19 h; (ii) AcOH, heat, 2 h; (iii) NaH, THF, *n*-octyl bromide, heat 4 h; (iv) 50% TFA in  $\text{CH}_2\text{Cl}_2$ , stirred for 3 h; (v) 1,3-dicyanatobenzene, *N,N*-diisopropyl ethylamine stirred in  $\text{CH}_2\text{Cl}_2$  for 9 h.

The fluorescence titration of **185** was performed with the tetrabutylammonium salts of tartaric and mandelic acids. The receptor, **185** exhibited clear fluorometric discrimination for D and L tartarates, while a low level of discrimination was found for mandelates. Interestingly, the compound, **186** exhibited a small preference for D-tartrate with the enantiomeric fluorescence difference ratio (ef) of 1.44, which signifies the steric crowding around the binding zone in **185** as the key feature for its enantioselective sensing of tartrate.

Katagiri et al. [82] reported a new achiral host on the basis of Cu(II) complex of pyridine-benzimidazole, **192**,  $[\text{Cu}(\text{bmb-bpy})(\text{H}_2\text{O})(\text{OTf})_2]$  where (bmb-bpy = 6,6'-bis[(1-methylbenzimidazol-2-yl)thio)methyl]-2,2'-bipyridine) (Figure 16) for the enantioselective and chemoselective recognition of chiral carboxylic acids. Hence, the binding of chiral carboxylic acids, 2-phenylbutyric acid (PBA), 2-phenylpropionic acid (PPA), 2-bromopropionic acid (BPA) and *N*-*boc*-2-piperidinecarboxylic acid (PCA) to  $[\text{Cu}(\text{bmb-bpy})(\text{H}_2\text{O})(\text{OTf})_2]$  produced an exciton-coupled circular dichroism signal. The (*R*)-PBA, (*R*)-PPA, (*R*)-PCA gave the positive first Cotton effect and negative second Cotton effect, while (*S*)-showed the negative first Cotton effect and positive second Cotton effect. Further, the opposite (*S*) enantiomers exhibited the mirror image relationship. The linear discriminant analysis (LDA) allowed the assignment of the absolute configuration, the five replicates for the each enantiomers of each carboxylic acids were analyzed at four different wavelength (333, 313, 295, and 285 nm). The LDA plot of chiral carboxylic acids with a positive first Cotton effect appear at a negative position on F1-axis, whereas the plots of the negative first Cotton effect appear at a positive

position. A stronger CD intensity shows a larger absolute value of F1, whereas a weaker CD intensity shows a smaller absolute value. F2-axis shows a small difference in the CD profile for each sample. Furthermore, enantiomeric excess of chiral carboxylic acids, have established using the eight unknown samples in the range of  $-100\%$  (S) to  $+100\%$  (R) plotted on the calibration line with linear regression.

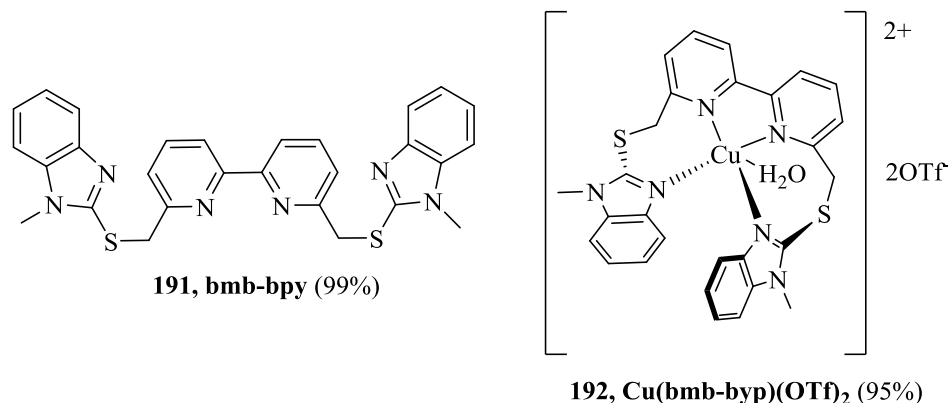


**Figure 16.** Pyridine-benzimidazole-based host **191**, **192**.

### 6.3. Triazole Ring Containing Receptors

Triazole has both pyridine and pyrrole type of nitrogens and satisfactory basic character. The chiral center can be easily attached by N-alkylation or N-acylation reactions. Presence of multiple ligating centers and aromatic nature were good enough reasons to attract attention of chiral chemists. Triazole linked hosts are considered to be better chelators for chiral guests for its electron rich nature due to the presence of three nitrogen atoms adjacent to each other. As per reports, the orientation of nitrogen atom at the third position is important for chiral discrimination of amino acids [69]. The general structural design existing in the triazole based receptors discussed in this report, incorporates one or more triazole motifs at terminal ends separated by a chiral spacer to form a molecular cleft. Triazoles could be further attached to chiral arms which function as chiral discriminators. Few macrocyclic receptors are also prepared in which triazoles are placed in macrocyclic cavity, with nitrogen atoms facing inwards to enable participation during recognition events. (Chart 5).

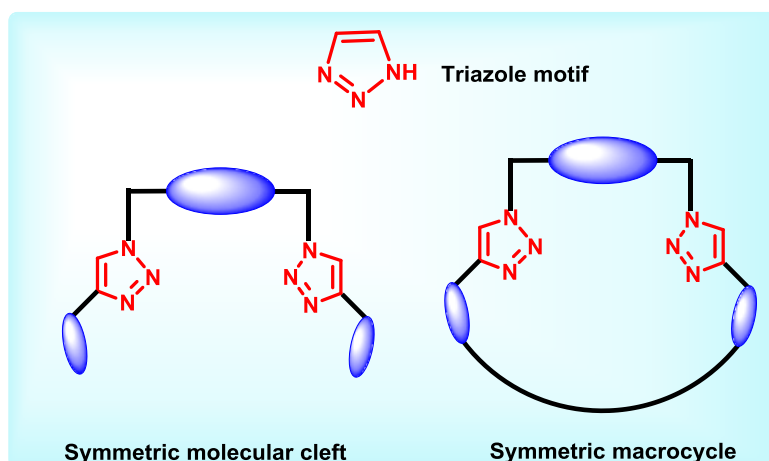


**Chart 5.** General design of triazole containing hosts.

Sato et al. [83] synthesized the new triazole linked hosts, (**193**, **194**) (Figure 17) by versatile, rapid and high yield copper catalyzed Huisgen-1,3-dipolar cycloaddition (Click Chemistry) of linker azide with saccharide alkyne. These two compounds, **193**, **194** then were investigated for the chiral



recognition ability. It was established that the orientation of nitrogen atoms at the 3-position of triazole rings was the most important factor for the enantiodiscrimination of amino acid esters. Thus, UV titrations revealed the triazole linked host **193** exhibited the chiral recognition preference for (*R*)-alanine isopropyl ester with  $K_R/K_S = 2.13$  and for host **194** the strong complexes were formed with both the enantiomers of alanine isopropyl ester but no enantioselectivity observed. Further, the similar recognition ability of alanine isopropyl ester by the host **193** and **194** corroborated by the Fast Atom Bombardment Mass spectroscopy method.

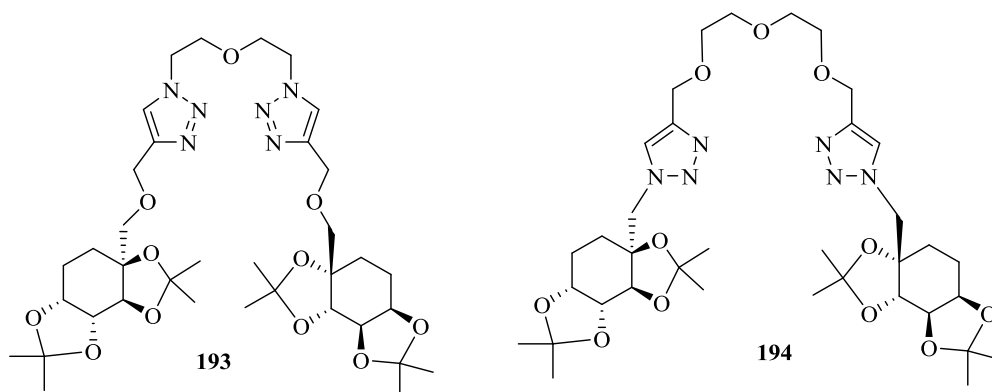
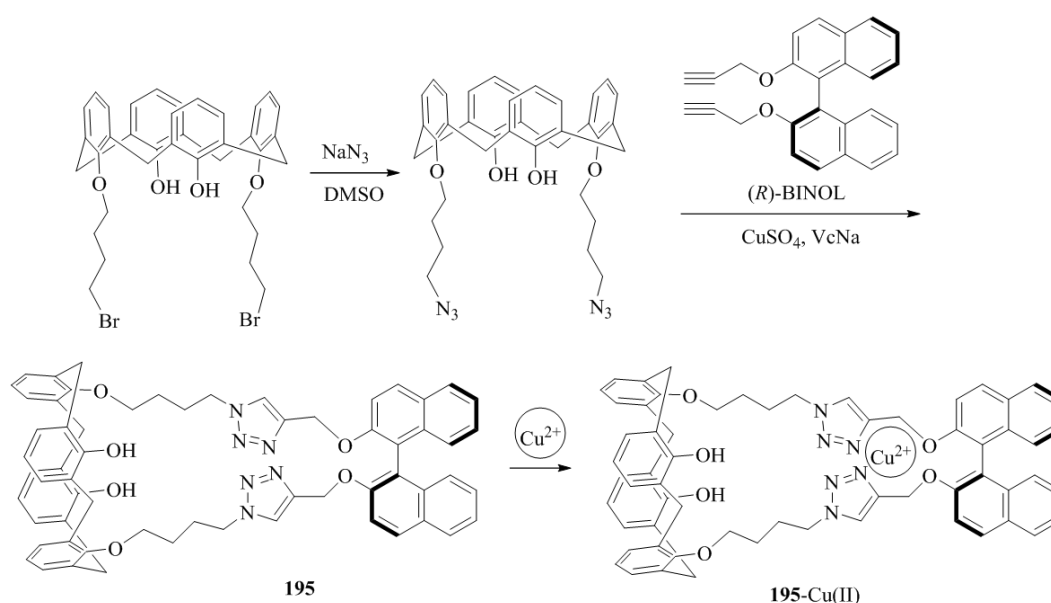


Figure 17. Triazole linked host compounds, **193** and **194**.

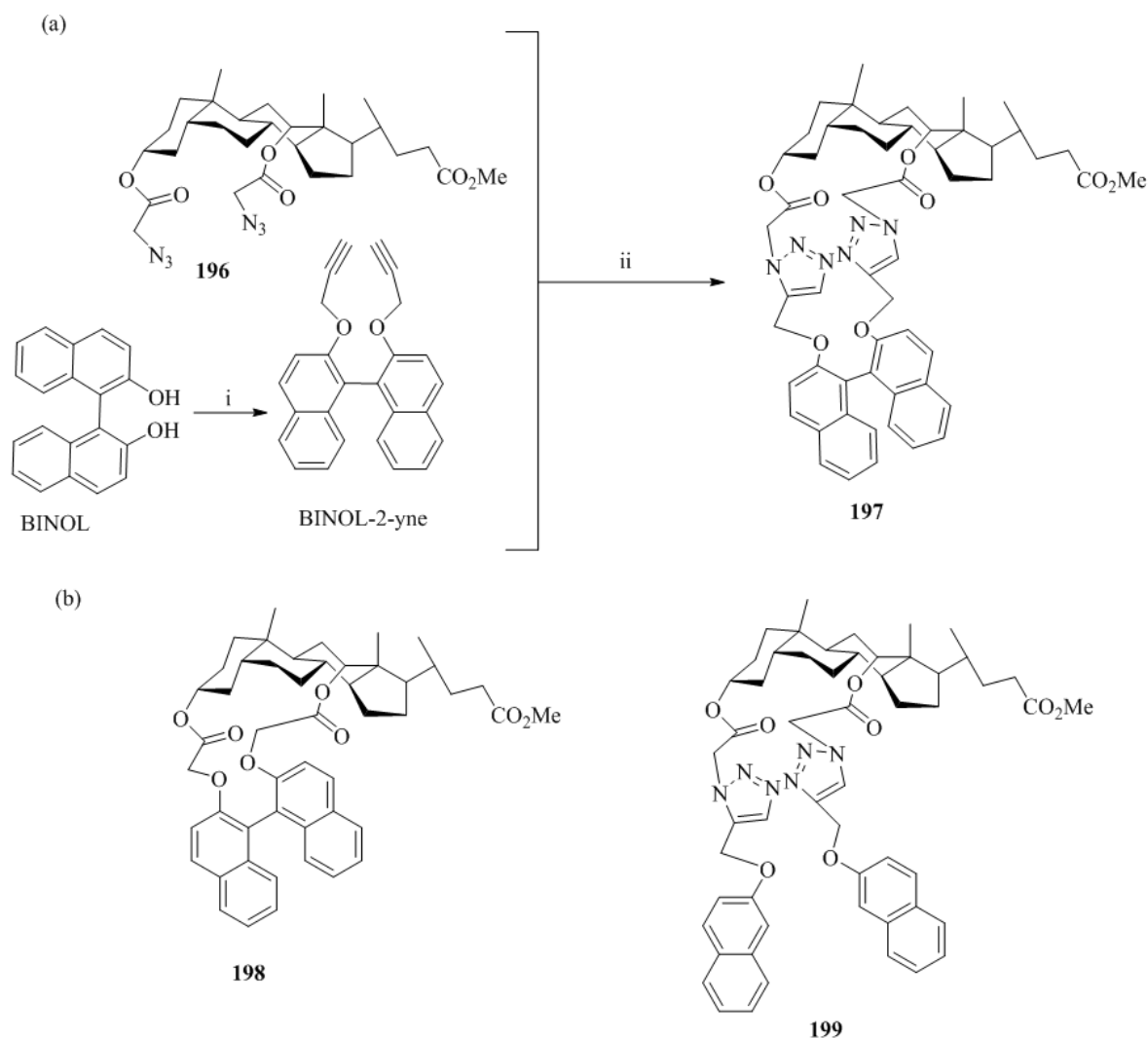
Li et al. [84] synthesized the fluorescent calix-[4]arene bearing a chiral 1,1'-bi-2-naphthol unit-based receptor, **195** (Scheme 34). The in situ generated complex Cu(II)-**195** were evaluated for the chiral discrimination of performance of the, (*R*)- and (*S*)-Mandelic acid using fluorimeter. The fluorescent intensity of Cu(II)-**195** complex upon addition of (*R*)-Mandelic acid increased 6.35 fold and with (*S*)-Mandelic acid increased up to 4.87 fold. Thus, the enantiomeric fluorescence difference was found to be 1.69. The tartaric acid and malic acid were also investigated and showed the increased in the fluorescence intensity for *R* enantiomers over the *S* enantiomers. Further, by using the dynamic light scattering, for mandelic acid a remarkable 100-fold detection sensitivity was increased with the detection limit of  $2.0 \times 10^{-7}$  M as compared to fluorescent method.



Scheme 34. Synthesis of calix-[4]arene, **195** bearing a chiral 1,1'-bi-2-naphthol and its Cu complex.



Ju et al. [85] synthesized **197** (Cyclic Deoxycholate-Triazole-BINOL conjugate) (Scheme 35) from azido-deoxycholic acid ester **196** and BINOL-2-yne via the “CuAAC” click reaction. This macrocycle is able to serve as a fluorescent turn-off sensor for  $\text{Hg}^{2+}$  ion due to the 1,2,3-triazole motif, which has an outstanding binding ability to transition metal ions. Furthermore, the corresponding  $[\mathbf{197} \cdot \text{Hg}^{2+}]$  complex exhibited recognition ability for amino acids with certain enantioselectivity (Table 18). Hence, L-amino acids showed larger  $K_a$  as compared to D-amino acids. The stronger interaction of  $[\mathbf{197} \cdot \text{Hg}^{2+}]$  complex with L-amino acids than with D-amino acids is a result of the chiral spatial structure provided by the deoxycholic acid scaffold.



**Scheme 35.** (a) Synthesis of **197**; (b) Structure of control molecules **198** and **199**.

**Table 18.** Association constants between  $[\mathbf{197} \cdot \text{Hg}^{2+}]$  or  $[\mathbf{199} \cdot \text{Hg}^{2+}]$  complex and amino acids.

Amino Acids	$[\mathbf{197} \cdot \text{Hg}^{2+}]$			$[\mathbf{199} \cdot \text{Hg}^{2+}]$		
	$K_L$ ( $10^5 \text{ M}^{-1}$ )	$K_D$ ( $10^5 \text{ M}^{-1}$ )	$K_L/K_D$	$K_L$ ( $10^5 \text{ M}^{-1}$ )	$K_D$ ( $10^5 \text{ M}^{-1}$ )	$K_L/K_D$
Ala	1.284	1.252	1.026	0.4664	0.4646	1.004
Val	1.226	1.199	1.023	0.4358	0.4352	1.001
His	2.201	2.002	1.100	0.8610	0.8455	1.018
Cys	2.510	2.121	1.183	1.630	1.616	1.008
Met	2.032	1.841	1.104	0.7667	0.7764	0.9875

#### 6.4. Benzo-Fused Furan Heterocycles Containing Receptors

Benzo-fused furans are electron rich units and hence are expected to exhibit anisotropic effects due to the presence of ring current. There are innumerable heterocycles containing benzo-fused furans. The use of this heterocyclic unit in stereo-discrimination reactions are very few. One solution to this situation was to incorporate this unit in receptors with different elements of chirality, such as the presence of chiral axis.

The benzofuran containing hosts are bestowed with excellent fluorescence properties and hence are ideal substrates for development of fluorescent sensor. Our group has designed and synthesized several interesting receptors with benzofuran motifs. The receptors discussed here originate from synthetically simple benzofuran motif which are axially linked or helically linked benzofuran rings (Chart 6). Benzofuran units can be used as a synthon to prepare crowded binols and the free hydroxyl groups of the furo fused binols can be exploited to synthesize macrocycles.

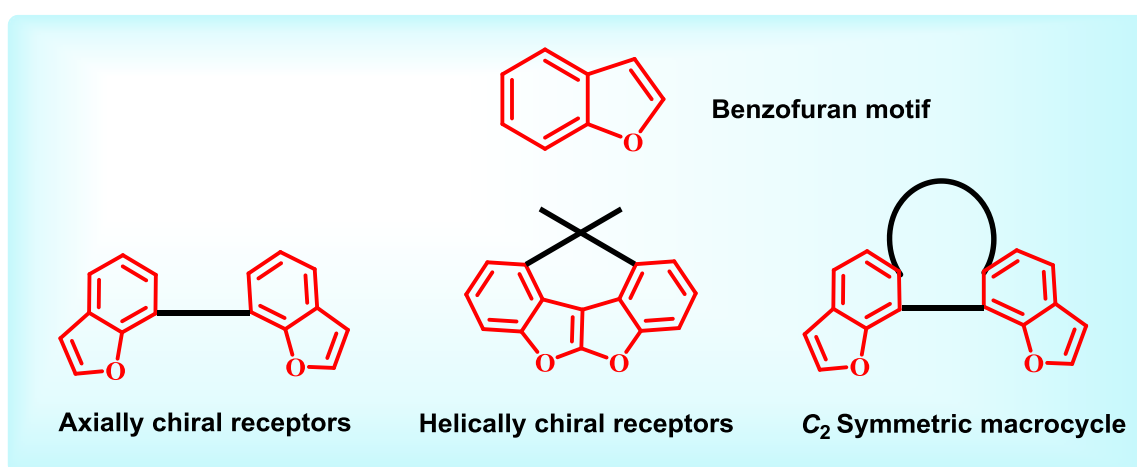
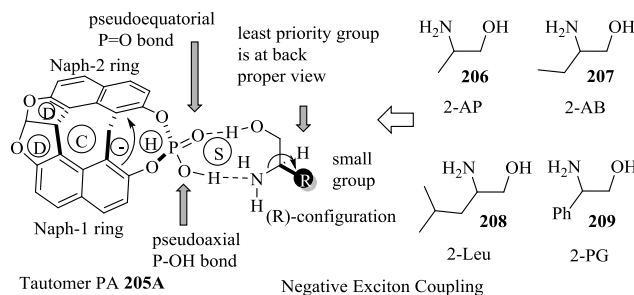
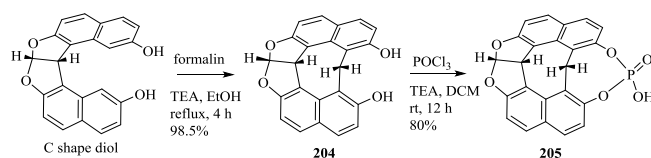
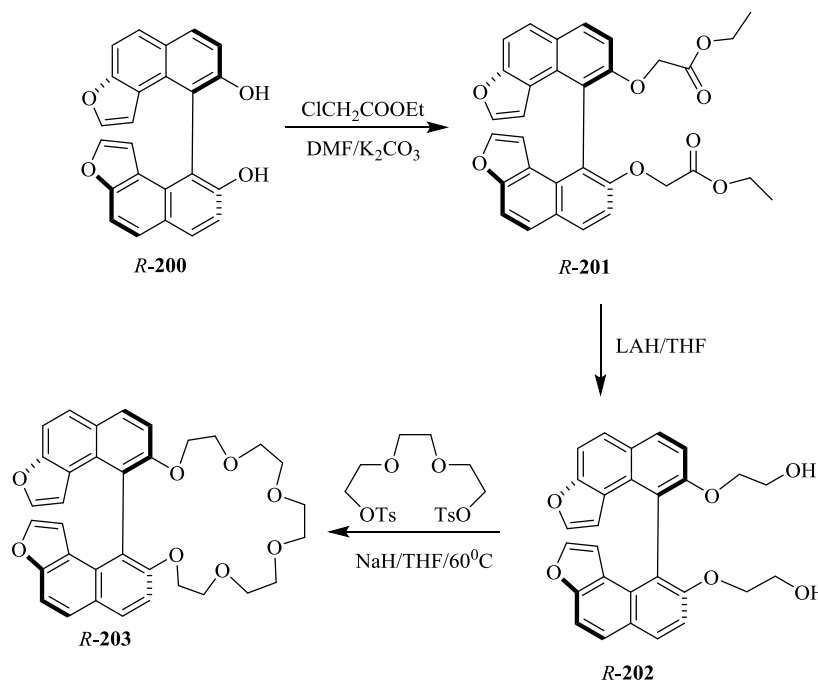


**Chart 6.** General design of benzofuran containing hosts.

Our group [86–89] synthesized several furan ring incorporated chiral receptors. In 2007 [37] the synthesis of chiral furo fused BINOL-based crown ether, (*R*)-**203** has been reported (Scheme 36). Parent furo fused BINOL, **200** was alkylated with ethyl chloroacetate followed by the corresponding reduction and treatment with triethylene glycol tosylate to yield (*R*)-**203**.

The furo-fused BINOL derivative (*R*)-**203** has the following special features: *C*<sub>2</sub> symmetry, a sufficiently enlarged dihedral angle for better stereo-discrimination and modified electronic properties as compared to BINOL. This macrocycle (*R*)-**203** was useful as an enantioselective chiral sensor for phenylethylamine and ethyl ester of valine. Fusion of furan to BINOL resulted in a highly stereodiscriminating backbone for the chiral crown moiety. This receptor, (*R*)-**203** exhibited fluorescence enhancement differences of 2.97 and 2.55 times between two enantiomers of phenylethylamine and ethyl ester of valine, correspondingly. The ratio of association constants for two diastereomeric complexes on the basis of two enantiomers of these guests was found to be 11.30 and 7.02, respectively.

Further in 2016 [25] the *Cs*-symmetric rigid organophosphoric acid host, **205** (Scheme 37) was developed by the treatment of helicene diol [72], **204** with phosphoryl chloride and explored for the supramolecular induced circular dichroism sensing of chiral amino alcohol. The study revealed that the rigidity of tautomers, **205A** (Figure 18) or **205B** (Figure 19) and bulkiness of chiral amino alcohols were responsible for the resultant ICD signals (Table 19).



In the case of amino alcohols, **206–209** (Figure 18) with small substituents such as  $-\text{CH}_3$ ,  $-\text{C}_2\text{H}_5$ , or  $-\text{CH}_2\text{CH}(\text{CH}_3)_2$  present at the stereogenic center, the tautomer **205A** of achiral phosphoric acid **205** is preferred. This could be possible due to cooperative hydrogen bonding, amino group of guest accepts the acidic hydrogen  $\text{P}-\text{O}-\text{H}$  of **205A**, occupying a pseudoaxial position, whereas the alcohol part of the chiral guest acts as a hydrogen bond donor to  $\text{P}=\text{O}$  of the PA group, with a pseudoequatorial position on the H ring. The resultant nine membered spirocyclic hydrogen-bonded S ring is able to transfer the information on the R/S configuration at the stereogenic center of guest to host via H ring, directly attached to the chromophores, exhibited the corresponding ICD signal (negative exciton coupling). The R-enantiomers of chiral amino alcohol gave the negative sign in the ICD spectrum while S-enantiomer exhibited the mirror image.

Intriguingly, the chiral amino alcohols, **210–213** (Figure 19) with bulky substituent at the stereogenic center on interaction with the achiral phosphoric acid preferred the 189B tautomer to result into reversed induced CD pattern to the amino alcohols with small substituent at stereogenic center. This is attributed owing to the amino group of guest hydrogen bonded with an acidic P–O–H group, occupies a pseudoequatorial position. Simultaneously, the –OH group acts as hydrogen bond donor to the P=O group of **205B** and occupies a pseudoaxial position to the rigid, conformationally locked H ring, the newly formed. Resulted complex of host and guest able to transfer the chiral information of guest by the S-ring to H ring and to the chromophore of the host to induced the signals in the CD. Thus, this mechanistic demonstration exemplified the binding mode of the host dependent on the bulk of the substituent present at stereogenic center of guest chiral amino alcohols.

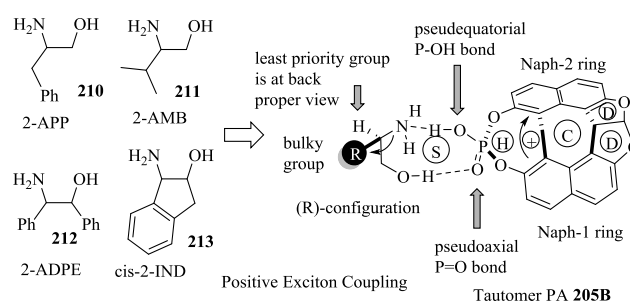


**Figure 19.** Proposed exciton coupling model for amino alcohols, **210–213** having bulky R group, binding with tautomer, **205B**.

Complexation of host phosphoric acid, **205A** mode, with guest, **206** (2-AP) gave the highest  $\Delta \epsilon$  value at  $498.65 \text{ cm}^{-1} \text{ M}^{-1}$ . Similarly, the 205B mode resulted in highest  $\Delta \epsilon$  value of  $641.13 \text{ cm}^{-1} \text{ M}^{-1}$  for **211** (2-AMB) (Table 19).

**Table 19.** ICD Results for Amino Alcohols, **206–213** with **205**.

Guests	First CE	Second CE	$\Delta \epsilon (\text{cm}^{-1} \text{ M}^{-1})$	$g = \Delta \epsilon / \epsilon \times 10^{-3}$ (at First CE)	Binding Mode
(R)- <b>206</b>	–	+	498.65	35.9	A
(R)- <b>207</b>	–	+	121.10	15.16	A
(R)- <b>208</b>	–	+	85.48	10.8	A
(R)- <b>209</b>	–	+	7.12	10.0	A
(R)- <b>210</b>	+	–	124.66	10.5	B
(R)- <b>211</b>	+	–	641.13	9.3	B
(1R,2S)- <b>212</b>	+	–	4.63	0.1	B
(1R,2S)- <b>213</b>	+	–	3.21	0.4	B

Subsequently in 2017, [48] Hasan et al. developed the dioxo[6]helicenes-based supramolecular chirogenic system (**214**) for chiral recognition of enantiopure *trans*-1,2-cyclohexanediamine (Figure 20). The host, **214** was obtained using the reaction of dioxo[6]helicenes and (1S)-camphanic chloride and the enantioselective fluorescence study revealed that **214** serves as a turn-on fluorescent sensor for *trans*-cyclohexyl diamine with the excellent enantioselective factor,  $\alpha = K_{SS}/K_{RR} = 6.3$  in benzene as a solvent.

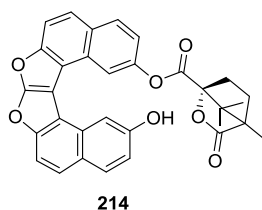


**Figure 20.** Helicene camphanate.

### 6.5. Receptors with Nitrogen and Oxygen Containing Five Membered Heterocycles

Chiral Oxazolines and oxazolidinones have played one of the most noticeable roles [90,91] in chiral processes, by providing Evans' chiral auxiliaries, chiral organo-catalysts and chiral metal-based catalysts. The use of these molecules in the chiral receptors has received some attention. Oxazoline coordinates to a wide range of transition metals. Stereochemical outcome of the metal catalyzed reaction is strongly governed by the favorable placement of stereogenic centre, the chelating nitrogen atom of oxazoline ligand and the metal ion.

The oxazoline based  $C_3$ -symmetric receptors discussed in this report have tripod like structures with terminal oxazolines or in another case, the free arms of the tripod linked to benzene motif, forming a molecular cage (Chart 7). The types of interactions which are observed in such hosts are  $\pi$ - $\pi$  interactions due to aromatic oxazoline rings and tripodal hydrogen bonding interactions due to the flexible arms containing oxazolines.

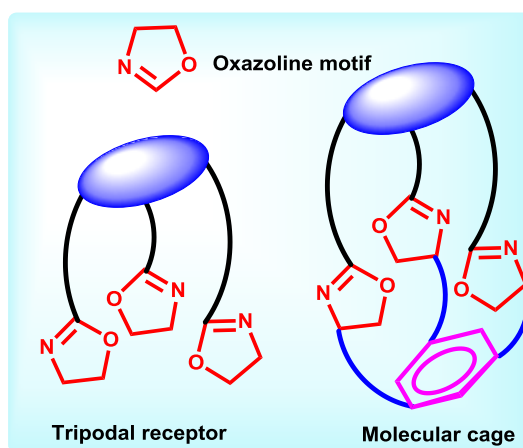


Chart 7. General design of oxazoline containing receptors.

In 2003, Ahn et al. [22] developed the benzene-based tripodal  $C_3$ -symmetric oxazoline receptors, **215a–c** (Figure 21) for the chiral molecular recognition of  $\alpha$ -chiral primary ammonium ions (Table 20). Surprisingly, a good level of the enantioselectivity was observed by one of the receptors **215a**, as it provides the  $C_3$  symmetric chiral environment on guest binding. The general results of chiral discrimination for  $\alpha$ -substituted guests revealed that the  $\pi$ - $\pi$  interaction is an important factor. Binding studies using NMR and isothermal titration calorimetry confirmed the host guest complexes formation influenced by the enthalpy changes and minor negative contribution of entropy changes.

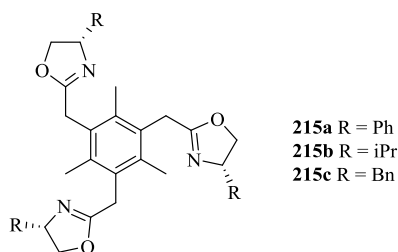


Figure 21.  $C_3$ -symmetric oxazoline receptors, **215a–c**.

The same group [92] later established the use of  $C_3$  symmetric receptor, **215a** for the enantioselectivity of  $\beta$ -chiral primary ammonium ions by utilizing a bifurcated H-bonding. Further, the extraction experiments confirmed that this interaction plays a crucial role in the chiral discrimination between the host and guest. The X-ray data proved the existence of such H-bonding.

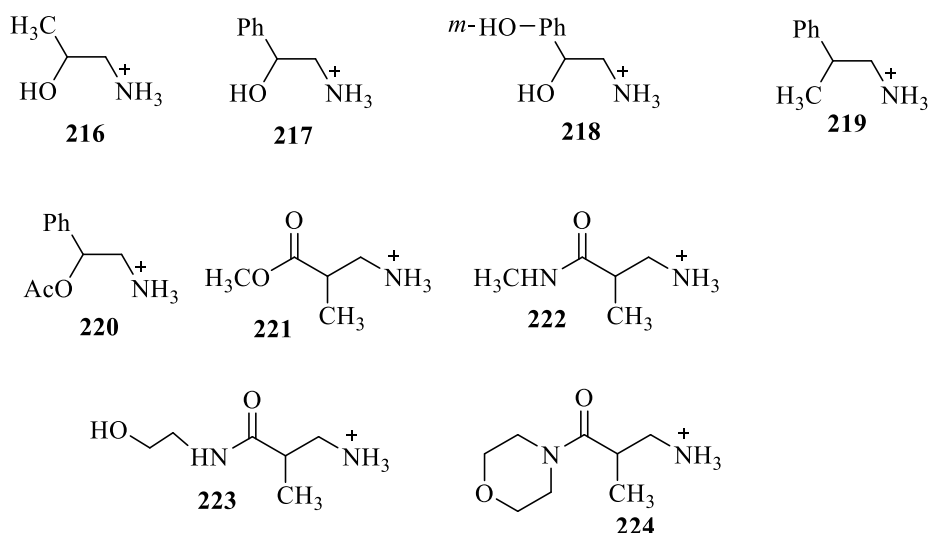
Hence, this article demonstrated that this type of binding is suitable for the chiral molecular recognition with  $C_3$ -symmetric tripodal oxazoline receptors and further extended toward ammonium ions of  $\alpha$ -,  $\beta$ -, and  $\alpha$ ,  $\beta$ -chiralprimary amines Tables 21 and 22.

**Table 20.** Enantioselective binding of Tris(oxazoline), **215a** toward Racemic Ammonium Salts.

Racemic Ammonium Guest	Enantioselectivity <sup>a</sup>	Extraction (%) <sup>b</sup>
$\alpha$ -phenylethylamine	71(R):29(S)	82
$\alpha$ -(1-naphthyl)ethylamine	70:30	99
Phenylglycine methyl ester	78(S):22(R)	60
Tryptophan methyl ester	67(S):33(R)	57 <sup>c</sup>
Alanine methyl ester	53(S):47(R)	41
Phenylalanine methyl ester	55(S):45(R)	36

<sup>a</sup> Enantioselectivity of the ammonium ion extracted from excess racemic salts ( $\text{RNH}_3^+\text{Cl}^-$ , 10 M equivalent, 0.5 M in  $\text{D}_2\text{O}$ ; 0.6 M  $\text{NaPF}_6$ ) by tris(oxazoline) **215a** (0.05 M in  $\text{CDCl}_3$ ) at 25 °C. <sup>b</sup> Percentage of the ammonium salts extracted into  $\text{CDCl}_3$  with respect to tris(oxazoline) **1a**. <sup>c</sup> Extraction at 45 °C.

**Table 21.** Selective binding of **215a** toward racemic ammonium salts of  $\beta$ -chiral amines, **216–224**.



Entry	Racemic Guest	Enantioselectivity <sup>a</sup>	Extraction (%) <sup>b</sup>
1	<b>216</b>	63:37 <sup>c</sup>	50
2	<b>217</b>	75:25	60
3	<b>218</b>	72:28	40
4	<b>219</b>	50:50	97
5	<b>220</b>	58:42	72
6	<b>221</b>	58:42	71
7	<b>222</b>	71:29	<5
8	<b>223</b>	61:39	10
9	<b>224</b>	83:17	<5

<sup>a</sup> Enantiomeric ratio of the extracted guest from excess racemic salts (10 M equiv., 0.5 M in  $\text{D}_2\text{O}$ ) by PhBTO **215a** (0.05 M in  $\text{CDCl}_3$ ) at 25 °C. <sup>b</sup> Percentage of the ammonium salt extracted into  $\text{CDCl}_3$  with respect to PhBTO **215a**.

<sup>c</sup> Major: (R)- isomer.

Removing the  $\beta$ -OH group from **225**, as in **226** or **227**, (Figure 22) results in low enantioselectivities, hence indicating that the secondary H-bond interaction is critical to secure the necessary environment for chiral discrimination as confirmed by the crystallographic structure of the corresponding **215–225** complex.

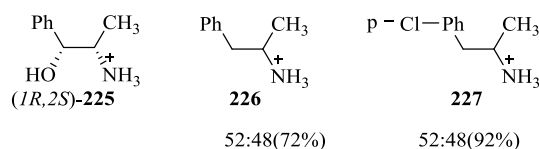
**Table 22.** Selective Binding of **215** toward Racemic Ammonium Salts of  $\alpha$ -alkyl-substituted Chiral Amine.

228                      229

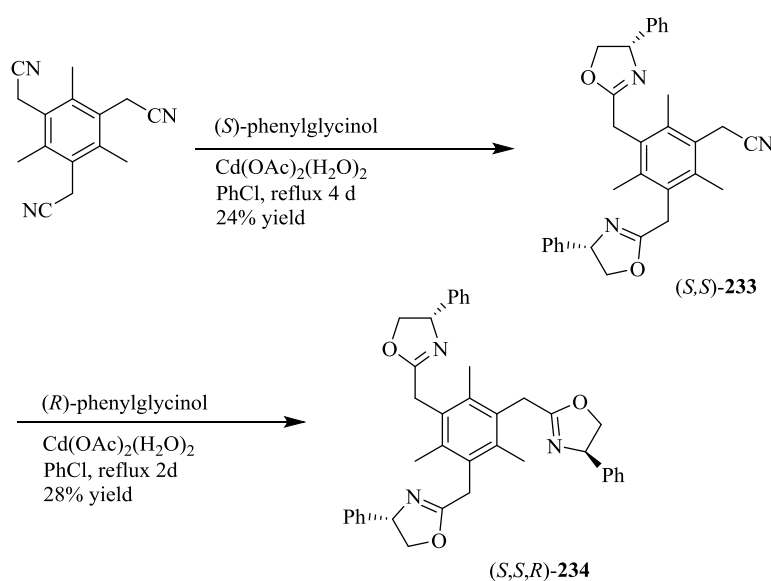
230                      231                      232

Entry	Racemic Guest	Enantioselectivity	Extraction (%)
1	<b>228</b>	66:34 <sup>c</sup>	74
2	<b>229</b>	61:39	20
3	<b>230</b>	56:44	26
4	<b>231</b>	53:37 <sup>c</sup>	41
5	<b>232</b>	55:45 <sup>c</sup>	36

<sup>a</sup> Enantiomeric ratio of the extracted guest from excess racemic salts (10 M equiv., 0.5 M in D<sub>2</sub>O) by **215** (0.05 M in CDCl<sub>3</sub>) at 25 °C. <sup>b</sup> Percentage of the ammonium salt extracted into CDCl<sub>3</sub> with respect to **215**. <sup>c</sup> Major: (S)-isomer.

**Figure 22.** Chiral ammonium analytes, **225–227**.

In the next article [93] the development of a benzene-based tripodal oxazoline receptor with C<sub>1</sub>-symmetry, **234** upon changing the symmetry of chiral environment from C<sub>3</sub> to C<sub>1</sub> was reported (Scheme 38). The synthetic strategy was based on the coupling of tris-(cyanomethyl)mesitylene with (S)-phenylglycinol in the presence of 5 mol % Cd(OAc)<sub>2</sub> to furnish (S,S)-bis(oxazoline), **233** and subsequent treatment with (R)-phenylglycinol under the similar reaction conditions afforded (S,S,R)-**234** in 28% isolated yield.

**Scheme 38.** Synthesis of (S,S,R)-**234**.

Subsequently, **234–237** were explored for the chiral discrimination by using extraction experiment. The tripodal receptors with two phenylglycinol-derived oxazolines displayed significant enantioselectivity for racemic  $\alpha$ -chiral ammonium ions (Table 23, entries 1–8). It was revealed that the changing receptor's symmetry, from  $C_3$  to  $C_1$ , causes intense improvement in the binding mode and chiral recognition. Table 24 shows that **234** was more enantioselective than other hosts, but less selective than **235**. However, **234** gave significantly lower values of the % extraction than other receptors. Furthermore, the receptor **236** and **237** (Figure 23) extracted (*S*)- $\alpha$ -phenylethylammonium ion preferentially over the (*R*)-guest demonstrated the reverse sense of the chiral discrimination in comparison with that of **234**.

**Table 23.** Enantioselective Extraction Experiments Using **234–237** towards  $\alpha$ -Chiral Organoammonium Guests.

Entry	Receptor	Ammonium Guest	Enantioselectivity	Extraction (%)
1	<b>235</b>	PhCH(NH <sub>3</sub> <sup>+</sup> ) CH <sub>3</sub>	71( <i>R</i> ):29( <i>S</i> )	82
2	<b>235</b>	PhCH(NH <sub>3</sub> <sup>+</sup> ) CO <sub>2</sub> Me	78( <i>S</i> ):22( <i>R</i> )	60
3	<b>234</b>	PhCH(NH <sub>3</sub> <sup>+</sup> ) CH <sub>3</sub>	64( <i>R</i> ):36( <i>S</i> )	51
4	<b>234</b>	PhCH(NH <sub>3</sub> <sup>+</sup> ) CO <sub>2</sub> Me	70( <i>S</i> ):30( <i>R</i> )	22
5	<b>236a</b>	PhCH(NH <sub>3</sub> <sup>+</sup> ) CH <sub>3</sub>	59( <i>S</i> ):41( <i>R</i> )	100
6	<b>236a</b>	PhCH(NH <sub>3</sub> <sup>+</sup> ) CO <sub>2</sub> Me	62( <i>S</i> ):38( <i>R</i> )	91
7	<b>236b</b>	PhCH(NH <sub>3</sub> <sup>+</sup> ) CH <sub>3</sub>	58( <i>S</i> ):42( <i>R</i> )	80
8	<b>236b</b>	PhCH(NH <sub>3</sub> <sup>+</sup> ) CO <sub>2</sub> Me	69( <i>S</i> ):31( <i>R</i> )	69
9	<b>236c</b>	PhCH(NH <sub>3</sub> <sup>+</sup> ) CH <sub>3</sub>	50( <i>S</i> ):50( <i>R</i> )	-
10	<b>237</b>	PhCH(NH <sub>3</sub> <sup>+</sup> ) CH <sub>3</sub>	50( <i>S</i> ):50( <i>R</i> )	70

**Table 24.** Enantioselective Binding of Receptors, **235**, **240a**, and **240b** toward Organoammonium Ions **98** and Ala Methyl Ester.

Receptor-Guest	Temp (°C)	Enantioselectivity	Binding (%) <sup>a</sup>
<b>235</b> -( <i>R,S</i> )- <b>98</b>	25	71( <i>R</i> ):29( <i>S</i> ) <sup>c</sup>	82
<b>240a</b> -( <i>R,S</i> )- <b>98</b>	−30	57( <i>R</i> ):43( <i>S</i> )	~100
	−50	60( <i>R</i> ):40( <i>S</i> )	~100
<b>240b</b> -( <i>R,S</i> )- <b>98</b>	−30		
	−50	61( <i>R</i> ):39( <i>S</i> )	73
<b>235</b> -( <i>R,S</i> )-Ala Methyl ester	25	47( <i>R</i> ):53( <i>S</i> ) <sup>c</sup>	41
<b>240a</b> -( <i>R,S</i> )-Ala Methyl ester	10	61( <i>R</i> ):39( <i>S</i> )	62
	−10	60( <i>R</i> ):40( <i>S</i> )	65
	−30	61( <i>R</i> ):39( <i>S</i> )	67
	−50	64( <i>R</i> ):36( <i>S</i> )	68
<b>240b</b> -( <i>R,S</i> )-Ala Methyl ester	−10	64( <i>R</i> ):36( <i>S</i> )	79
	−30	66( <i>R</i> ):34( <i>S</i> )	83
	−50	72( <i>R</i> ):28( <i>S</i> )	76

<sup>a</sup> Percentage of receptor-guest adduct with respect to unbound guest, calculated for 1 equiv. of receptor.

Further this group [94] reported the preparation of chiral cage-like receptors, **240a** and **240b** (Scheme 39) via the reaction of corresponding 3-hydroxyphenyl-substituted tripodal oxazolines, **238** with capping molecules, **239**. The chiral recognition behavior of **240a** and **240** was studied for two typical chiral guests;  $\alpha$ -phenylethylammonium **98** and alanine methyl ester as  $\alpha$ -aryl- and  $\alpha$ -alkyl substitutedamines by using <sup>1</sup>H NMR (Table 24). However, **240** preferentially binds to (*R*)-**98** with a lower enantioselectivity as compared to **202**. Furthermore, **240** is able to recognize alanine methyl ester with excellent enantioselectivity (7:3), but chiral discrimination is not effective in the case of **235**. The degree of chiral discrimination with the cage-like receptors is distinctive from the open sensors, attributed to narrowed space offered for the guest.



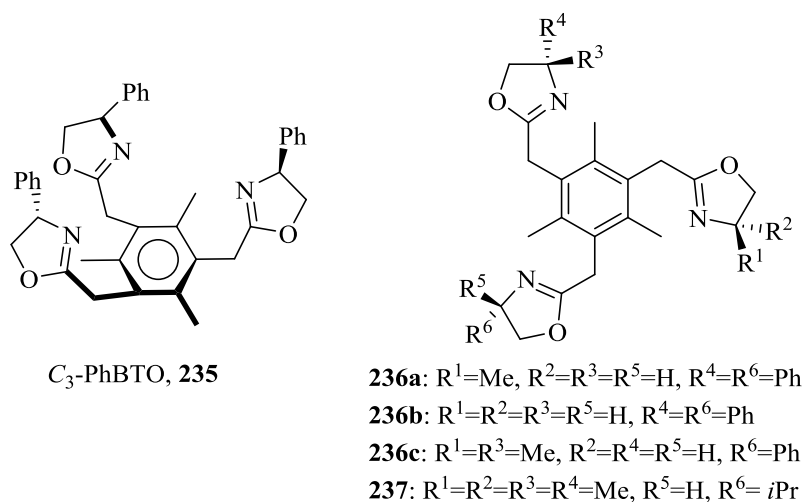
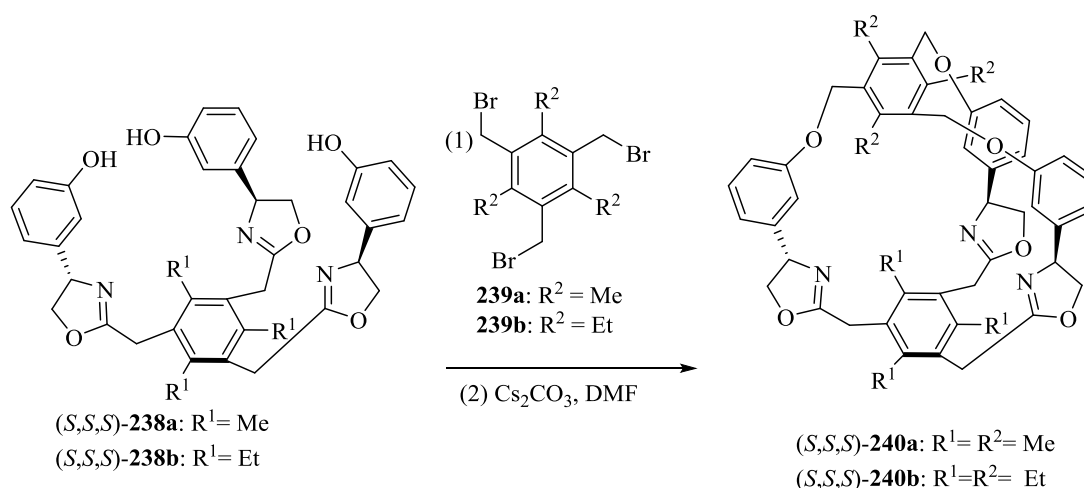


Figure 23. Receptor 235, 236, and 237.



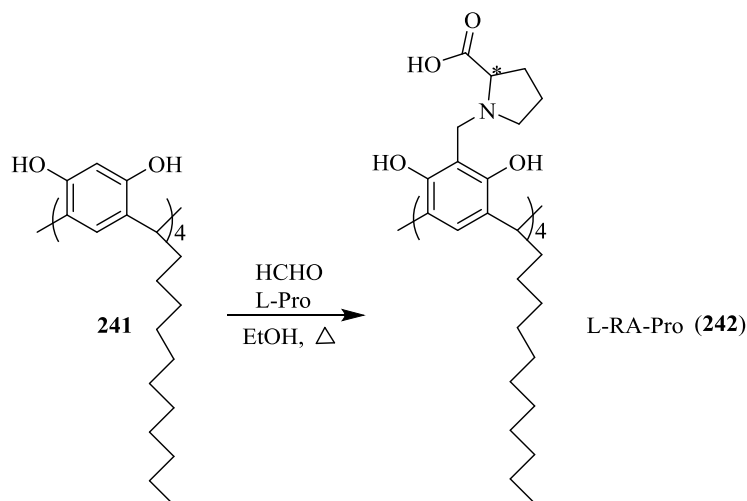
Scheme 39. Synthesis of cage-like receptors, (S,S,S)-240a and (S,S,S)-240b.

## 7. Miscellaneous Heterocyclic Receptors

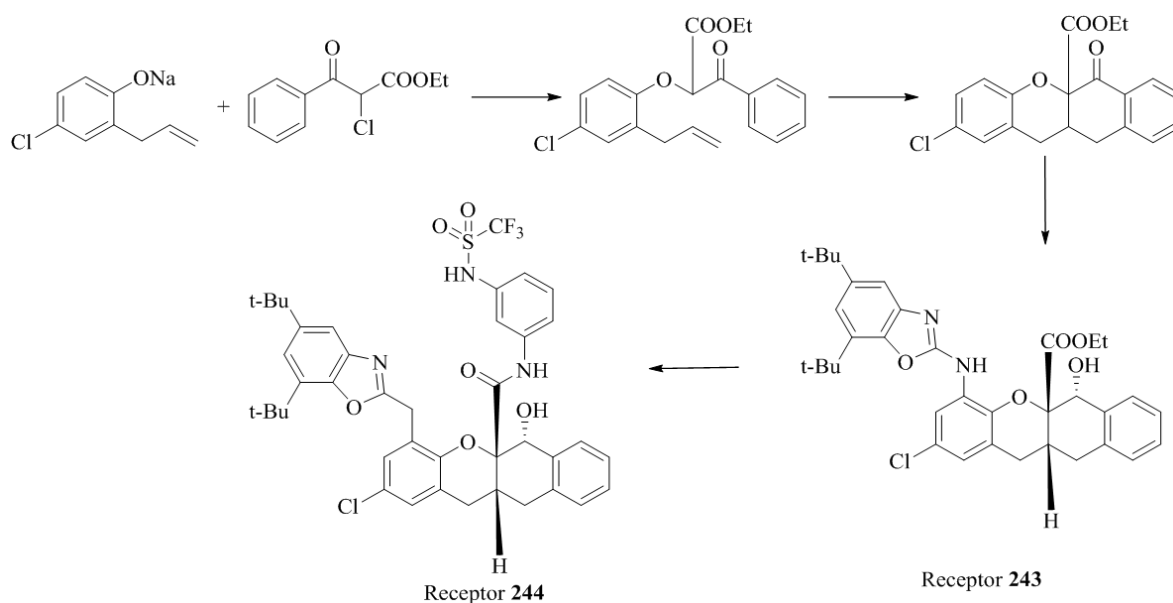
Apart from the heterocycles mentioned above, there exists a group of heterocyclic receptors which have a few but significant experimental findings. Given below is the group of such group used in chiral recognition receptors. Hegner et al. [28] described the synthesis of chiral amphiphilic calix[4]resorcinarene, tetrakis(*N*-methylprolyl)tetraundecylcalix-[4]resorcinarene, **242** (Scheme 40), bearing four *L*-prolyl moieties at the macrocyclic upper rim and four undecyl chains at the lower rim. The methodology consists of the Mannich-type reaction of tetraundecylcalix[4]resorcinarene, **241**, *L*-proline, and formaldehyde to yield the desired product. The supramolecular complex of calixresorcinarene and Cu(II) displayed the enantioselective recognition properties for phenylalanine with the stronger binding for *D*-phenylalanine.

Moran et al. [95] synthesized the *cis*-tetrahydrobenzoxanthene receptors, **243**, **244** by following the synthetic route given in Scheme 41. The binding properties of **243** have been evaluated by <sup>1</sup>H NMR titration with decanoic acid and Cbz-glycine (Cbz = benzyloxycarbonyl) to give  $K_a = 1.2 \times 10^4 \text{ M}^{-1}$  and  $1.5 \times 10^4 \text{ M}^{-1}$ , respectively. However, the titration of a racemic mixture of **243** with the amino acid derivatives, such as Cbz-phenylglycine, exhibited the association ( $K_a = 2.3 \times 10^4 \text{ M}^{-1}$ ) but neither splitting of the <sup>1</sup>H NMR signals of host nor chiral discrimination were observed. Further, the receptor, **243** was converted to **244** by treatment with the lithium salt of *m*-phenylenediamine, followed by the

reaction with trifluoromethanesulfonic anhydride. The titrations of racemic host carried out with enantiomeric pure guests (amino acid derivatives, Table 25), resulted in splitting of the  $^1\text{H}$ -NMR signals of **244**, owing to the chiral discrimination, and confirming significant enantioselectivity for **244**. The racemic receptor, **244** then was treated with ethoxycarbonyl-L-leucine and two corresponding enantiomers of the host have been separated on preparative TLC.



Scheme 40. Synthetic route to L-RA-Pro, **242**.

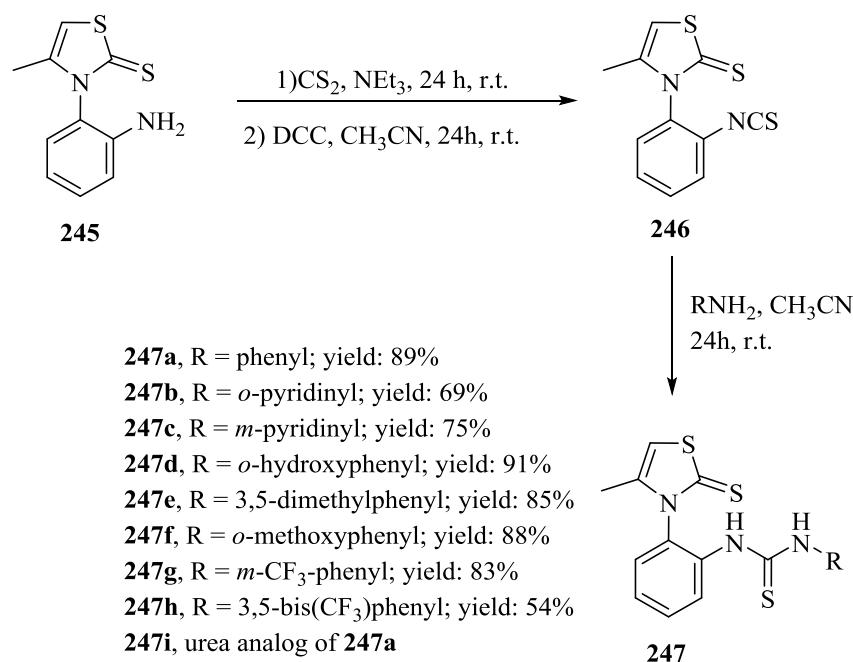


Scheme 41. *cis*-tetrahydrobenzoxanthene receptors **243**, **244**.

Table 25. Enantioselective discrimination for receptor, **244** with different guests in  $\text{CDCl}_3$  at 20 °C.

Guest	$K_a$
Ethoxycarbonyl-L-proline	57.0
Cbz-L-phenylglycine	16.0
Cbz-L-phenylalanine	15.0
Ethoxycarbonyl-L-alanine	8.4
Ethoxycarbonyl-L-leucine	7.6
BOC-L-leucine	4.0

Roussel et al. [96] reported the non-racemic atropisomeric 1-(2-(4-methyl-2-thioxothiazol-3(2*H*)-yl)phenyl)-3-(hetero)aryl(thio)ureas, **247a–h** (Scheme 42). The synthesis was carried out on the basis of parent enantiopure amino-thiazoline-2-thione, **245**, which was converted into the corresponding isothiocyanate, **246** followed by the reaction with the desired aniline derivatives. These thioureas were investigated as neutral anion receptors for the chiral recognition of some amino-acids derivatives using NMR showing moderate binding affinities and discrimination (Table 26). It was exemplified that the intramolecular H-bonding apparently play a noticeable role in the fine tuning of binding and lead to the activation or deactivation depending upon the interaction site.



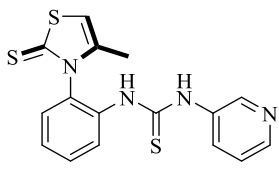
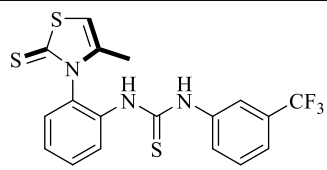
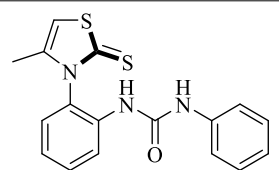
**Scheme 42.** Synthesis of thiourea, **247a–h** from amino-2-thiazoline, **245**.

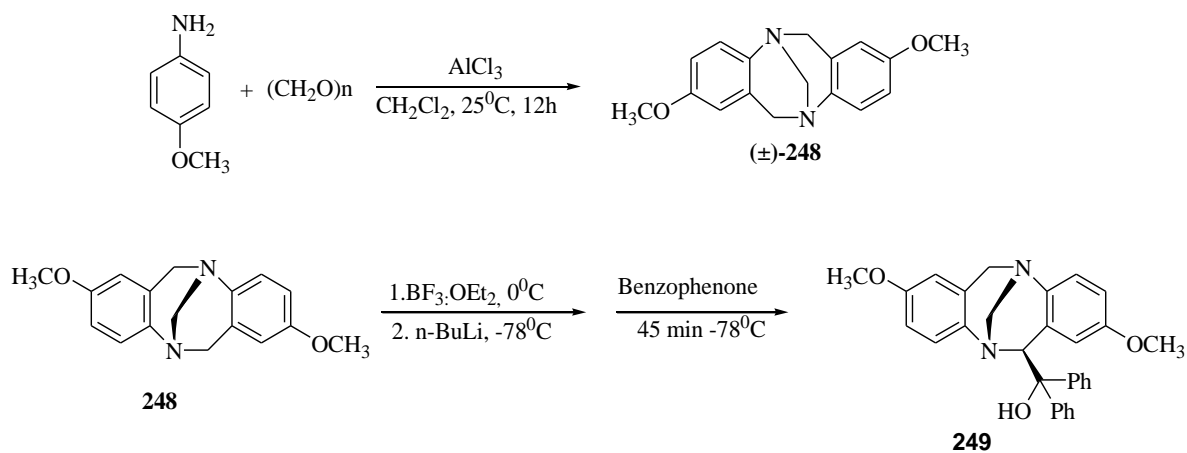
Periasamy et al. [97] synthesized the Troger's base, **248** (Scheme 43) by reported synthetic methodology via the reaction of *p*-anisidine with paraformaldehyde in the presence of AlCl<sub>3</sub> and followed by the enantioseparation with *O,O'*-dibenzoyl-L-tartaric acid as a resolving agent. Further, the amino alcohol, **249** was prepared from the chiral methoxy Troger's base, **248** by using a standard procedure for the  $\alpha$ -alkylation of tertiary amines. These chiral compounds, **248** and **249** demonstrated a good chiral recognition behavior for several carboxylic acids as determined by NMR (Table 27).

**Table 26.** Binding constant ( $K_a$ ) for the 1:1 complexes formed between thioureas, **247a,c,g** and urea **247i** and tetrabutylammonium salts of some *N*-Acetyl amino-acid or naproxen in CD<sub>3</sub>CN at 20 °C (<sup>1</sup>H NMR titration).

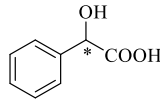
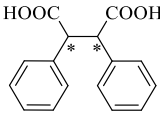
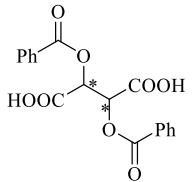
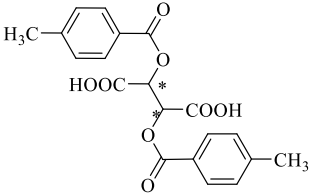
Chiral Selectors	N-Ac-amino acid Tetrabutyl Ammonium Salt	Association Constants (M <sup>−1</sup> )	Discrimination
 <b>247a (aR)</b>	(L)- <i>N</i> -Ac-Phe-COO <sup>−</sup>	540	L/D 1.60 D/L 1.15 <sup>a</sup>
	(D)- <i>N</i> -Ac-Phe-COO <sup>−</sup>	330	
	(L)- <i>N</i> -Ac-Val-COO <sup>−</sup>	600	
	(D)- <i>N</i> -Ac-Val-COO <sup>−</sup>	700	

Table 26. Cont.

Chiral Selectors	N-Ac-amino acid Tetrabutyl Ammonium Salt	Association Constants (M <sup>-1</sup> )	Discrimination
 <b>247c (aS)</b>	(L)-N-Ac-Phe-COO <sup>-</sup> (D)-N-Ac-Phe-COO <sup>-</sup>	1150 2300	D/L 2.00
 <b>247g (aS)</b>	(L)-N-Ac-Phe-COO <sup>-</sup> (D)-N-Ac-Phe-COO <sup>-</sup>	800 960	D/L 1.20 <sup>a</sup>
 <b>247i (aR)</b>	(L)-N-Ac-Phe-COO <sup>-</sup> (D)-N-Ac-Phe-COO <sup>-</sup> (L)-N-Ac-Val-COO <sup>-</sup> (D)-N-Ac-Val-COO <sup>-</sup>	1250 1550 2150 2350	L/D 1.25 <sup>a</sup> D/L 1.10 <sup>a</sup>
(aR) 247i (aS) 247i	(L)-N-Ac-Leu-COO <sup>-</sup>	2750 3900	1.42
(aR) 247i (aS) 247i	(S)-Naproxenate	1330 1900	1.43
(aR) 247i (aS) 247i	(L)-N-Ac-Trp-COO <sup>-</sup>	825 1150	1.47

<sup>a</sup> Ratio less than 1.3 are under the limit of confidence.**Scheme 43.** Synthetic methodology for Troger's base, **248** and its amino alcohol derivative, **249**.

**Table 27.** Chemical Shift changes ( $\Delta\delta$ ) and chemical shift non-equivalence ( $\Delta\Delta\delta$ ) observed in  $^1\text{H}$  NMR spectra of guest acids in the presence of hosts, **248** and **249**.

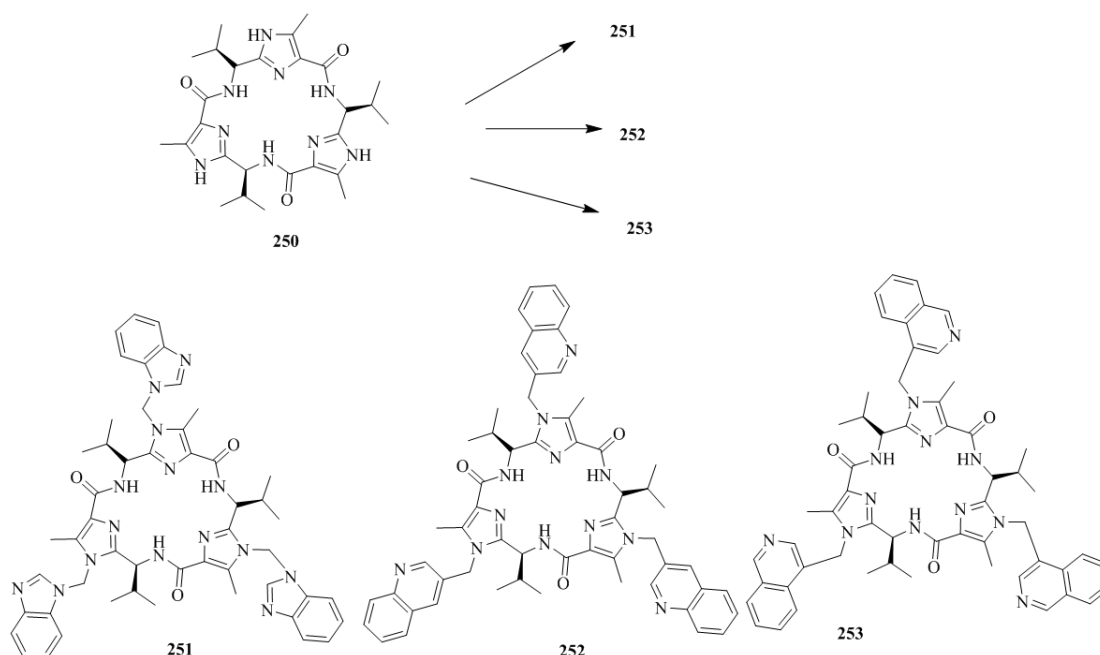
Guests	Observed Signals	$\Delta\delta(\text{ppm})$		$\Delta\Delta\delta\text{ (Hz)}$	
		<b>248</b>	<b>249</b>	<b>248</b>	<b>249</b>
 Mandelic acid	–CH	–0.13 –0.12 –0.205 –0.217	–0.122 –0.14 –	4 4.8 <sup>b</sup>	7.2 –
 2,3-diphenylsuccinic acid	–CH	–0.08 –0.11	–	12	0
 O,O'-dibenzoyl tartaric acid	Ortho CH of phenyl ring	–0.060 –0.008	–0.101 –0.137	21.2	14.4 <sup>c</sup>
 O,O'-ditoluoyl tartaric acid	Ortho CH of toluoyl ring	–0.001 –0.050	–0.05 0.102	20.8	20.4 <sup>c</sup>

The chiral recognition study (Table 27) established that the chiral methoxy Troger's base **248** exhibited better enantiodiscrimination towards the  $C_2$ -symmetric acids such as 2,3-diphenylsuccinic acid, *o,o'*-dibenzoyl tartaric acid, and *o,o'*-ditoluoyl tartaric acid. Whereas, the  $C_1$ -symmetric **249** was showed better discrimination towards unsymmetrical acids mandelic acid and 1,1'-binaphthyl-2,2'-diylphosphoric acid.

Haberhauer et al. [98] synthesized the  $C_3$ -symmetric imidazole-containing macrocyclic peptide receptors, (**251**–**253**) (Scheme 44) with different binding arms. The simple using *N*-alkylation of known scaffold, **250** with the corresponding halogenomethyl compounds afforded the desired receptors.

These hosts were employed as chiral scaffolds for the enantioselective recognition of chiral primary organoammonium ions by using the  $^1\text{H}$  NMR titration techniques. The arms of receptors, nitrogen-containing aromatic heterocycles were selected as simple units due to their rigidity, bulkiness, and ability to transfer the chiral information of the scaffold to the active binding site, thereby making the enantioselective discrimination possible. The results obtained for the chiral discrimination with several guests are summarized in Tables 28 and 29. The binding constant of receptors **251**–**253** with perchlorate salts of (*R*)-PEA and (*S*)-PEA were determined Table 28. The benzimidazole receptor, **251** on interaction with the (*R*)-PEA and (*S*)-PEA influenced the protons towards upfield around 0.10 ppm. The titration curve obtained demonstrated the pseudo linear progression, and found smaller binding constants less than  $1\text{ M}^{-1}$  owing to receptor, **251** could not orient basic nitrogens of benzimidazole in such a way to form the stable complex. For the quinoline receptor **252**, obtained the quite low value of binding constant as  $200\text{ M}^{-1}$  for (*R*)-PEA and  $480\text{ M}^{-1}$  for (*S*)-PEA respectively for both enantiomers with maximum 0.03 ppm and 0.06 ppm chemical shift. In the case of isoquinoline receptor, **253** large

chemical shift around 0.3 ppm observed with binding constants,  $4500\text{ M}^{-1}$  for (*S*)-PEA and  $30,000\text{ M}^{-1}$  for (*R*)-PEA.



**Scheme 44.** Synthesis of  $C_3$ -symmetric imidazole-containing macrocyclic peptides receptor (**251–253**).

**Table 28.** Binding constants  $K_a$  ( $\text{M}^{-1}$ ) for the formation of 1:1 complexes of **218–220** with the perchlorates of (*R*)- and (*S*)- $\alpha$ -phenylethylamine in  $\text{CDCl}_3$  at 298 K <sup>a</sup>.

Entry	Guest	218	219	220
1	( <i>R</i> )-PEA	<1	$200(\pm 30)$	$30000(\pm 11000)$ <sup>b</sup>
2	( <i>S</i> )-PEA	<1	$480(\pm 60)$	$4500(\pm 590)$

<sup>a</sup> The association constants  $K_a$  ( $\text{M}^{-1}$ ) for the formation of 1:1 complexes were measured using  $^1\text{H}$  NMR spectroscopic titrations. <sup>b</sup> A host concentration of  $2.5 \times 10^{-4}\text{ M}$  was used for titration studies, because of the high binding constant.

For the titration of quinoline receptor **252** with other guests (Table 29) revealed the maximum chemical shift observed in the range of 0.01 ppm and 0.05 ppm and binding constants for the complexes were more similar for (*R*)-PEA and (*S*)-PEA. Further, quite small binding constant were obtained for **251**\*(*R*)-AH and **251**\*(*S*)-AH with the respective values of  $360\text{ M}^{-1}$  and  $100\text{ M}^{-1}$ . More interestingly, high enantioselectivities were furnished for the complexes of **252** with (*R*)-BA vs. (*S*)-BA and for the complexes of **252** with (*R*)-PAM vs. (*S*)-PAM. Intriguingly, the binding constant values of isoquinoline receptor **253** with the both the enantiomers of guests were found to be ten times larger than that of quinolone receptor **252**. In general comparison of receptors **252** and **253** exemplified the high sensitivity to small change in the guest molecules.

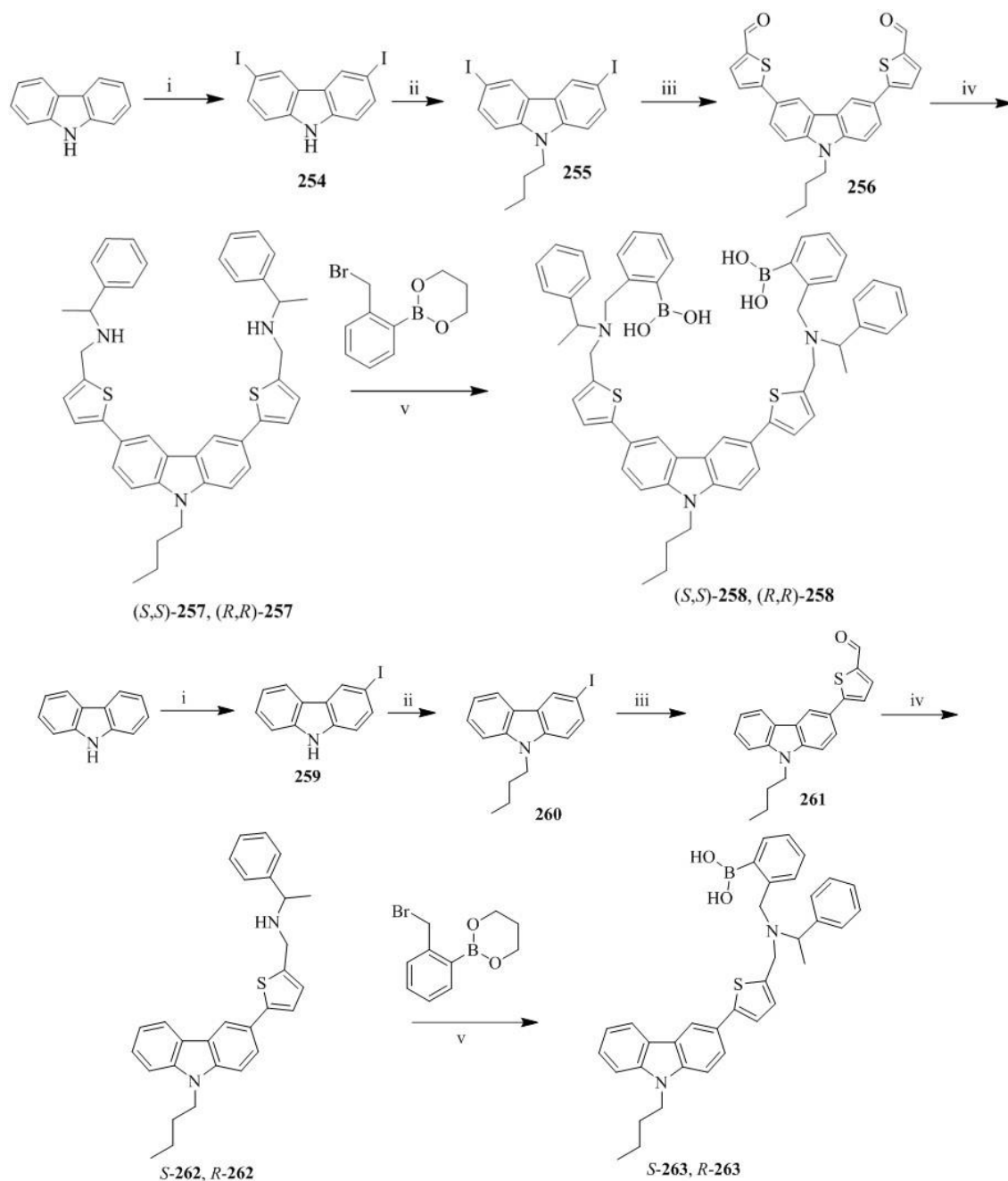
Zhao et al. [38] prepared the chiral fluorescent bisboronic acid sensors, **258**, **263** with 3,6-dithiophen-2-yl-9H-carbazole as a fluorophore (Scheme 45). The thiophene units were used to extend the  $\pi$ -conjugation of carbazole and to enhance the electron-donating ability of fluorophore. The synthetic strategy was based on the first iodination of carbazole core and subsequent attachment of 2-formyl-5-thiopheneboronic acid to the carbazole moiety by Pd(0)-catalyzed Suzuki cross-coupling. The chirogenic center was introduced by reductive amination with  $\alpha$  benzylamine. Finally, the boronic acid units were attached by a simple *N*-alkylation with 2-(2-bromomethylphenyl)-1,3,2-dioxaborinane. The monoboronic acid sensor, **230** was also prepared from mono iodinate carbazole in the similar manner and used for comparison in the binding studies.

**Table 29.** Binding constants  $K_a$  ( $M^{-1}$ ), maximum observed chemical shifts ( $\Delta \delta_{\max}$ ), Gibbs free energy changes ( $-\Delta G_0$ ), selectivity coefficients, and differences of the Gibbs free energy changes ( $\Delta \Delta G_0$ ) above) for the formation of 1:1 complexes of **219** and **220** with different salts of  $\alpha$ -chiral primary organoammonium ions in  $CDCl_3$  at 298 K.

Guest	$K_s$	$\Delta \delta_{\max}$	Selectivity Coefficients	$-\Delta G_0$ kJ mol $^{-1}$	$\Delta \Delta G_0$ kJ mol $^{-1}$
252*(R)-PEA	200( $\pm$ 40)	0.03		13.1	
252*(S)-PEA	480( $\pm$ 70)	0.06	2.4	15.3	−2.2
252*(R)-PAM	16,000( $\pm$ 4900)	0.01		24	
252*(S)-PAM	1900( $\pm$ 500)	0.02	8.4	18.7	5.3
252*(R)-BA	130( $\pm$ 40)	0.01		12.1	
252*(S)-BA	940( $\pm$ 240)	0.01	7.2	17	−4.9
252*(R)-NEA	—	—d		—	
252*(S)-NEA	d	—d	—	—	—
252*(R)-BEA	560( $\pm$ 210)	0.01		15.7	
252*(S)-BEA	540( $\pm$ 50)	0.05	1.0	15.6	0.1
252*(R)-AH	360( $\pm$ 70)	0.01		14.6	
252*(S)-AH	100( $\pm$ 20)	0.02	3.6	11.4	3.2
253*(R)-PEA	30,000( $\pm$ 11,000)	0.25		25.5	
253*(S)-PEA	4500( $\pm$ 590)	0.30	6.7	20.8	4.7
253*(R)-PAM	2000( $\pm$ 240)	0.22		18.8	
253*(S)-PAM	1100( $\pm$ 270)	0.22	1.8	17.4	1.5
253*(R)-BA	1600( $\pm$ 260)	0.17		18.3	
253*(S)-BA	2400( $\pm$ 930)	0.20	1.5	19.3	−1.0
253*(R)-NEA	1000( $\pm$ 180)	0.06		17.1	
253*(S)-NEA	610( $\pm$ 110)	0.06	1.6	15.9	1.2
253*(R)-BEA	6600( $\pm$ 1600)	0.30		21.8	
253*(S)-BEA	3200( $\pm$ 450)	0.28	2.1	20	1.8
253*(R)-AH	9700( $\pm$ 3100)	0.13		22.7	
253*(S)-AH	2400( $\pm$ 710)	0.16	4.0	19.3	3.5

The host containing diboronic acid, **258** exhibited the enantioselective recognition of tartaric acid at acidic pH, and the enantioselectivity was found to be 3.3. The L-tartaric acid showed 5 fold enhancements in the fluorescence while for D-tartaric acid exhibited 3 fold enhancement in the fluorescence. Thus, fluorescence enhancement factor ( $I_F^{\text{Sample}}/I_F^{\text{Blank}}$ ) for **258** upon interaction with tartaric acid was 3.5-fold at pH 3.0. Further, **258** was useful for the enantioselective recognition of D- and L-mandelic acid, whereas **263** containing monoboronic acid failed to display the corresponding chiral recognition of these guests.

Pu and coworkers [99] developed the H<sub>8</sub>-BINOL-aminemolecules, (S)-**264**–(S)-**267** as a promising new class of the enantioselective fluorescent sensors by using their recently developed one-step reaction of H<sub>8</sub>BINOL with in situ generated aminomethanol (Scheme 46). The NMR studies revealed that the difference between the fluorescence spectra of (S)-**264**–(S)-**267** apparently arises from the different capability of their nitrogen atoms to form intramolecular hydrogen bonds. When (S)-**267** was treated with enantiomer (R)-MA result into the substantial fluorescent enhancement with  $I_R/I_0 = 3.2$ . This was anticipated that the involvement of nitrogen of (S)-**267** in the complexation with (R)-MA to form a structurally more rigid fluorophore. However, for (S)-MA, the fluorescence enhancement was smaller with  $I_R/I_0 = 2.1$ . This indicates that (S)-**267** is a promising candidate for the enantioselective fluorescent recognition of MA in the shorter emission wavelength. Greater fluorescence enhancement at the short wavelength ( $\lambda_{em} = 330$  nm) was observed upon the interaction of (S)-**268** (Figure 24) with (R)-MA, whereas (S)-MA gave smaller enhancement at the same wavelength. Thus, a good enantioselective fluorescent response was observed in this case with ef = 3.5. This study demonstrated that the H<sub>8</sub>BINOL-based molecules are promising as a new class of the enantioselective fluorescent sensors.

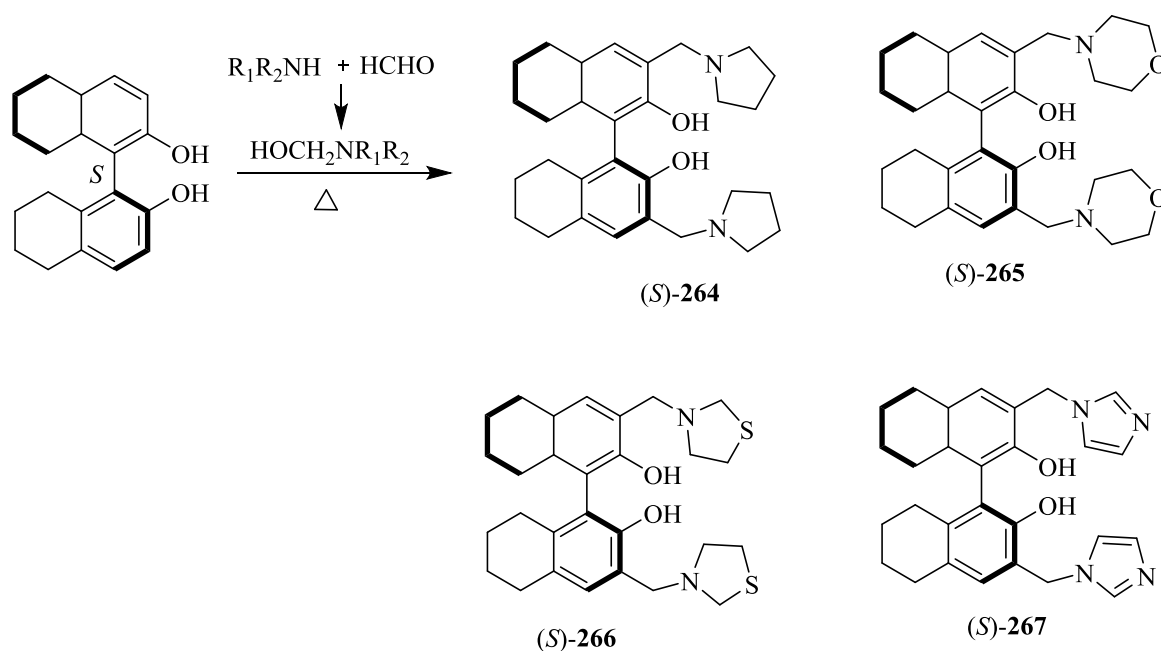


**Reagents and conditions:** (i) KI, KIO<sub>3</sub>, CH<sub>3</sub>COOH, reflux, 10 min, 42.1%; (ii) NaH, DMF, n-C<sub>4</sub>H<sub>9</sub>Br, rt 1 h, 85.0%; (iii) THF, K<sub>2</sub>CO<sub>3</sub>, Pd(PPh<sub>3</sub>)<sub>4</sub>, 5-formylthiophene-2-boronic acid, N<sub>2</sub> atmosphere, reflux, 10 h, 62.4%; (iv) R- and S-1-phenylethanamine, DCM, ethanol, reflux, 8 h, then NaBH<sub>4</sub>, rt 1 h, 79.4% (S,S-12), 64.6% (R,R-12); (v) acetonitrile, DCM, K<sub>2</sub>CO<sub>3</sub>, 2-(2-bromomethylphenyl)-1,3,2-dioxaborinane, reflux, 10 h, 27.5% (S,S-1), 31.2% (R,R-1); (vi) KI, KIO<sub>3</sub>, CH<sub>3</sub>COOH, reflux, 10 min, 40.0%; (vii) NaH, DMF, n-C<sub>4</sub>H<sub>9</sub>Br, rt 1 h, 90.2%; (viii) THF, K<sub>2</sub>CO<sub>3</sub>, Pd(PPh<sub>3</sub>)<sub>4</sub>, 5-formylthiophene-2-boronic acid, N<sub>2</sub> atmosphere, reflux, 10 h, 52.0%; (ix) R- and S-1-phenylethanamine, DCM, ethanol, reflux, 8 h, then NaBH<sub>4</sub>, rt 1 h, 71.2% (S-16), 78.4% (R-16); (x) acetonitrile, DCM, K<sub>2</sub>CO<sub>3</sub>, 2-(2-bromomethylphenyl)-1,3,2-dioxaborinane, reflux, 10 h, 42.0% (S-2), 44.5% (R-2).

**Scheme 45.** Synthesis of bisboronic acid sensors, **258**, **263** bearing 3,6-dithiophen-2-yl-9H-carbazole as a fluorophore.

Jurczak et al. [31] prepared the tweezer-type compound, **271** by functionalization of 7,7'-diamino 2,2'-diindolylmethane, **269** with peracetylated D-glucuronic acid (**270**) (Figure 25), as a source of chirality, to form the corresponding amide linkage. Similarly, the reference receptor, **272** was synthesized from 7-aminoindole.





**Scheme 46.** Synthesis of the H<sub>8</sub>BINOL-amine compounds, (S)-264–(S)-267.

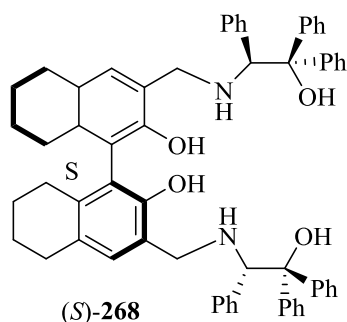


**Figure 24.** H<sub>8</sub>BINOL-amino alcohol, (S)-268.

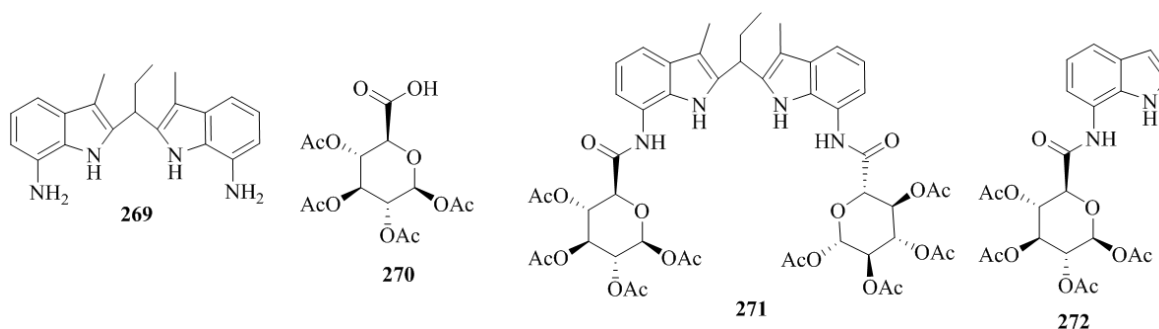
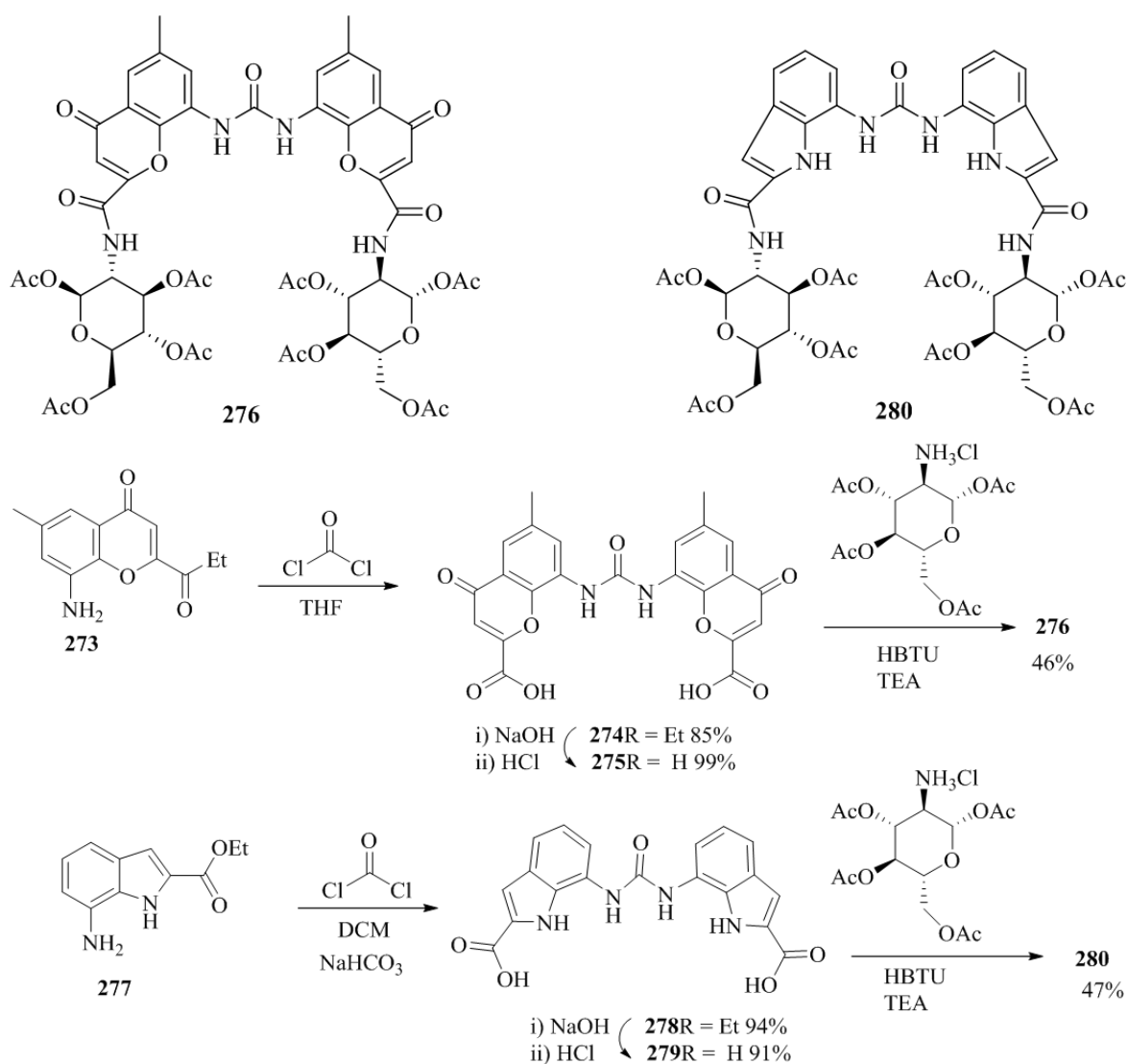


**Figure 25.** Structures of 7,7'-diamino-2,2'-dindolylmethane (**269**), peracetylated D-glucuronic acid, **270**, and chiral anion receptors **271** and **272**.

The enantioselective recognition of **271** and **272** were studied by <sup>1</sup>H NMR titrations for model chiral anionic guests; *S*-(+)-mandelate or *R*-(−)-mandelate. It was found that the association constant of (*R*)-MA is larger than that of (*S*)-MA. ROESY spectrum of the host-guest system between **271** and (*R*)-MA shows the corresponding correlations between the aromatic protons of guest and sugar protons (H3 and H5) of host. For weaker bounded (*S*)-MA, additional cross peaks were also found indicating a

deeper penetration of the anion into the receptor cavity. This was also confirmed by different ROESY signals arising from the (*R*)-mandelate protons and sugar moiety protons of host.

The same group [100] developed the chromenone- and indole–urea-based  $C_2$ -symmetrical receptors, **276** and **280** functionalized with easily accessible 1,3,4,6-tetra-*O*-acetyl-D-glucosamine, starting from amines **273** and **277** (Scheme 47). Subsequently, the condensation with phosgene resulted in **274** and **278** followed by the hydrolysis of ester groups to yield **275** and **279**. These acid compounds were then coupled with the D-glucosamine derivative to furnish the desired products, **276** and **280**.

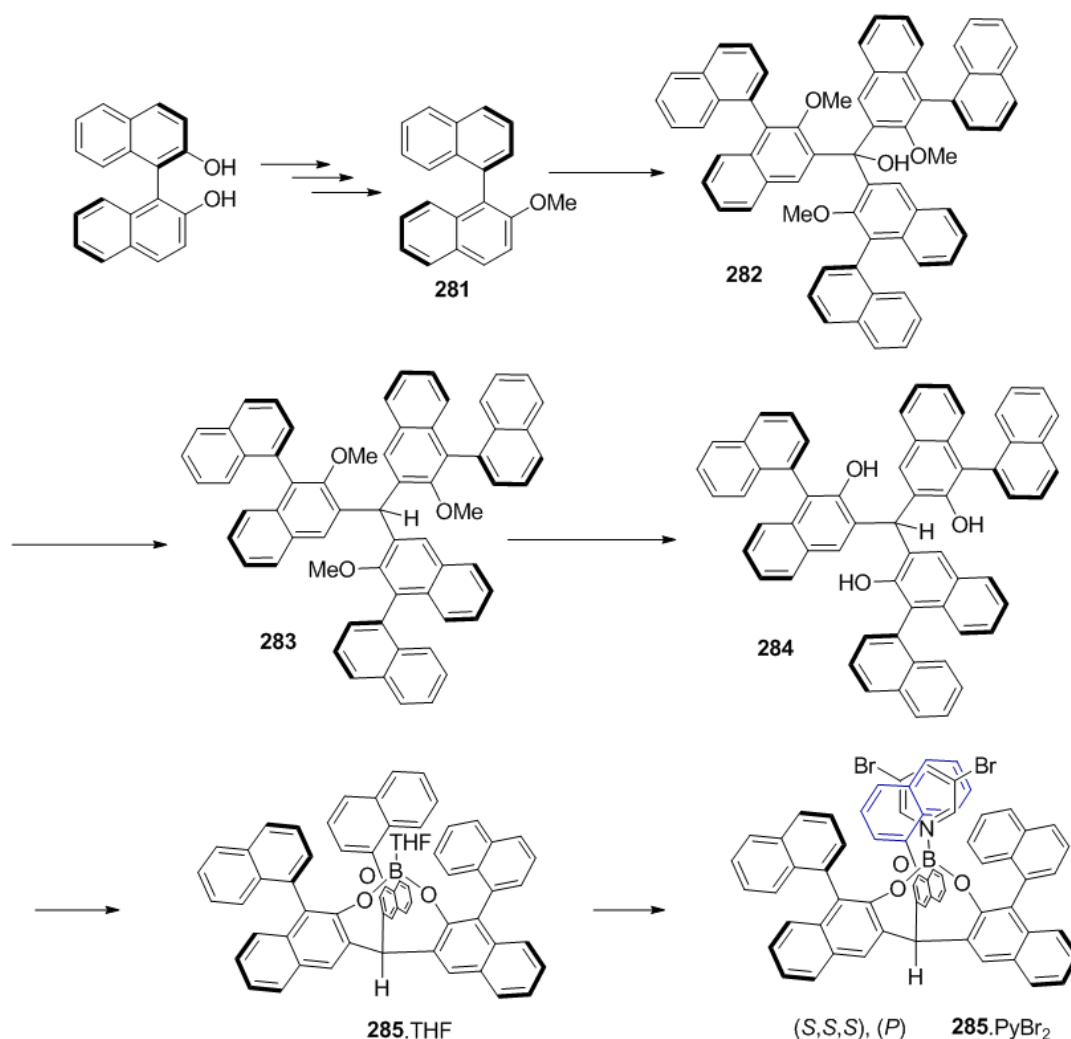


**Scheme 47.** Synthesis of receptors **276** and **280**.

The receptors, **276** and **280** were evaluated for their binding properties with various anions derived from chiral acids and having a stereogenic center in the  $\alpha$  position. It was observed that **276** binds the *S* enantiomers of anions more strongly than the *R* enantiomers in all cases, with the enantioselectivities in the range of 1.2–2.0. A similar trend but with weaker preference for binding the *S* enantiomers was observed for **280** in the most cases. Also, **276** recognizes the chiral guests by steric interaction with the sugar moieties. This hypothesis was further supported by the relative stability constants ( $K_S/K_R$ ) in the mandelate anion series. Hence, reducing the steric hindrance on the  $\alpha$  carbon in the anion by substituting Ph with  $\text{PhCH}_2$  results in increasing the overall stability constants and decreasing the  $K_S/K_R$  value, whereas enhancing this steric hindrance by replacing the hydrogen atom

with the  $\text{CF}_3$  group significantly decreases both the stability constants and the  $K_S/K_R$  value. In the case of **280** the sugar parts do not interact with the side chain of anions during the complexation, which was explained by the weak enantiodiscrimination.

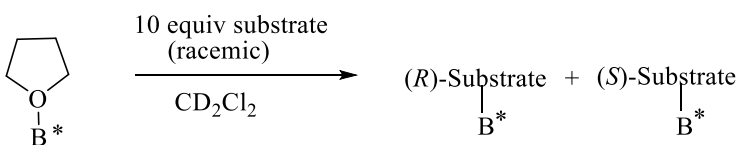
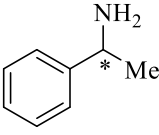
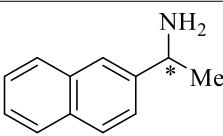
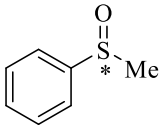
Yasuda et al. [101] prepared the cage-shaped borate, **285** starting from readily available (*R*)-BINOL, which was converted to methoxybinaphthyl, **281** followed by lithiation at the ortho-position and subsequent condensation with ethyl chloroformate to yield tris(2-methoxybinaphthyl)methanol, **282** (Scheme 48). Further reduction of **282** with a  $\text{Me}_2\text{SiHCl}/\text{InCl}_3$  system and deprotection of the methoxy groups afforded tris(2-hydroxybinaphthyl) methane, **284** with the axial chirality at all three binaphthyl moieties. Finally, mixing **284** with  $\text{BH}_3 \cdot \text{THF}$  generated the cage shaped borate, **285**, which was subsequently converted to **285**·PyBr<sub>2</sub>.



**Scheme 48.** Synthesis of homochiral cage-shaped borate, **285** with  $C_3$ -symmetry.

The chiral recognition of a mixture of the excess amount of racemic phenyl ethyl amine **98** with **285**·THF in  $\text{CD}_2\text{Cl}_2$  have been studied by  $^1\text{H}$  NMR measurement. The ratio between the *R* and *S* enantiomers of phenyl ethyl amine, 1-(2-naphthyl)ethylamine and adducts with **285** found to be 18:1, 23:1 respectively (entry 1, 2 in Table 30), showing the highly enantioselective recognition. Further, the *R* and *S* enantiomers ratio for the racemic methyl phenyl sulfoxide with host **285**, was observed to be 7:1 owing to low Lewis basicity of the sulfoxide as compared to amines.

**Table 30.** Recognition of chiral substrates by complexation with **285**.THF.

		
Entry	Substrate	R/S <sup>a</sup>
1	 <b>98</b>	18:1 <sup>b</sup>
2	 <b>99</b>	23:1 <sup>c</sup>
3	 <b>286</b>	7:1 <sup>d</sup>

<sup>a</sup> The ratios and absolute configurations except entry 3 were determined by <sup>1</sup>H NMR measurement; <sup>b</sup> heating for 43 h at 80 °C; <sup>c</sup> heating for 216 h at 80 °C; <sup>d</sup> the absolute configuration was not determined.

## 8. Summary

Chiral molecular recognition is a crucial branch of modern chemistry facilitating the qualitative and quantitative analysis of chiral molecules. It is also a basis of the industrially relevant chromatographic technique for bulk separation of racemates. There exists a huge global market for chiral separation technology for qualitative and quantitative estimations of chiral analytes. This review focuses on chiral supramolecular systems with the presence of heterocyclic ring(s) in the host structures. The hosts with the pyridine ring(s) form the major group in both the macrocyclic structures and the open chain tweezers. So far, different spectral and analytical techniques to detect and to estimate the binding between the host and the guest with a noticeable difference in the association constants of two enantiomeric guests have been employed. The fluorescence and NMR spectroscopic methods have been more commonly used for the chiral recognition purpose. Different types of intermolecular interactions between the corresponding hosts and guests involved in each supramolecular system have been proposed and discussed. An additional method on the basis of induced chirality detected by CD has been included in the review, though strictly speaking it is amplification of chirality of the guests based on supramolecular interactions between achiral host and chiral guests. Hosts with presence of different chiral elements have been employed. So far the incorporation of heterocyclic units in chiral hosts seems to be driven by ease of access, presence of aromatic ring and presence of multiple ligating centers. Though crowns and macrocycles of different sizes have been employed for chiral recognition studies, size-dependent enantio-discrimination factor has been noticed only in the last few years. Given the importance of chiral analysis, this branch is poised to achieve momentum in the coming decade.

**Acknowledgments:** Authors thank Mohammed Hasan and Sushil Khot for critical reading and suggestions. Vaibhav N. Khose thanks UGC-NET for the JRF and SRF awards. Victor Borovkov acknowledges funding from the European Union's Seventh Framework Programme for Research, Technological Development, and Demonstration under Grant Agreement no. 621364 (TUTIC-Green).

**Conflicts of Interest:** The authors declare no conflict of interest.

## References

1. Zupancic, V.; Kikelj, D. Chiral drugs in pharmaceutical industry-development and applications. *Farm. Vestnik* **2001**, *52*, 259–272.
2. Gao, Y.; Boschetti, E.; Guerrier, L. Synthesis and separation of optically active compounds. Part I. *Ann. Pharm. Fr.* **1994**, *52*, 184–203. [[PubMed](#)]
3. Hembury, G.A.; Borovkov, V.V.; Inoue, Y. Chirality sensing supramolecular systems. *Chem. Rev.* **2008**, *108*, 1–73. [[CrossRef](#)] [[PubMed](#)]
4. Ball, P. Giving life a hand. *Chem. World* **2007**, *4*, 30–31.
5. Talele, T.T. Natural-products-inspired use of the gem-dimethyl group in medicinal chemistry. *J. Med. Chem.* **2017**. [[CrossRef](#)] [[PubMed](#)]
6. Blaskovich, M.A.T. Unusual amino acids in medicinal chemistry. *J. Med. Chem.* **2016**, *59*, 10807–10836. [[CrossRef](#)] [[PubMed](#)]
7. Karnik, A.V.; Patil, S.T.; Patnekar, S.S.; Semwal, A. A convenient route to optically active  $\gamma$ -substituted  $\gamma$ -lactones. *New J. Chem.* **2004**, *28*, 1420–1422. [[CrossRef](#)]
8. Karnik, A.V.; Kamath, S.S. Cascade enantioselective synthesis of  $\gamma$ -aryl- $\gamma$ -butyrolactones with a delayed stereoselective step. *Tetrahedron* **2008**, *64*, 2992–2996. [[CrossRef](#)]
9. Tawde, T.S.; Wagh, S.J.; Sapre, J.V.; Khose, V.N.; Badani, P.M.; Karnik, A.V. Reversal of enantioselectivity induced by the achiral part of an organocatalyst in a Diels-Alder reaction. *Tetrahedron Asymmetry* **2016**, *27*, 130–135. [[CrossRef](#)]
10. Buchbauer, G.; Shafii-Tabatabai, A. Enones of (+)- and (–)-3-pinane: Influence of chirality on flavour. *Flavour Fragr. J.* **2003**, *18*, 441–445. [[CrossRef](#)]
11. Leffingwell, J.C.; Leffingwell, D. Chiral chemistry in flavours & fragrances. *Spec. Chem. Mag.* **2011**, *31*, 30–33.
12. Pietropaolo, A. *Ideas in Chemistry and Molecular Sciences: Where Chemistry Meets Life*; Pignataro, B., Ed.; Wiley: Hoboken, NJ, USA, 2010; pp. 293–312.
13. Venkatakrishnarao, D.; Sahoo, C.; Mamonov, E.A.; Novikov, V.B.; Mitetelo, N.V.; Naraharisetty, S.G.; Murzina, T.V.; Chandrasekar, R. Chiral organic photonics: Self-assembled micro-resonators for an enhanced circular dichroism effect in the non-linear optical signal. *J. Mater. Chem. C* **2017**, *5*, 12349–12353. [[CrossRef](#)]
14. Cram, D.J. The design of molecular hosts, guests, and their complexes. *Science* **1988**, *240*, 760–767. [[CrossRef](#)] [[PubMed](#)]
15. Bao, W.; Wang, Z.; Li, Y. Synthesis of chiral ionic liquids from natural amino acids. *J. Org. Chem.* **2003**, *68*, 591–593. [[CrossRef](#)] [[PubMed](#)]
16. Bako, P.; Fenichel, L.; Toke, L. A Novel diaza-crown ether and cryptands from glucopyranose and their complex-forming properties. *Eur. J. Org. Chem.* **1990**, *1990*, 1161–1164. [[CrossRef](#)]
17. Bako, P.; Vizvardi, K.; Toppet, S.; Eycken, E.; Hoornaert, G.; Fenichel, L.; Toke, L. Synthesis, extraction ability and application in asymmetric synthesis of aza crown ethers derived from D-glucose. *Tetrahedron* **1998**, *54*, 14975–14988. [[CrossRef](#)]
18. Bradshaw, J.S.; Huszthy, P.; McDaniel, C.W.; Oue, M.; Zhu, C.Y.; Izatt, R.M.; Lifson, S. Enantiomeric recognition of organic ammonium salts by chiral pyridino-18-crown-6 ligands: A short review. *J. Coord. Chem.* **1992**, *27*, 105–114. [[CrossRef](#)]
19. Fernandez-Gonzalez, A.; Guardia, L.; Badía-Laiño, R.; Díaz-García, M. Mimicking molecular receptors for antibiotics—analytical implications. *Trends Anal. Chem.* **2006**, *25*, 949–957. [[CrossRef](#)]
20. Kaushansky, K. Small molecule mimics of hematopoietic growth factors: Improving on Mother Nature? *Leukemia* **2001**, *15*, 673–674. [[CrossRef](#)] [[PubMed](#)]
21. Dickert, F.L. Biomimetic receptors and sensors. *Sensors* **2014**, *14*, 22525–22531. [[CrossRef](#)] [[PubMed](#)]
22. Kim, S.; Kim, K.; Jung, J.; Shin, S.; Ahn, K. Unprecedented Chiral Molecular Recognition in a  $C_3$ -Symmetric Environment. *J. Am. Chem. Soc.* **2002**, *124*, 591–596. [[CrossRef](#)] [[PubMed](#)]

23. Kim, J.; Seo, J.; Yim, E.; Jin, Y.; Song, S.; Suh, H. Enantiomeric recognition in host-guest complexation using chiral bis-pyridino-18-crown-6 ethers, by electrospray ionization mass spectrometry (ESI-MS) enantiomer-labelled (EL) guest method. *Bull. Korean Chem. Soc.* **2008**, *9*, 1069–1072.
24. Lu, Q.; Hou, J.; Wang, J.; Xu, B.; Zhang, J.; Yu, X. Multichannel Chromogenic and Chiral Anions Recognition by Imidazolium Functionalized BINOL Derivatives. *Chin. J. Chem.* **2013**, *31*, 641–650. [[CrossRef](#)]
25. Hasan, M.; Khose, V.N.; Pandey, A.D.; Borovkov, V.; Karnik, A.V. Tailor-Made Supramolecular Chirogenic System Based on Cs-Symmetric Rigid Organophosphoric Acid Host and Amino Alcohols: Mechanistic Studies, Bulkiness Effect, and Chirality Sensing. *Org. Lett.* **2016**, *18*, 440–443. [[CrossRef](#)] [[PubMed](#)]
26. Artz, S.P.; de Grandpre, M.P.; Cram, D.J. Host-guest complexation. Search for new chiral hosts. *J. Org. Chem.* **1985**, *50*, 1486–1496. [[CrossRef](#)]
27. Ozer, H.; Kocakaya, S.O.; Akgun, A.; Hosgoren, H.; Togrul, M. The enantiomeric recognition of chiral organic ammonium salts by chiral pyridino-macrocycles bearing aminoalcohol subunits. *Tetrahedron Asymmetry* **2009**, *20*, 1541–1546. [[CrossRef](#)]
28. Shahgaldian, P.; Pieleś, U.; Hegner, M. Enantioselective recognition of phenylalanine by a chiral amphiphilic macrocycle at the air-water interface: A copper-mediated mechanism. *Langmuir* **2005**, *21*, 6503–6507. [[CrossRef](#)] [[PubMed](#)]
29. Lu, Q.; Dong, L.; Zhang, J.; Li, J.; Jiang, L.; Huang, Y.; Qin, S.; Hu, C.; Yu, X. Imidazolium-functionalized binol as a multifunctional receptor for chromogenic and chiral anion recognition. *Org. Lett.* **2009**, *11*, 669–672. [[CrossRef](#)] [[PubMed](#)]
30. Zhao, H.; Hua, W. Synthesis and characterization of pyridine-based polyamido-polyester optically active macrocycles and enantiomeric recognition for D- and L-amino acid methyl ester hydrochloride. *J. Org. Chem.* **2000**, *65*, 2933–2938. [[CrossRef](#)] [[PubMed](#)]
31. Granda, J.M.; Jurczak, J. Sweet anion receptors: Recognition of chiral carboxylate anions by D-glucuronic-acid-decorated diindolylmethane. *Org. Lett.* **2013**, *15*, 4730–4733. [[CrossRef](#)] [[PubMed](#)]
32. De la Torre, M.F.; Campos, E.G.; Gonzalez, S.; Moran, J.R.; Caballero, M.C. Binding properties of an abiotic receptor for complexing carboxylates of  $\alpha$ -heterocyclic and  $\alpha$ -keto acids. *Tetrahedron* **2001**, *57*, 3945–3950. [[CrossRef](#)]
33. Tejada, A.; Oliva, A.I.; Simon, L.; Grande, M.; Caballero, M.; Moran, J.R. A macrocyclic receptor for the chiral recognition of hydroxycarboxylates. *Tetrahedron Lett.* **2000**, *41*, 4563–4566. [[CrossRef](#)]
34. You, J.; Yu, X.; Zhang, G.; Xiang, Q.; Lan, J.; Xie, R. Novel chiral imidazole cyclophane receptors: Synthesis and enantioselective recognition for amino acid derivatives. *Chem. Commun.* **2001**, *0*, 1816–1817. [[CrossRef](#)]
35. Pandey, A.; Mohammed, H.; Karnik, A. Chiral benzimidazole-derived mono azacrowns: Synthesis and enantiomer recognition studies with chiral amines and their ammonium salts. *Tetrahedron Asymmetry* **2013**, *24*, 706–712. [[CrossRef](#)]
36. Pandey, A.D.; Mohammed, H.; Pissurlenkar, R.S.; Karnik, A.V. Size-induced chiral discrimination switching by (S)-(–)-2-( $\alpha$ -hydroxyethyl)-benzimidazole-derived azacrowns. *ChemPlusChem* **2015**, *80*, 475–479. [[CrossRef](#)]
37. Upadhyay, S.P.; Pissurlenkar, R.S.; Coutinho, E.C.; Karnik, A.V. Furo-fused BINOL based crown as a fluorescent chiral sensor for enantioselective recognition of phenylethylamine and ethyl ester of Valine. *J. Org. Chem.* **2007**, *72*, 5709–5714. [[CrossRef](#)] [[PubMed](#)]
38. Wu, Y.; Guo, H.; James, T.D.; Zhao, J. Enantioselective recognition of mandelic acid by a 3,6-dithiophen-2-yl-9H-carbazole-based chiral fluorescent bisboronic acid sensor. *J. Org. Chem.* **2011**, *76*, 5685–5695. [[CrossRef](#)] [[PubMed](#)]
39. Shcherbakova, E.G.; Brega, V.; Minami, T.; Sheykhi, S.; James, T.D.; Anzenbacher, P. Toward fluorescence-based high-throughput screening for enantiomeric excess in amines and amino acid derivatives. *Chem. Eur. J.* **2016**, *22*, 10074–10080. [[CrossRef](#)] [[PubMed](#)]
40. Jo, H.H.; Lin, C.Y.; Anslyn, E.V. Rapid optical methods for enantiomeric excess analysis: From enantioselective indicator displacement assays to exciton-coupled circular dichroism. *Acc. Chem. Res.* **2014**, *47*, 2212–2221. [[CrossRef](#)] [[PubMed](#)]
41. Velazquez, H.A.; Hamelberg, D. Electrochemical detection. In *Chemosensors: Principles, Strategies, and Applications*, 1st ed.; Wang, B., Anslyn, E.V., Eds.; John Wiley & Sons, Inc.: Hoboken, NJ, USA, 2011.
42. Lynnf, B.C.; Tsessarskaja, M.; Schall, O.F.; Hernandez, J.C.; Watanabe, S.; Takahashit, T.; Kaifer, A.; Gokel, G.W. Hydrogen bonding in macrocyclic receptor systems. *Supramol. Chem.* **1993**, *1*, 253–260. [[CrossRef](#)]

43. Muehldorf, A.V.; Engen, D.V.; Warner, J.C.; Hamilton, A.D. Aromatic-aromatic interactions in molecular recognition: A family of artificial receptors for thymine that shows both face-to-face and edge-to-face orientations. *J. Am. Chem. Soc.* **1988**, *110*, 6561–6562. [[CrossRef](#)]
44. Mecozzi, S.; West, A.P.; Dougherty, D.A. Cation- $\pi$  interactions in aromatics of biological and medicinal interest: Electrostatic potential surfaces as a useful qualitative guide. *Proc. Natl. Acad. Sci. USA* **1996**, *93*, 10566–10571. [[CrossRef](#)] [[PubMed](#)]
45. Price, S.L.; Stone, A.J. The electrostatic interactions in van der Waals complexes involving aromatic molecules. *J. Chem. Phys.* **1987**, *86*, 2859–2868. [[CrossRef](#)]
46. Gibb, B.C. Van der waals interactions and the hydrophobic effect. In *Chemosensors: Principles, Strategies, and Applications*, 1st ed.; Wang, B., Anslyn, E.V., Eds.; John Wiley & Sons, Inc.: Hoboken, NJ, USA, 2011.
47. Mei, X.; Wolf, C. Enantioselective sensing of chiral carboxylic acids. *J. Am. Chem. Soc.* **2004**, *126*, 14736–14737. [[CrossRef](#)] [[PubMed](#)]
48. Hasan, M.; Khose, V.N.; Mori, T.; Borovkov, V.; Karnik, A.V. Sui Generis Helicene-Based Supramolecular Chirogenic System: Enantioselective Sensing, Solvent Control, and Application in Chiral Group Transfer Reaction. *ACS Omega* **2017**, *2*, 592–598. [[CrossRef](#)]
49. Li, G.; Cao, J.; Zong, W.; Lei, X.; Tan, R. Enantiodiscrimination of carboxylic acids using the diphenylprolinol NMR chiral solvating agents. *Org. Chem. Front.* **2016**, *3*, 96–102. [[CrossRef](#)]
50. Fukui, F.; Fukushima, Y. NMR Determinations of the Absolute Configuration of  $\alpha$ -Chiral Primary Amines. *Org. Lett.* **2010**, *12*, 2856–2859. [[CrossRef](#)] [[PubMed](#)]
51. Parker, D. NMR determination of enantiomeric purity. *Chem. Rev.* **1991**, *91*, 1441–1457. [[CrossRef](#)]
52. Davankov, V.A. Separation of enantiomeric compounds using chiral HPLC systems. A brief review of general principles, advances, and development trends. *Chromatographia* **1989**, *27*, 475–482. [[CrossRef](#)]
53. Kim, J.; Lee, J.; Lee, S.; Seo, J.; Hong, J.; Suh, H. Chiral molecular recognition in fast atom bombardment mass spectrometry (FAB-MS) enantiomerlabeled (EL) guest method using new chiral bis-pyridino-18-crown-6. *Bull. Korean Chem. Soc.* **2002**, *23*, 543–544.
54. Bayly, S.R.; Chen, G.Z.; Beer, P.D. Electrochemical Detection. In *Chemosensors: Principles, Strategies, and Applications*, 1st ed.; Wang, B., Anslyn, E.V., Eds.; John Wiley & Sons, Inc.: Hoboken, NJ, USA, 2011.
55. Shaw, S.A.; Aleman, P.; Vedejs, E. Development of chiral nucleophilic pyridine catalysts: Applications in asymmetric quaternary carbonsynthesis. *J. Am. Chem. Soc.* **2003**, *125*, 13368–13369. [[CrossRef](#)] [[PubMed](#)]
56. Ishii, T.; Fujioka, S.; Sekiguchi, Y.; Kotsuki, H. A new class of chiral pyrrolidine-pyridine conjugate base catalysts for use in asymmetric Michael addition reactions. *J. Am. Chem. Soc.* **2004**, *126*, 9558–9559. [[CrossRef](#)] [[PubMed](#)]
57. Ager, D.J.; Prakash, I.; Schaad, D.R. 1,2-amino alcohols and their heterocyclic derivatives as chiral auxiliaries in asymmetric synthesis. *Chem. Rev.* **1996**, *96*, 835–876. [[CrossRef](#)] [[PubMed](#)]
58. Fu, G.C. Asymmetric Catalysis with “Planar-Chiral” Derivatives of 4-(Dimethylamino)pyridine. *Acc. Chem. Res.* **2004**, *37*, 542–547. [[CrossRef](#)] [[PubMed](#)]
59. Jolly, S.T.; Bradshaw, J.S.; Izatt, R.M. Synthetic chiral macrocyclic crown ligands: A short review. *J. Heterocycl. Chem.* **1982**, *19*, 3–18. [[CrossRef](#)]
60. Bradshaw, J.S.; Peter Huszthy, P.; Redd, J.T.; Zhang, X.X.; Wang, T.; Hathaway, J.K.; Young, J.; Izatt, R.M. Enantiomeric recognition of chiral ammonium salts by chiral pyridino- and pyrimidino-18-crown-6 ligands: Effect of structure and solvents. *Pure Appl. Chem.* **1995**, *67*, 691–695. [[CrossRef](#)]
61. Chu, I.; Dearden, D.V.; Bradshaw, J.S.; Huszthy, P.; Izatt, R.M. Chiral host-guest recognition in an ion-molecule reaction. *J. Am. Chem. Soc.* **1993**, *115*, 4318–4320. [[CrossRef](#)]
62. Hellier, P.C.; Bradshaw, J.S.; Young, J.J.; Zhang, X.X.; Izatt, R.M. Chiral pyridine-based macrobicyclic clefts: Synthesis and enantiomeric recognition of ammonium salts. *J. Org. Chem.* **1996**, *61*, 7270–7275. [[CrossRef](#)] [[PubMed](#)]
63. Asakawa, M.; Brown, C.L.; Pasini, D.; Stoddart, J.F.; Wyatt, P.G. Enantioselective recognition of amino acids by axially-chiral  $\pi$ -electron-deficient receptors. *J. Org. Chem.* **1996**, *61*, 7234–7235. [[CrossRef](#)] [[PubMed](#)]
64. Somogyi, L.; Huszthy, P.; Bradshaw, J.S.; Izatt, R.M.; Hollosi, M. Enantiomeric recognition of aralkyl ammonium salts by chiral pyridino-18-crown-6 ligands: Use of circular dichroism spectroscopy. *Chirality* **1997**, *9*, 545–549. [[CrossRef](#)]
65. Gavin, J.A.; Garcia, M.E.; Benesi, A.J.; Mallouk, T.E. Chiral molecular recognition in a tripeptide benzylviologen cyclophane host. *J. Org. Chem.* **1998**, *63*, 7663–7669. [[CrossRef](#)]



66. Du, C.; You, J.; Yu, X.; Liu, C.; Lan, J.; Xie, R. Homochiral molecular tweezers as hosts for the highly enantioselective recognition of amino acid derivatives. *Tetrahedron Asymmetry* **2003**, *14*, 3651–3656. [[CrossRef](#)]
67. Chen, X.; Du, D.; Hua, W. Synthesis of novel chiral polyamide macrocycles containing pyridyl side-arms and their molecular recognition properties. *Tetrahedron Asymmetry* **2003**, *14*, 999–1007. [[CrossRef](#)]
68. Ema, T.; Tanida, D.; Sakai, T. Versatile and practical macrocyclic reagent with multiple hydrogen-bonding sites for chiral discrimination in NMR. *J. Am. Chem. Soc.* **2007**, *129*, 10591–10596. [[CrossRef](#)] [[PubMed](#)]
69. Heckel, T.; Winkel, A.; Wilhelm, R. Chiral ionic liquids based on nicotine for the chiral recognition of carboxylic acids. *Tetrahedron Asymmetry* **2013**, *24*, 1127–1133. [[CrossRef](#)]
70. Ma, F.; Ai, L.; Shen, X.; Zhang, C. New macrocyclic compound as chiral shift reagent for carboxylic acids. *Org. Lett.* **2007**, *9*, 125–127. [[CrossRef](#)] [[PubMed](#)]
71. Chen, X.; Huang, Z.; Chen, S.; Li, K.; Yu, X.; Pu, L. Enantioselective gel collapsing: A new means of visual chiral sensing. *J. Am. Chem. Soc.* **2010**, *132*, 7297–7299. [[CrossRef](#)] [[PubMed](#)]
72. Seker, S.; Baris, D.; Arslan, N.; Turgut, Y.; Lu, N.P.; Togrul, M. Synthesis of rigid and C<sub>2</sub>-symmetric pyridino-15-crown-5 type macrocycles bearing diamide-diester functions: Enantiomeric recognition for chiral primary organoammonium perchlorate salts. *Tetrahedron Asymmetry* **2014**, *25*, 411–417. [[CrossRef](#)]
73. Deniz, P.; Turgut, Y.; Togrul, M.; Hosgoren, H. Pyridine containing chiral macrocycles: Synthesis and their enantiomeric recognition for amino acid derivatives. *Tetrahedron* **2011**, *67*, 6227–6232. [[CrossRef](#)]
74. Ghosh, K.; Majumdar, A. L-Amino acid derived pyridinium-based chiral compounds and their efficacy in chiral recognition of lactate. *RSC Adv.* **2015**, *5*, 24499–24506. [[CrossRef](#)]
75. Khanvilkar, A.N.; Bedekar, A.V. Synthesis and characterization of chiral aza-macrocycles and study of their enantiomer recognition ability for organo-phosphoric acid and phosphonic acid derivatives by <sup>31</sup>P NMR and fluorescence spectroscopy. *Org. Biomol. Chem.* **2016**, *14*, 2742–2748. [[CrossRef](#)] [[PubMed](#)]
76. Gonzalez, S.; Pelaez, R.; Sanz, F.; Jimenez, M.B.; Moran, J.R.; Caballero, M.C. Macrocyclic chiral receptors toward enantioselective recognition of naproxen. *Org. Lett.* **2006**, *8*, 4679–4682. [[CrossRef](#)] [[PubMed](#)]
77. Barnhill, D.K.; Sargent, A.L.; Allen, W.E. Participation of host spacer atoms in carboxylic acid binding: Implications for amino acid recognition. *Tetrahedron* **2005**, *61*, 8366–8371. [[CrossRef](#)]
78. Su, X.; Luo, K.; Xiang, Q.; Lan, J.; Xie, R. Enantioselective recognitions of chiral molecular tweezers containing imidazoliums for amino acids. *Chirality* **2009**, *21*, 539–546. [[CrossRef](#)] [[PubMed](#)]
79. Luo, K.; Jiang, H.; You, J.; Xiang, Q.; Guoa, S.; Lan, J.; Xie, R. Chiral di-imidazolium molecular tweezers: Synthesis and enantioselective recognition for amino acid derivatives. *Lett. Org. Chem.* **2006**, *3*, 363–367.
80. Munusamy, S.; Muralidharan, V.P.; Iyer, S.K. Enantioselective recognition of unmodified amino acids by ligand-displacement assays with in situ generated 1:1 Cu(II)-BINOL imidazole complex. *Sens. Actuators B Chem.* **2017**, *250*, 244–249. [[CrossRef](#)]
81. Ghosh, K.; Sarkar, T. L-Valine derived benzimidazole based bis-urea in enantioselective fluorescence sensing of L-tartrate. *Tetrahedron Lett.* **2013**, *54*, 4568–4573. [[CrossRef](#)]
82. Zhao, S.; Ito, S.; Ohba, Y.; Katagiri, H. Determination of the absolute configuration and identity of chiral carboxylic acids using a Cu(II) complex of pyridine-benzimidazole-based ligand. *Tetrahedron Lett.* **2014**, *55*, 2097–2100. [[CrossRef](#)]
83. Sato, H.; Shizuma, M. Triazole-linked host compounds for chiral-discrimination toward amino acid ester guests. *J. Oleo Sci.* **2008**, *57*, 503–511. [[CrossRef](#)] [[PubMed](#)]
84. Miao, F.; Zhou, J.; Tian, D.; Li, H. Enantioselective recognition of mandelic acid with (R)-1,1-bi-2-naphthol-linked calix[4]arene via fluorescence and dynamic light scattering. *Org. Lett.* **2012**, *14*, 3572–3575. [[CrossRef](#)] [[PubMed](#)]
85. Wu, J.; Lu, J.; Liu, J.; Zheng, C.; Gao, Y.; Hu, J.; Ju, Y. A deoxycholic acid-based macrocycle: Recognition of mercury ion and cascade enantioselective sensing toward amino acids. *Sens. Actuators B* **2017**, *241*, 931–937. [[CrossRef](#)]
86. Karnik, A.V.; Upadhyay, S.P.; Gangrade, M.G. [9,9']Bi[naphtho(2,1-b)furanyl]-8,8'-diol, a furo-fused BINOL derivative: Synthesis, resolution and determination of absolute configuration. *Tetrahedron Asymmetry* **2006**, *17*, 1275–1280. [[CrossRef](#)]
87. Upadhyay, S.P.; Karnik, A.V. Enantioselective synthesis of (R) and (S)-[9,9']bi[naphtho(2,1-b)furanyl]-8,8'-diol. A furo-fused BINOL derivative. *Tetrahedron Lett.* **2007**, *48*, 317–318. [[CrossRef](#)]
88. Kotwal, S.B.; Pandey, A.D.; Khose, V.N.; Karnik, A.V. A convenient route to enantiomerically enriched furo-fused BINOL derivative. *Indian J. Chem. B* **2015**, *54*, 940–943.



89. Hasan, M.; Pandey, A.D.; Khose, V.N.; Mirgane, N.A.; Karnik, A.V. Sterically congested chiral 7,8-dioxo[6]helicene and its dihydro analogues: Synthesis, regioselective functionalization, and unexpected domino prins reaction. *Eur. J. Org. Chem.* **2015**, *17*, 3702–3712. [[CrossRef](#)]
90. Ollevier, T. Iron bis(oxazoline) complexes in asymmetric catalysis. *Catal. Sci. Technol.* **2016**, *6*, 41–48. [[CrossRef](#)]
91. Wolf, C.; Xu, H. Asymmetric catalysis with chiral oxazolidine ligands. *Chem. Commun.* **2011**, *47*, 3339–3350. [[CrossRef](#)] [[PubMed](#)]
92. Kim, S.; Kim, K.; Kim, Y.K.; Shin, S.K.; Ahn, K.H. Crucial role of three-center hydrogen bonding in a challenging chiral molecular recognition. *J. Am. Chem. Soc.* **2003**, *125*, 13819–13824. [[CrossRef](#)] [[PubMed](#)]
93. Kim, J.; Kim, S.; Seong, H.R.; Ahn, K.H. Breaking the C<sub>3</sub>-symmetry of chiral tripodal oxazolines: Enantio-discrimination of chiral organoammonium ions. *J. Org. Chem.* **2005**, *70*, 7227–7231. [[CrossRef](#)] [[PubMed](#)]
94. Sambasivan, S.; Kim, S.; Choi, U.M.; Rhee, Y.M.; Ahn, K.H. C<sub>3</sub>-symmetric cage-like receptors: Chiral discrimination of R-chiral amines in a confined space. *Org. Lett.* **2010**, *12*, 4228–4231. [[CrossRef](#)] [[PubMed](#)]
95. Oliva, A.I.; Simon, L.; Hernandez, J.V.; Muniz, F.M.; Lithgow, A.; Jimenez, A.; Moran, J.R. Enantioselective recognition of  $\alpha$ -amino acid derivatives with a *cis*-tetrahydrobenzoxanthene receptor. *J. Chem. Soc. Perkin Trans.* **2002**, *2*, 1050–1052. [[CrossRef](#)]
96. Roussel, C.; Roman, M.; Andreoli, F.; Del Rio, A.L.; Faure, R.; Vanthuyne, N. Non-racemic atropisomeric (thio)ureas as neutral enantioselective anion receptors for amino-acid derivatives: Origin of smaller K<sub>ass</sub> with thiourea than urea derivatives. *Chirality* **2006**, *18*, 762–771. [[CrossRef](#)] [[PubMed](#)]
97. Satishkumar, S.; Periasamy, M. Chiral recognition of carboxylic acids by Troeger's base derivatives. *Tetrahedron Asymmetry* **2009**, *20*, 2257–2262. [[CrossRef](#)]
98. Schnopp, M.; Haberhauer, G. Highly selective recognition of  $\alpha$ -chiral primary organoammonium ions by C<sub>3</sub>-symmetric peptide receptors. *Eur. J. Org. Chem.* **2009**, 4458–4467. [[CrossRef](#)]
99. Yu, S.; DeBerardinis, A.M.; Turlington, M.; Pu, L. Study of the Fluorescent Properties of partially hydrogenated 1,1'-Bi-2-naphthol-amine molecules and their use for enantioselective fluorescent recognition. *J. Org. Chem.* **2011**, *76*, 2814–2819. [[CrossRef](#)] [[PubMed](#)]
100. Lichosyt, D.; Wasilek, S.; Jurczak, J. Stereoselective chirality extension of *syn,anti*- and *syn,syn*-oxazine and stereochemical analysis of chiral 1,3-oxazines: Stereoselective total syntheses of (+)-1-deoxygalactonojirimycin and (–)-1-deoxygulonojirimycin. *J. Org. Chem.* **2016**, *81*, 7342–7348. [[CrossRef](#)] [[PubMed](#)]
101. Konishi, A.; Nakaoka, K.; Maruyama, H.; Nakajima, H.; Eguchi, T.; Baba, A.; Yasuda, M. C<sub>3</sub>-symmetric boron lewis acid with a cage-shape for chiral molecular recognition and asymmetric catalysis. *Chem. Eur. J.* **2017**, *23*, 1273–1277. [[CrossRef](#)] [[PubMed](#)]

